

# **For Reference**

---


**NOT TO BE TAKEN FROM THIS ROOM**



Ex libris  
UNIVERSITATIS  
ALBERTAENSIS







Digitized by the Internet Archive  
in 2022 with funding from  
University of Alberta Library

<https://archive.org/details/Dingwell1984>



THE UNIVERSITY OF ALBERTA

Investigations of the role of fluorine in silicate melts :  
implications for igneous petrogenesis.

by

Donald Bruce Dingwell



A THESIS

SUBMITTED TO THE FACULTY OF GRADUATE STUDIES AND RESEARCH  
IN PARTIAL FULFILMENT OF THE REQUIREMENTS FOR THE DEGREE  
OF Doctor of Philosophy

Department of Geology

EDMONTON, ALBERTA

Fall 1984





## Dedication

This thesis is dedicated to my parents, Phyllis and Bruce.





## ABSTRACT

The results of five separate studies on the properties of fluorine- and water-bearing silicate melts are presented in this thesis. Each study represents an attempt to evaluate the effects of fluorine on polymerized silicate melts by studying melt properties. The melt properties studied are viscosity, fluorine diffusivity, melt-vapor partitioning and water solubility.

The effect of fluorine on melt viscosities of five compositions in the system  $\text{Na}_2\text{O}-\text{Al}_2\text{O}_3-\text{SiO}_2$  was investigated at one atmosphere and 1000-1600°C by concentric-cylinder viscometry. The compositions chosen were albite, jadeite and nepheline on the join  $\text{NaAlO}_2-\text{SiO}_2$  and two others off the join at 75 mole percent  $\text{SiO}_2$ , one peralkaline and one peraluminous. Fluorine reduces the viscosities and activation energies of all melts investigated. The viscosity-reducing power of fluorine increases with the  $\text{SiO}_2$  content of melts on the join  $\text{NaAlO}_2-\text{SiO}_2$  and is a maximum at  $\text{Na}/\text{Al}(\text{molar})=1$  for melts containing 75 mole percent  $\text{SiO}_2$ . Fluorine and water have similar effects on aluminosilicate melt viscosities, probably due to depolymerization of these melts by replacement of  $\text{Si}-\text{O}(\text{Si},\text{Al})$  bridges with  $\text{Si}-\text{OH}$  and  $\text{Si}-\text{F}$  bonds, respectively. The viscous flow of phonolites, trachytes and rhyolites will be strongly affected by fluorine.

The chemical diffusion of fluorine in jadeite melt was investigated from 10 to 15 kbars and 1200 to 1400°C using





diffusion couples of jadeite melt and fluorine-bearing jadeite melt (6.3wt.% F). The diffusion profile data indicate that the diffusion process is concentration-independent, binary, F-O interdiffusion. The F-O interdiffusion coefficient ranges from  $1.3 \times 10^{-7}$  to  $7.1 \times 10^{-7}$  cm<sup>2</sup>/sec. The Arrhenius activation energy of diffusion ranges from 36 to 39 kcal/mole as compared with 19 kcal/mole for fluorine tracer diffusion in a lime-aluminosilicate melt. The diffusivities of various cations are significantly increased by the addition of fluorine or water to a silicate melt.

The chemical diffusion of fluorine in five melts in the system Na<sub>2</sub>O-Al<sub>2</sub>O<sub>3</sub>-SiO<sub>2</sub> was investigated at 1200-1400°C and 1 atm. Spheres of the same melts that were used for viscometry were suspended from Pt loops in a flow of oxygen gas, at high temperature. The resulting volatilization of fluorine was investigated by microprobe scans for Na, Al, Si and F, across quenched, sectioned spheres. Profiles of fluorine concentration can be reduced to yield a bulk diffusion coefficient for F-O interdiffusion. Fluorine diffusivity decreases along the join NaAlO<sub>2</sub>-SiO<sub>2</sub> from nepheline to albite. At 75 mole % SiO<sub>2</sub>, fluorine diffusion is slower in albite than in peraluminous and peralkaline melts. Fluorine diffusion in albite melt is significantly slower than water diffusion in obsidian melt.

The solubilities of water in six melts in the system K<sub>2</sub>O-Na<sub>2</sub>O-Al<sub>2</sub>O<sub>3</sub>-SiO<sub>2</sub> were determined at 930-1630 bars and





800°C. The solubilities were determined by micromanometric measurement of H<sub>2</sub>O in quenched melts. The solubilities at 970 bars for the granitic and phonolitic minimum melts are 2.88 ±0.10 wt% and 5.01 ±0.14 wt%, respectively. Both peralkaline and peraluminous granitic melts have higher H<sub>2</sub>O solubilities than the 1 kbar P(H<sub>2</sub>O) minimum melt. Fluorine decreases the solubility of water in granitic melts.

The partitioning of Na, K, Al, and Si between fluorine-bearing haplogranitic melts and a coexisting fluid phase was investigated at 1 kbar and 800°C. Fluorine significantly increases the solubility of Na, K, Al and Si in the fluid phase. The largest increase is for aluminum suggesting that fluorine is coordinated by aluminum in one or more aluminofluoride or alkali aluminofluoride complexes under these conditions. The results provide experimental confirmation of the mobility of aluminum observed in many fluorine-rich magmato-hydrothermal systems.



## Acknowledgements

I am indebted to Dr. Chris Scarfe for helping me to formulate, carry out and complete this thesis. He has allowed me to pursue several interesting research projects in the last four years, all the while managing to keep on schedule and in good spirits. I thank Drs. B.E. Nesbitt , F.J. Longstaffe and T.H. Etsell for serving on my committee. I wish to thank the following for technical assistance and consultation, ; J.M. Duke for providing fluorine analyses by neutron activation, D.J. Cronin and D. Kauffman for assistance with viscometry, D.M. Harris for vacuum fusion micromanometric analyses of water, A. Stelmach for assistance with atomic absorption analyses and S. Launspach for assistance with electron microprobe operation and data reduction. Many thanks go to Mark Brearley, Todd Dunn, Jim Dickinson and Dave Harris for their comments on earlier drafts of portions of this thesis and for numerous discussions of the research contained herein. Finally, thank-you to all of my friends at University of Alberta for making it fun to be in geology.





## Table of Contents

Chapter	Page
I. Introduction .....	1
A. Opening comments .....	1
B. Background .....	1
C. Objectives .....	4
Viscometry .....	5
Diffusion .....	5
Water solubility .....	6
Melt-fluid partitioning .....	7
Summary .....	7
II. Viscometry .....	8
A. Introduction .....	8
B. Experimental method .....	9
C. Results .....	15
D. Discussion .....	18
Comparison with previous work. ....	18
Structural implications .....	23
Comparison with water .....	26
Geological applications .....	28
E. Summary and conclusions .....	32
III. High pressure diffusion .....	34
A. Introduction .....	34
B. Experimental method .....	35
C. Results .....	39
D. Discussion .....	47
Comparison with oxygen diffusion .....	47





Comparison with tracer diffusion .....	48
Comparison with Si-Ge and Al-Ga interdiffusion .....	48
Compensation relationships .....	52
Effect of water and fluorine on cationic diffusivities .....	54
Geological applications .....	55
E. Summary and conclusions .....	57
IV. One atmosphere diffusion .....	58
A. Introduction .....	58
B. Experimental method .....	58
C. Data reduction .....	62
D. Results .....	63
E. Discussion .....	67
Comparison with viscosity data .....	67
Pressure dependence of F-O interdiffusion in jadeite melt .....	68
Comparison with water .....	70
Diffusion mechanisms .....	74
V. Water solubility .....	77
A. Introduction .....	77
B. Experimental and analytical procedures .....	79
C. Results .....	84
Pressure dependence .....	84
Effects of Na-K exchange .....	87
Dependence of solubility on the alkali/aluminum ratio .....	87
Solubility in a phonolite liquid .....	90
Effect of fluorine on solubility .....	90



D. Discussion .....	92
Comparison with earlier determinations .....	92
E. Geological application .....	96
VI. Major element partitioning .....	99
A. Introduction .....	99
B. Experimental and analytical methods .....	100
C. Results .....	105
D. Discussion .....	112
E. Geological implications .....	113
VII. Summary and conclusions .....	119
A. Summary of results .....	119
B. Conclusions .....	121
Melt structure .....	121
Geological implications .....	122
Bibliography .....	125





## List of Figures

1. Figure 1. Common and extreme ranges of fluorine content of granites and related rocks.....	2
2. Figure 2. Melt compositions used in viscometry projected into the system $\text{Na}_2\text{O}-\text{Al}_2\text{O}_3-\text{SiO}_2$ .....	10
3. Figure 3. Newtonian behavior of fluorine-bearing albite melt.....	12
4. Figure 4. Viscosities of fluorine-bearing melts and base melts.....	16
5. Figure 5. Decreases in activation energy of viscous flow for fluorine-bearing melts .....	20
6. Figure 6. Effect of fluorine on slag viscosities.....	22
7. Figure 7. Comparison of the effects of water and fluorine on melt viscosity .....	27
8. Figure 8. The effect of fluorine on the viscosities of phonolites, trachytes and rhyolites.....	30
9. Figure 9. Profile of diffusion couple for fluorine in jadeite melt.....	41
10. Figure 10. Reduced diffusion-couple profile. ....	43
11. Figure 11. Fluorine diffusion data in jadeite melt at 10, 12.5 and 15 kilobars.....	44
12. Figure 12. Tracer diffusion in a lime-aluminosilicate melt.....	49
13. Figure 13. Pressure dependence of F-O, Al-Ga and Si-Ge interdiffusion .....	51
14. Figure 14. Compensation plot for silicate melt diffusivities.....	53





15. Figure 15. Concentration profiles of Na, Al, Si and fluorine in a 1 atmosphere diffusion experiment.....	61
16. Figure 16. Reduced diffusion profiles from time series experiments .....	64
17. Figure 17. Results of 1 atmosphere diffusion experiments.....	65
18. Figure 18. Pressure dependence of fluorine diffusion in jadeite melt. ....	69
19. Figure 19. Chemical diffusion of fluorine in albite melt and water in rhyolite melts.....	72
20. Figure 20. Alkali tracer diffusion in rhyolite melts..	76
21. Figure 21. Starting compositions in the system $K_2O-Na_2O-Al_2O_3-SiO_2$ .....	80
22. Figure 22. Effect of pressure on water solubility.....	85
23. Figure 23. Effect of the alkali/aluminum ratio on water solubility .....	88
24. Figure 24. Effect of fluorine on water solubility.....	91
25. Figure 25. Solubility determinations in natural and synthetic granitic melts.....	93
26. Figure 26. Fluorine-free compositions in the system $K_2O-Na_2O-Al_2O_3-SiO_2$ .....	101
27. Figure 27. Reversals and time series experiments in molar Na-K-Al-Si space.....	104
28. Figure 28. Solute yields for Na, K, Al and Si.....	106
29. Figure 29. Solute yields for fluorine.....	109
30. Figure 30. Results of partitioning experiments in haplogranite-HF-H <sub>2</sub> O.....	110



31. Figure 31. Comparison with boron-bearing and  
chlorine-bearing fluid compositions .....114



## List of Tables

1. Table 1. Analyses of glasses used for viscometry.....	14
2. Table 2. Viscosity results and computed Arrhenius parameters.....	17
3. Table 3. Analyses of starting glasses for high pressure diffusion experiments.....	36
4. Table 4. Conditions and results of high pressure diffusion experiments.....	45
5. Table 5. Arrhenius parameters for high pressure diffusion.....	46
6. Table 6. Experimental results for 1 atmosphere diffusion.....	66
7. Table 7. Arrhenius parameters for 1 atmosphere diffusion.....	66
8. Table 8. Experimental determinations of water solubility .....	82
9. Table 9. Effect of pressure on the solubility of water.....	86
10. Table 10. Dependence of the equimolar solubility of water on the alkali/aluminum ratio.....	89
11. Table 11. Analyses of starting glasses for partitioning experiments .....	102
12. Table 12. Analyses of the quenched vapor phase.....	107
13. Table 13 Melt/vapor distribution coefficients.....	111





## I. Introduction

### A. Opening comments

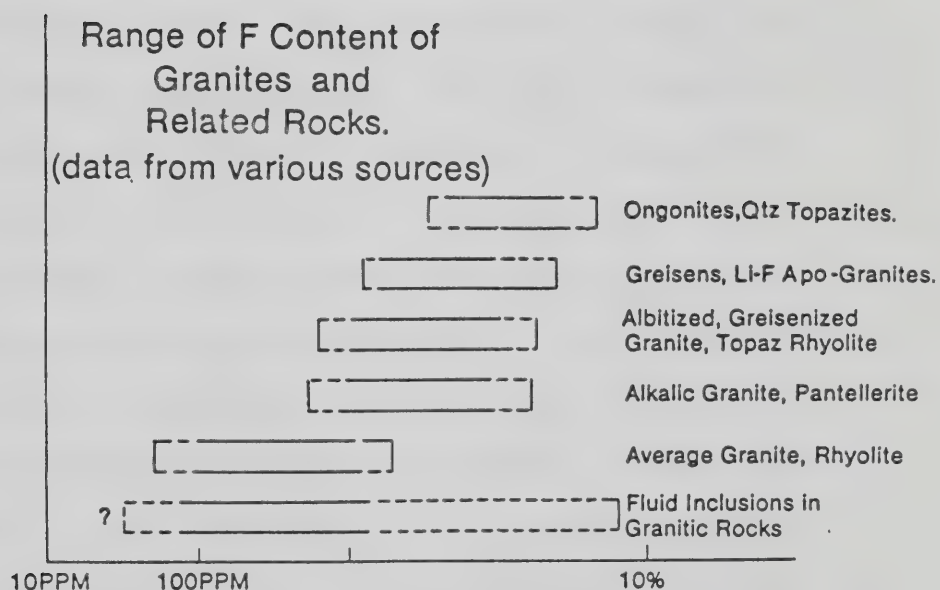
An accurate knowledge of the physical and chemical properties of silicate melts is essential for a discussion of the processes involved in igneous petrogenesis. This thesis contains five investigations into silicate melt properties which have direct consequences for the petrogenesis of many igneous rocks. Fluorine-rich igneous rocks occur in a variety of settings, both intrusive and extrusive, and the chemistry of fluorine-rich magmas can be wet or dry, peralkaline or peraluminous (Bailey, 1977). Typical and extreme ranges of fluorine contents of granitic and related rocks are shown in Figure 1. It is well known that fluorine significantly modifies several of the physical properties of synthetic aluminosilicate melts (see below) and, therefore, it is expected that fluorine-rich geological melts may behave differently than fluorine-free melts of equivalent composition. This thesis comprises a series of studies which investigate the role of fluorine in silicate melts of geologic interest by examining some of the chemical and physical properties of fluorine-bearing melts.

### B. Background

Previous work on the role of fluorine in silicate melts can be grouped into two categories. Firstly, there has been a long discussion in the ceramics literature on the role of



Figure 1. Common and extreme ranges of fluorine contents of granites and related rocks.







fluorine in silicate melts and glasses at one atmosphere. Studies have been conducted on viscosity (Schwerin, 1934; Owens-Illinois Glass Company, 1944; Kozakevitch, 1954; Bills, 1963; Hirayama and Camp, 1969; Rau *et al.*, 1977), electrical conductivity (Shinozaki *et al.*, 1977), infrared and Raman spectroscopy (Kumar *et al.*, 1965; Takusagawa, 1980; Dumas *et al.*, 1982), volatilization (Kumar *et al.*, 1961; Kogarko *et al.*, 1968; Al-Dulaimy, 1978), melting curves (Kogarko and Krigman, 1973) and opalescence (Rothwell, 1956). With the exception of some of the viscosity work, all these studies have been conducted on depolymerized, Al-poor melts. The major conclusion to be drawn from these ceramic studies is that fluorine is incorporated in dry, aluminum-free melts by forming Si-F bonds, replacing the oxygen in Si-O-Si bridges, and resulting in the formation of  $\text{SiO}_3\text{F}$  units (Rabinovich, 1967). Rabinovich (1983) has discussed the consequences of structural reorganization during slow cooling of fluorine-bearing silicate melts (i.e. opalescence) and the increasing volatilization of fluorine as alkali fluorides with decreasing temperature. Studies which suggest the predominance of alkali-fluoride bonds in silicate melts (Kogarko *et al.*, 1968; Kogarko and Krigman, 1973) have probably undergone the type of structural reorganization described by Rabinovich (1983) or have been conducted on extremely alkaline, depolymerized melts.



The second body of data on fluorine in silicate melts comes from extensive phase equilibria work on wet, fluorine-bearing granitic and albite melts (Wyllie and Tuttle, 1961; Koster van Groos and Wyllie, 1968; Anfilogov *et al.*, 1973; Glyuk and Anfilogov, 1973a,b; Danckwerth, 1980; Manning, 1981). Despite the variety of synthetic and natural compositions used, almost all studies report the replacement of feldspar by quartz on the liquidus with sufficient addition of fluorine. This relative increase in quartz stability implies a decrease in the activity of  $\text{NaAlO}_2$ , relative to  $\text{SiO}_2$ , in the melt. Decreased  $\text{NaAlO}_2$  activity is not consistent with the solution of fluorine in these melts by the formation of  $\text{SiO}_3\text{F}$  complexes. Instead, Manning *et al.* (1980) have proposed the formation of Al-F complexes with Al in octahedral coordination.

### C. Objectives

This thesis is an attempt to evaluate the behavior of fluorine and fluorine-bearing melts in simplified chemical systems. The results of these studies are discussed in terms of their implications for the structural role of fluorine in silicate melts and the petrogenesis of fluorine-bearing igneous rocks. The thesis is written in the form of five separate papers (chapters 2 to 6) and therefore each chapter has its own introduction and conclusions. The conclusions of all studies are summarized in chapter 7.



## Viscometry

Chapter 2 is an investigation of the effect of fluorine on melt viscosities in the system  $\text{Na}_2\text{O}-\text{Al}_2\text{O}_3-\text{SiO}_2$ . Viscosity is a property which has been shown to vary greatly with melt composition in simple systems (e.g. Riebling, 1966) and which has been related to melt structure (Mysen *et al.*, 1980). The viscosity of igneous magmas is a critical parameter controlling their physical behavior during coalescence, ascent and emplacement/eruption (Harris *et al.*, 1970). The primary objective of this work was to quantify the viscosity-reducing effect of fluorine on relatively polymerized melts in the system  $\text{Na}_2\text{O}-\text{Al}_2\text{O}_3-\text{SiO}_2$ . The results indicate that the viscosity-reducing effect of fluorine is comparable to that of water. Fluorine and water probably remain stably dissolved in silicate melts by replacement of O in  $\text{Si}-\text{O}-(\text{Si},\text{Al})$  bridges with  $(\text{Si},\text{Al})-\text{F}$  and  $(\text{Si},\text{Al})-\text{OH}$ , respectively. The viscosity-reducing effect of fluorine is greatest in  $\text{SiO}_2$ -rich melts at low temperatures (600-800°C) where viscosity decreases several orders of magnitude with the addition of 1 wt% fluorine.

## Diffusion

Chapters 3 and 4 present data on the diffusivity of fluorine in melts of geologic interest. Diffusivities in silicate melts yield information on the structural nature of ionic transport in melts which can be usefully compared with viscosity and other melt properties to obtain a clearer





understanding of melt structure. The geologic applications of fluorine diffusivity concern bulk diffusion rates in relatively dry, fluorine-rich igneous magmas.

The chemical diffusion of fluorine has been studied at 1 atmosphere in five melts in the system  $\text{Na}_2\text{O}-\text{Al}_2\text{O}_3-\text{SiO}_2$  and at 10 to 15 kilobars in jadeite melt. The diffusion is a binary F-O exchange which is independent of concentration but strongly dependent on melt composition. Both fluorine and water significantly affect the diffusivities of other species in silicate melts and thus the bulk diffusivities of magmas are enhanced by their presence. There are several examples of relatively dry, fluorine-rich geologic melts whose kinetic behavior may be controlled their fluorine contents.

### **Water solubility**

Few properties of silicate melts are more influential in igneous petrogenesis than the solubility of water. Yet the data available for several natural melts contain significant discrepancies. Chapter 5 presents the results of water solubility determinations in haplogranitic melts using a new technique, vacuum fusion manometry. The solubility of water was measured in 1 kilobar thermal minimum, peralkaline and peraluminous granitic melts, in a phonolite melt and in fluorine-bearing granitic melts. Water solubility varies strongly with melt composition. The solubility of water in peralkaline and peraluminous melts is greater than in the 1



kilobar minimum granitic melt and the phonolite melt dissolves twice as much water as granitic melts. The addition of fluorine to the 1 kilobar minimum melt decreases the solubility of water slightly.

### **Melt-fluid partitioning**

The partitioning of elements between a melt and a coexisting fluid phase is a critical parameter in the evolution of magmato-hydrothermal systems.

Chlorine-dominated systems are common but fluorine-rich systems do exist. Chapter 6 reports partitioning data for Na, K, Al and Si in the system haplogranite-HF-H<sub>2</sub>O. Fluorine enhances the solubility of Na, K, Al and Si despite the high melt/fluid partition coefficient of fluorine itself.

Normalized fluid compositions in equilibrium with fluorine-bearing granitic melts are much more Al-rich than comparable chlorine-bearing and boron-bearing fluids. Fluorine does not suppress Al mobility in magmato-hydrothermal systems as chlorine does and therefore fluorine-rich systems can be expected to, and often do, exhibit evidence of extensive Al mobility.

### **Summary**

Chapter 7 is a brief summary of the geological and melt structural implications of the contents of chapters 2 to 6.





## II. Viscometry

### A. Introduction

It is well known in the glass and ceramics literature that the incorporation of fluorine into silicate melts has an important effect on their properties (Weyl, 1950; Eitel, 1965). More specifically, fluorine, as  $\text{CaF}_2$ , has been used in ceramics for several hundred years as a flux to promote fining or bubble removal from glass melts and more recently as a flux to aid the kinetics of slag-iron separation in steelmaking. The ceramics and glass literature contains a large body of data on the effect of fluorine additions to various slag compositions (Schwerin, 1934; Owens-Illinois Glass Company, General Research Laboratory, 1944; Kozakevitch, 1954; Bills, 1963; Hirayama and Camp, 1969). In the geological literature it has been shown that fluorine plays an important role in melt structure and properties (Wyllie and Tuttle, 1961; Manning, 1981).

For these reasons the effect of fluorine on the viscosity of melts in the system  $\text{Na}_2\text{O}-\text{Al}_2\text{O}_3-\text{SiO}_2$  was investigated. Temperature-viscosity relationships of fluorine-bearing melts of albite, jadeite, nepheline, one peralkaline and one peraluminous composition have been measured between 1000-1600°C. The results were then compared with available data from fluorine-free melts in  $\text{Na}_2\text{O}-\text{Al}_2\text{O}_3-\text{SiO}_2$ , with studies on fluorine-bearing slags, and



with data for hydrous rhyolites. From these comparisons it is inferred that (1) reductions in viscosity of polymerized melts occur by substitution of fluorine for bridging oxygens and (2) water and fluorine have similar effects on the viscosities of polymerized melts.

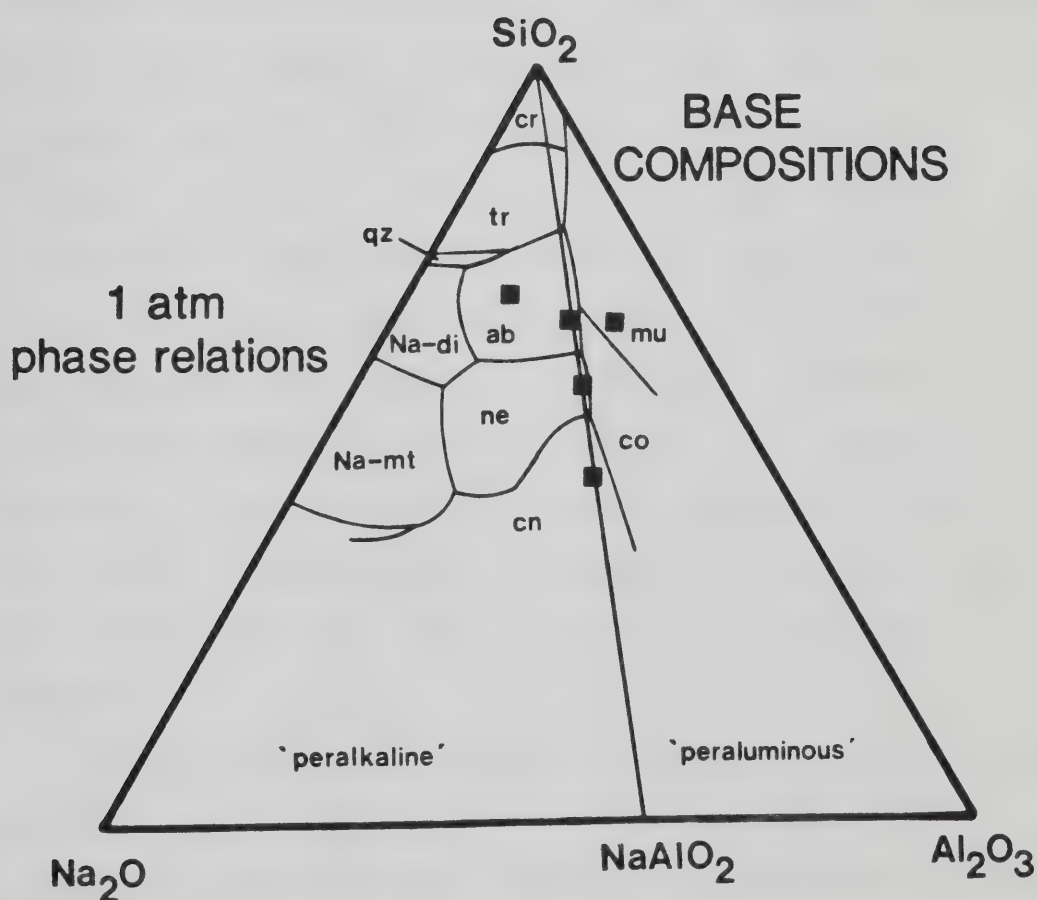
## B. Experimental method

The compositions studied were chosen to evaluate the influence of varying alkali/aluminum ratio and silica content on the viscosity of fluorine-bearing melts. The five base compositions are albite, jadeite, nepheline and two others with 75 mole percent  $\text{SiO}_2$ , one peralkaline and one peraluminous (Fig. 2). The system  $\text{Na}_2\text{O}-\text{Al}_2\text{O}_3-\text{SiO}_2$  was chosen because viscosities in the base system  $\text{Na}_2\text{O}-\text{Al}_2\text{O}_3-\text{SiO}_2$  have been studied by Riebling (1966) and the structure and physical properties of glasses and melts in this system have been investigated (Hunnold and Bruckner, 1979; Taylor and Brown, 1979; Navrotsky *et al.*, 1982; Seifert *et al.*, 1982). The normative compositions of many fluorine-rich igneous melts containing greater than 50 mole percent feldspars + feldspathoids are well represented by this system.

Fluorine was included in the melt compositions by substituting  $2\text{AlF}_3$  for some of the  $\text{Al}_2\text{O}_3$  of the base composition. Thus the substitution is essentially 2 moles of fluorine for one mole of oxygen, denoted by the exchange operator  $\text{F}_2\text{O}_{-1}$ . The starting compositions were synthesized from reagent grade sodium carbonate, alumina, aluminum



Figure 2. Melt compositions projected into  $\text{Na}_2\text{O}-\text{Al}_2\text{O}_3-\text{SiO}_2$ . One atm liquidus phase fields; cristobalite(cr), tridymite(tr), albite(ab), sodium disilicate(Na-di), sodium metasilicate(Na-mt), nepheline(ne), carnegieite(cn), corundum(co) and mullite(mu). The diagram is in weight percent.







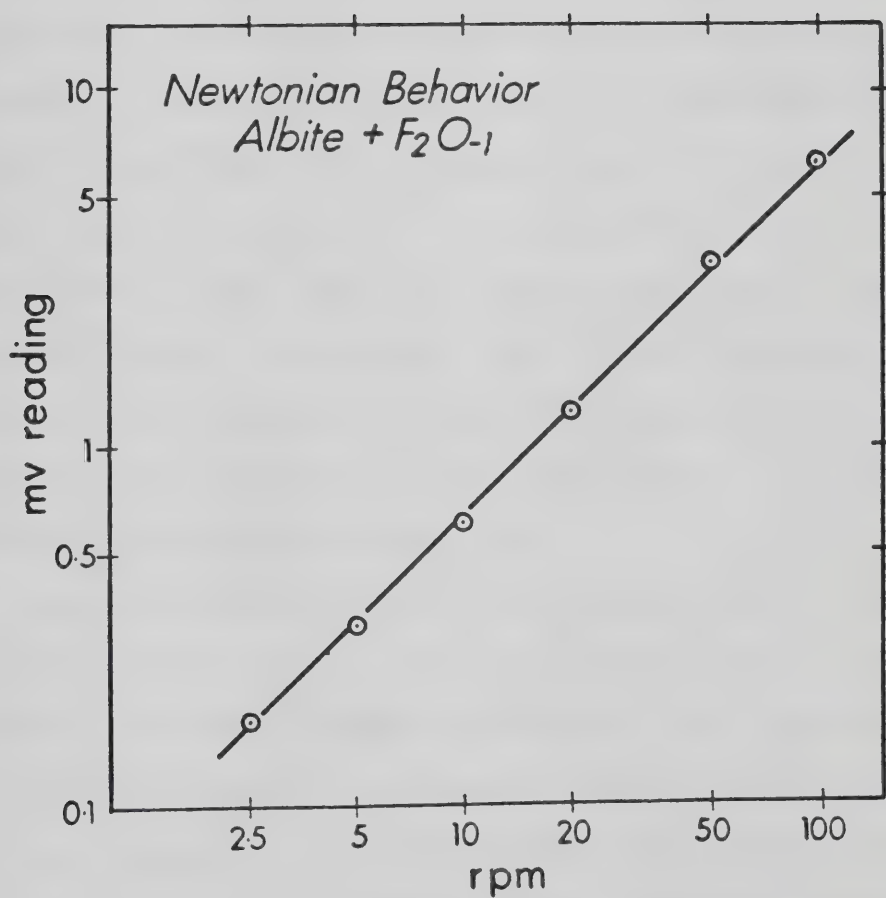
fluoride and purified quartz sand. Carbonate + oxides + fluoride, equivalent to a decarbonated weight of 600 grams, were mixed thoroughly for 12 hours and then fused in a 10.5 cm long by 5.5 cm diameter platinum crucible for 6 to 10 hours at 1600°C to ensure homogeneity and escape of air bubbles.

Viscosities were determined using a concentric cylinder viscometer which uses a Pt90Rh10 inner cylinder 5 cm long and 1.2 cm in diameter with conical ends. The inner cylinder is rotated and the resultant torque is measured and converted into a millivolt signal. The apparatus was calibrated with NBS standard lead-silica glass SRM #711 for which the viscosity-temperature relationship is well known. The viscosities are accurate to  $\pm 5\%$  with a precision of  $\pm 1\%$  and temperatures have uncertainties of  $\pm 1^\circ\text{C}$ . Measurements were made at 50°C intervals over the temperature range 1000-1600°C. Viscosities were independent of shear rate for all compositions (e.g. Fig. 3) indicating Newtonian behavior.

Volatilization of fluorine was significant during melt synthesis but not during viscosity measurement. The viscosity measurements were obtained at successively lower temperatures for each composition and then the highest temperature measurement was repeated. Due to the powerful viscosity-reducing effect of fluorine in these melts, returning to the high temperature data point for each composition is an excellent check for significant fluorine



Figure 3. Newtonian behavior of fluorine-bearing (5.8 wt.%) albite melt (data at 1500°C).





volatilization during measurements. High temperature readings at the start and finish of each set of measurements were within error, indicating that fluorine volatilization during the measurements was insignificant. According to the glass compositions analyzed after viscometry, there was no significant sodium loss.

Na, Al and Si contents of quenched melts (glasses) were determined, after completion of the viscosity measurements, by energy dispersive analysis using an ARL-SEMQ microprobe fitted with an EEDS-ORTEC energy dispersive system. Operating conditions were 15 kV, 4nA sample current and 240 second count times. The beam was rastered over a 20x20 micrometer area, a technique which proved adequate for avoiding volatilization of Na or F during analysis. The homogeneity of glasses was confirmed for Na, Al and Si by analysing six spots on each glass.

Fluorine contents were determined by neutron activation analysis. Twelve replicates of each glass were determined against a curve for reagent-grade  $\text{CaF}_2$ . The technique was verified with standard opal glass SRM #91 (5.72 wt.%F). Fluorine contents were combined with the raw spectra for Na, Al and Si as input for EDATA2 (Smith and Gold, 1979), allowing full ZAF reduction of the Na, Al and Si data (Table 1).





Table 1. Analyzed melt compositions\*

	Na	Al	Si	F	O	Total
Albite	8.31	9.15	31.54	5.8	44.5	99.30
Jadeite	11.17	12.75	26.72	6.3	43.0	99.94
Nepheline	15.97	17.57	19.40	5.2	41.1	99.24
Peralkaline	10.88	5.42	34.09	3.7	45.9	99.99
Peraluminous	6.14	10.87	31.58	5.4	45.5	99.49

\*Na, Al and Si determined by electron microprobe; F determined by neutron activation analysis; O by stoichiometry.

Errors for microprobe data expressed as percent of the amount present at 3 standard deviations: Na (4.3%), Al (2.0%), Si (1.0%).

Errors in fluorine determinations are  $\pm 0.1\text{wt}\%$  F at 1 standard deviation.



### C. Results

Fifty viscosity measurements were made on five compositions. The results are presented in Table 2 and in Figure 4. All five compositions show a log-linear dependence of viscosity on reciprocal temperature. Such behavior is described mathematically by the following Arrhenius equation

$$\log_{10}\eta = \log_{10}\eta_0 + E\eta/2.303RT$$

where  $\eta$  is the viscosity at temperature  $T$  (in K),  $\eta_0$  is a constant,  $R$  is the gas constant and  $E\eta$  is termed the activation energy of viscous flow. The method of least squares was used to fit the data to straight lines (Fig. 4) from which the Arrhenian parameters were determined. Above 1400°C, viscosities of the fluorine-bearing melts decrease in the order peraluminous > albite > jadeite > peralkaline > nepheline. Activation energies of viscous flow of fluorine-bearing melts decrease with increasing  $\text{SiO}_2$  along the join  $\text{NaAlO}_2\text{-SiO}_2$  from nepheline (58.0 kcal/mole) to albite (45.5 kcal/mole), and increase from the peralkaline melt (40.3 kcal/mole) to the peraluminous melt (68.7 kcal/mole) at 75 mole percent  $\text{SiO}_2$ . Different activation energies for the various melts result in two viscosity-temperature curve crossovers within the range of experimental measurements (Fig. 4). As a result, below 1350°C fluorine-bearing jadeite is more viscous than fluorine-bearing albite, and below 1400°C fluorine-bearing



Figure 4. Measured viscosities of fluorine-bearing melts (this study) and base melts (Riebling, 1966). Numbers on curves refer to the wt% of fluorine. Inset: Viscosities of vitreous and fluorine-bearing  $\text{SiO}_2$  (Rau *et al.*, 1977).

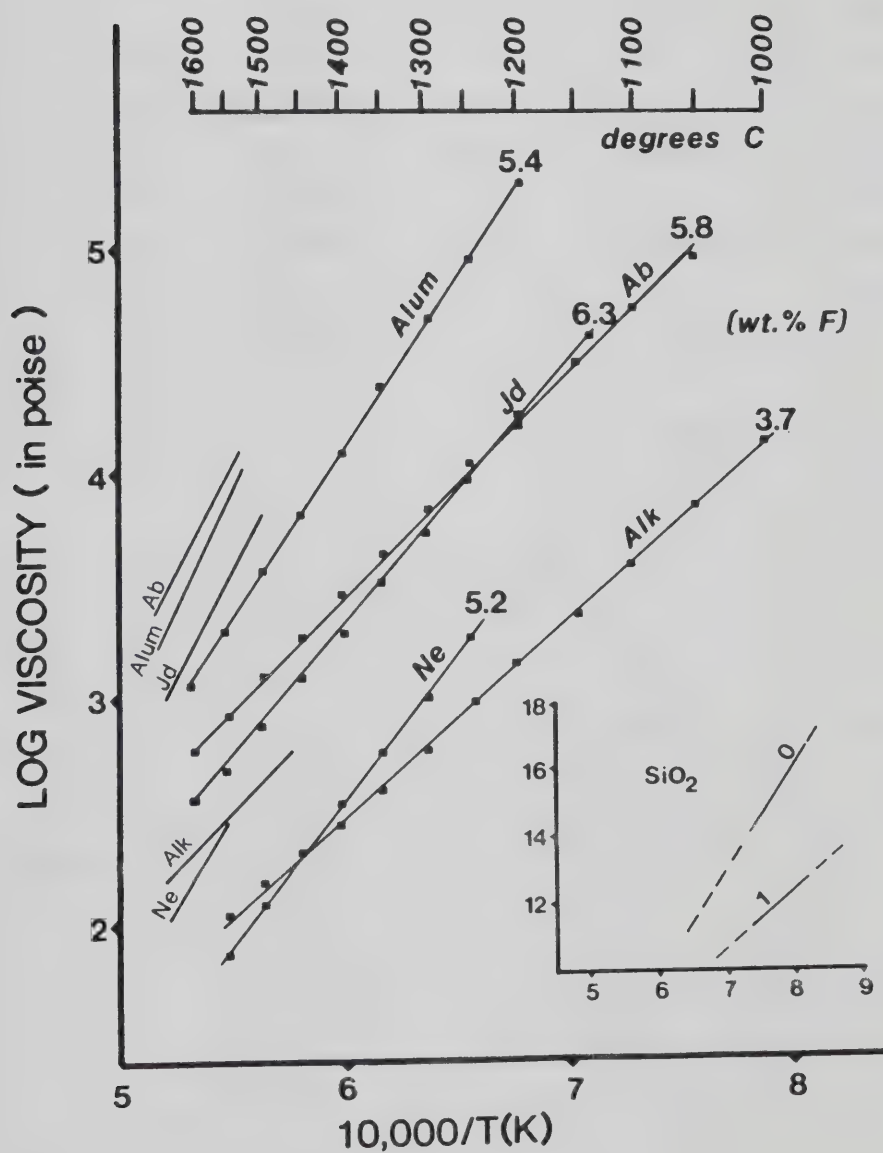






Table 2. Viscosity results and computed Arrhenian parameters

Temperature (degrees C)	Log <sub>10</sub> Viscosity (poise)				
	albite	jadeite	nepheline	peralkaline	peraluminous
1600	2.76	2.45	-	-	3.12
1550	2.93	2.68	1.87	2.04	3.33
1500	3.10	2.88	2.10	2.19	3.58
1450	3.28	3.08	2.31	2.32	3.82
1400	3.46	3.29	2.53	2.44	4.09
1350	3.65	3.51	2.76	2.59	4.38
1300	3.84	3.73	3.00	2.77	4.68
1250	4.05	3.97	3.26	2.97	4.96
1200	4.25	4.21	-	3.16	5.28
1150	4.50	4.62*	-	3.37	-
1100	4.73	-	-	3.60	-
1050	4.96	-	-	3.86	-
1000	-	-	-	4.14	-
Arrhenian parameters					
E <sub>n</sub> **	45.5	55.0	58.0	40.3	68.7
log <sub>10</sub> n <sub>0</sub>	-2.50	-3.92	-5.05	-2.81	-4.89

\* at 1137 degrees C

\*\*(in kcal/mole)



nepheline is more viscous than fluorine-bearing peralkaline melt (Fig. 4).

#### D. Discussion

##### Comparison with previous work.

Discussion of these data is facilitated by comparison with viscosities of equivalent fluorine-free melts in  $\text{Na}_2\text{O}-\text{Al}_2\text{O}_3-\text{SiO}_2$ . In Figure 4 we have included data from Riebling (1966) for the five base compositions and the data of Rau *et al.* (1977) for vitreous silica and fluorine-bearing silica. Figure 4 shows that the addition of fluorine strongly reduces the viscosity and the activation energy of all melts studied. These reductions (denoted  $\Delta\eta$  and  $\Delta E_a$ , respectively) are different in magnitude for each of the base compositions. The lowering of viscosities and activation energies of melts on the join  $\text{NaAlO}_2-\text{SiO}_2$  is a positive function of  $\text{SiO}_2$  content. For example, at  $1400^\circ\text{C}$  the viscosity reduction with the addition of 1 wt% fluorine (by substitution of fluorine for oxygen) to  $\text{SiO}_2$  is  $0.45 \log_{10}$  units. Under equivalent conditions, the viscosities of albite, jadeite and nepheline melts decrease 0.26, 0.19 and  $0.16 \log_{10}$  units/wt.% F, respectively. All activation energies for fluorine-bearing melts are reduced from the values for their fluorine-free counterparts: albite (85.3 kcal/mole), jadeite (86.8



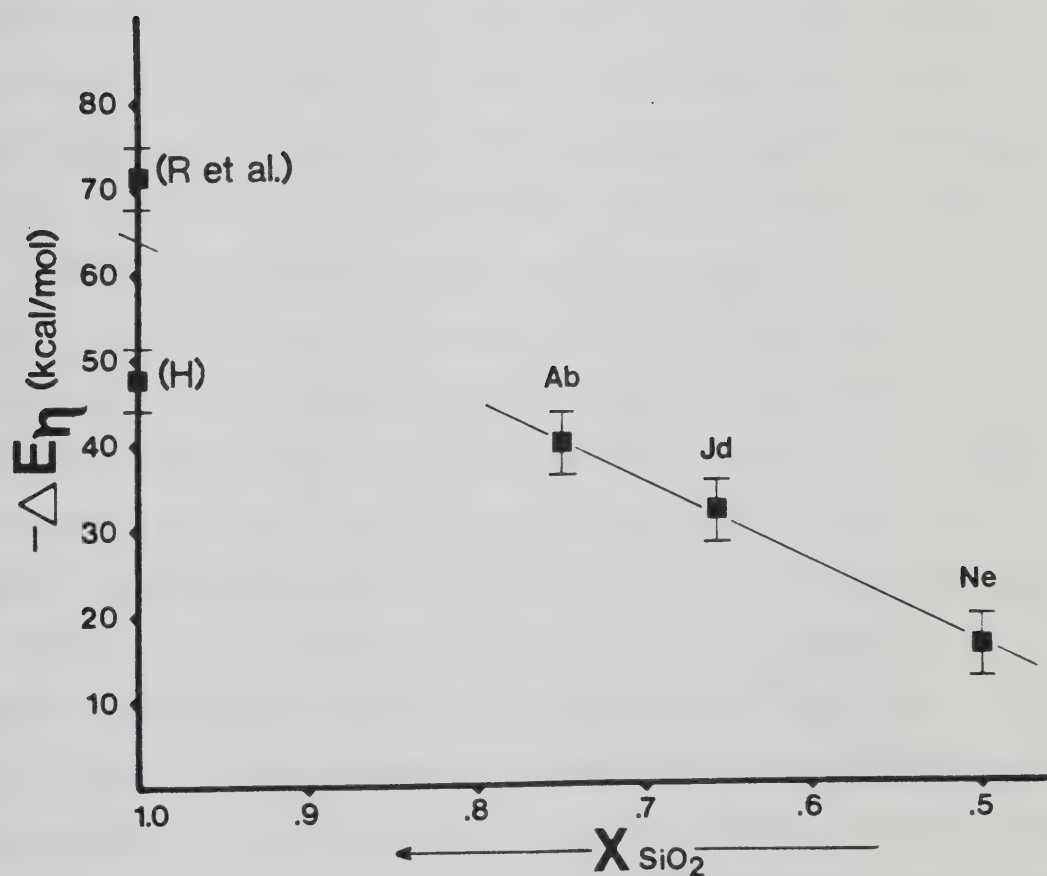
kcal/mole) and nepheline (74.2 kcal/mole) (Riebling, 1966). Interestingly, the decrease in activation energy of these three melts upon addition of fluorine is a linear function of mole fraction of  $\text{SiO}_2/(\text{SiO}_2+\text{NaAlO}_2)$  over the range of 0.5 to 0.75 (Fig. 5). This results in decreasing activation energies with increasing  $\text{SiO}_2$  content from fluorine-bearing nepheline to fluorine-bearing albite. Extrapolation of the line in Figure 5 to  $X(\text{SiO}_2)=1$  is not possible due to the large uncertainty in the activation energy of silica (see Hofmaier and Urbain, 1968) and the possibility that 1 and 6 wt% additions of fluorine may not have an equivalent effect on the activation energy of  $\text{SiO}_2$ . However, the activation energy decrease is larger for the addition of fluorine to silica than for the addition of fluorine to any Al-bearing melts.

The three melts studied at 75 mole percent  $\text{SiO}_2$  are: peralkaline, albite and peraluminous. At  $1400^\circ\text{C}$ , the albite melt undergoes the largest decrease in viscosity ( $0.26 \log_{10}$  units/wt.%F), whereas the peralkaline and peraluminous melts show smaller decreases of 0.16 and 0.14  $\log_{10}$  units/wt.%F, respectively. These three melts all experience decreases in activation energy with fluorine addition, but the peralkaline and peraluminous melts drop only 5 and 16 kcal/mole, respectively, compared to a 40 kcal/mole drop for albite. As a result the viscosities and activation energies increase in the order peraluminous > albite > peralkaline.





Figure 5. Decreases in activation energy of viscous flow ( $\Delta E_\eta$ ) as a function of mole fraction of  $\text{SiO}_2$  (R *et al.*=Rau *et al.*, 1977; H=Hofmaier and Urbain, 1968).



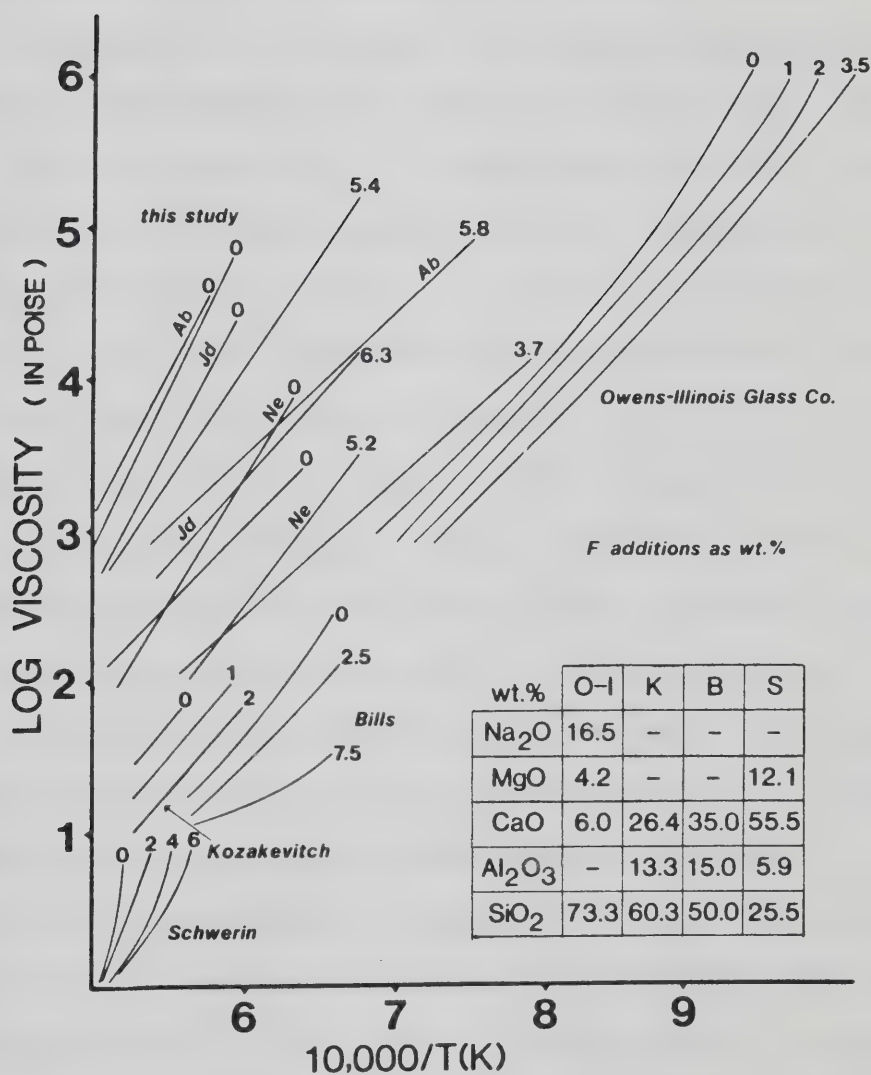


In summary, in order to account for the role of fluorine in melts in the system  $\text{Na}_2\text{O}-\text{Al}_2\text{O}_3-\text{SiO}_2$  any model must explain the following general features: 1) the decrease of all viscosities and activation energies with fluorine addition; 2) the positive dependence of  $dE_n$  and  $dn$  (see above) on  $\text{SiO}_2$  content for melts on the join  $\text{NaAlO}_2-\text{SiO}_2$  and the resulting negative dependence of  $E_n$  on  $\text{SiO}_2$  for fluorine-bearing melts on this join; and 3) the positive dependence of  $E_n$  and  $n$  on  $\text{Al}/\text{Na}$  at constant  $\text{SiO}_2$ , that contrasts with the presence of viscosity maxima at or near  $\text{Al}/\text{Na}$  (molar)=1 for fluorine-free melts (Riebling, 1966).

There have been several studies conducted on the effects of fluorine on viscosities of Al-poor slags (Schwerin, 1934; Owens-Illinois Glass Company, General Research Laboratory, 1944; Kozakevitch, 1954; Bills, 1963; Hirayama and Camp, 1969). The compositions of slags vary widely, especially in silica content (25 to 75 wt%) but, due to insufficient aluminum, none of the melts represents highly polymerized liquids such as those of the join  $\text{NaAlO}_2-\text{SiO}_2$ . Representative compositions and results from these studies are presented in Figure 6 with the results of the present study, thus providing a comparison of the effect of fluorine on polymerized and depolymerized melt viscosities. It is clear in Figure 6 that fluorine decreases the viscosities of all melts studied. However, the decreases in activation energy with fluorine addition are smaller for the depolymerized slags than for the polymerized melts in



Figure 6. Effect of fluorine on melt viscosity for several slag compositions. See text for references. Numbers on curves refer to wt.% fluorine added.







### Structural implications

The three-dimensional structure of melts on the join  $\text{NaAlO}_2\text{-SiO}_2$  has been discussed by several investigators (Riebling, 1966; Hunnold and Bruckner, 1979; Taylor and Brown, 1979; Navrotsky *et al.*, 1982; Seifert *et al.*, 1982). A continuous three-dimensional network of  $(\text{Al},\text{Si})\text{O}_4$  tetrahedra is stabilized by the inclusion of one network modifying Na atom per tetrahedrally coordinated Al atom. In such a structure all oxygen is bonded to two tetrahedrally-coordinated, network-forming cations to form oxygen bridges. In contrast, melts in  $\text{Na}_2\text{O}-\text{Al}_2\text{O}_3-\text{SiO}_2$  whose compositions lie off the join  $\text{NaAlO}_2\text{-SiO}_2$ , whether they are peralkaline or peraluminous, cannot maintain the structure of an uninterrupted three-dimensional network. These melts probably contain a discontinuous three-dimensional network perturbed by the presence of excess Na or Al atoms, coordinated by nonbridging oxygens (NBO) (Mysen *et al.*, 1980). The degree of polymerization of aluminosilicate melts may be represented by the ratio of NBO/T (where T represents a tetrahedrally-coordinated cation ; Mysen *et al.*, 1982). Analyses of the melts along the join  $\text{NaAlO}_2\text{-SiO}_2$  yield base compositions (projected from  $\text{F}_2\text{O}$ , (molar)) with NBO/T values close to zero (albite = 0.013; jadeite = 0.008; nepheline = 0.032). The peralkaline base composition yields NBO/T =





0.193. The peraluminous composition is difficult to deal with using the calculation procedure of Mysen *et al.* (1982) because of the uncertainty in assigning some or all of the aluminum to the value of T. If we assume as a limiting case that each tetrahedrally coordinated Al atom requires a Na atom for stabilization, then the maximum NBO/T for the peraluminous composition is 0.292. Viscosities in  $\text{Na}_2\text{O}-\text{Al}_2\text{O}_3-\text{SiO}_2$  (Riebling, 1966) appear to reflect the structural characteristics of these melts quite well. The presence of viscosity maxima at or near Na/Al (molar) = 1 along joins of constant silica content in  $\text{Na}_2\text{O}-\text{Al}_2\text{O}_3-\text{SiO}_2$  (Riebling, 1966) imply that at the 1:1 composition melts are completely polymerized (i.e. all Al is in tetrahedral coordination; Hunnold and Bruckner, 1979).

The viscous flow of pure silica involves an activation energy similar to the Si-O bond strength of Si-O-Si bridging bonds and thus viscous flow in  $\text{SiO}_2$  is thought to proceed by the breakage of such bridging bonds (Bockris and Reddy, 1970). Melts along the join  $\text{NaAlO}_2-\text{SiO}_2$  also require the breakage of bridging oxygen bonds but the average T-O-T bond strength is lowered from that of pure  $\text{SiO}_2$ . Peralkaline and peraluminous melts in  $\text{Na}_2\text{O}-\text{Al}_2\text{O}_3-\text{SiO}_2$  probably owe their lower viscosities to the smaller average size of flow units. Their lower activation energies may be due to a decrease in the number of bond breakages required for viscous flow.

Fluorine substitutes for oxygen in silicate melts (Rabinovich, 1983). If oxygen occurs in melts on the join



$\text{NaAlO}_2\text{-SiO}_2$  entirely as  $\text{Si-O-(Si,Al)}$  bridges, then fluorine must break oxygen bridges. It is clear from the viscosity data for fluorine-bearing silica (Rau *et al.*, 1977) that the exchange of  $\text{Si-O-Si}$  bridges for  $\text{Si-F}$  bonds occurs with a drastic change of melt viscosity (Fig. 4, inset). However, for melts along the join  $\text{NaAlO}_2\text{-SiO}_2$  the question is whether  $\text{Al-O}$  or  $\text{Si-O}$  bonds, or both, are the primary target for fluorine substitution. Fluorine-free melts have decreasing viscosities in the order albite > jadeite > nepheline, but similar activation energies (Riebling, 1966). The magnitude of the effect of fluorine on both activation energies and viscosities of melts on the join  $\text{NaAlO}_2\text{-SiO}_2$  is a positive function of  $\text{SiO}_2$  content. Figure 5 therefore supports the proposal that the decreasing efficiency of activation energy reduction with decreasing  $\text{SiO}_2$  content is a result of the decrease in the proportion of  $\text{Si-O-Si}$  bridges in these melts.

The three melts at 75 mole percent  $\text{SiO}_2$  vary in  $\text{Al/Na}$  and their viscosities and activation energies increase with  $\text{Al/Na}$ . Apparently the addition of fluorine to melts along this join eliminates the viscosity maximum at or near  $\text{Al/Na}=1$  for fluorine-free melts. Fluorine in the peralkaline and peraluminous melts may be substituting for non-bridging or bridging oxygens.

Breakage of  $\text{Si-O-Si}$  bridges can also explain the effect of fluorine on the viscosities of depolymerized melts such as those included in Figure 6. Melts shown in Figure 6 have



NBO/T ranging to 4.7 and thus are more depolymerized than the melts investigated in this study. Despite their calculated values of NBO/T, the  $\text{SiO}_2$ -poor melts probably contain some bridging oxygens (Gotz *et al.*, 1976; Smart and Glasser, 1978). Reduction of viscosities by fluorine addition to these melts may result from substitution of fluorine for bridging or nonbridging oxygens.

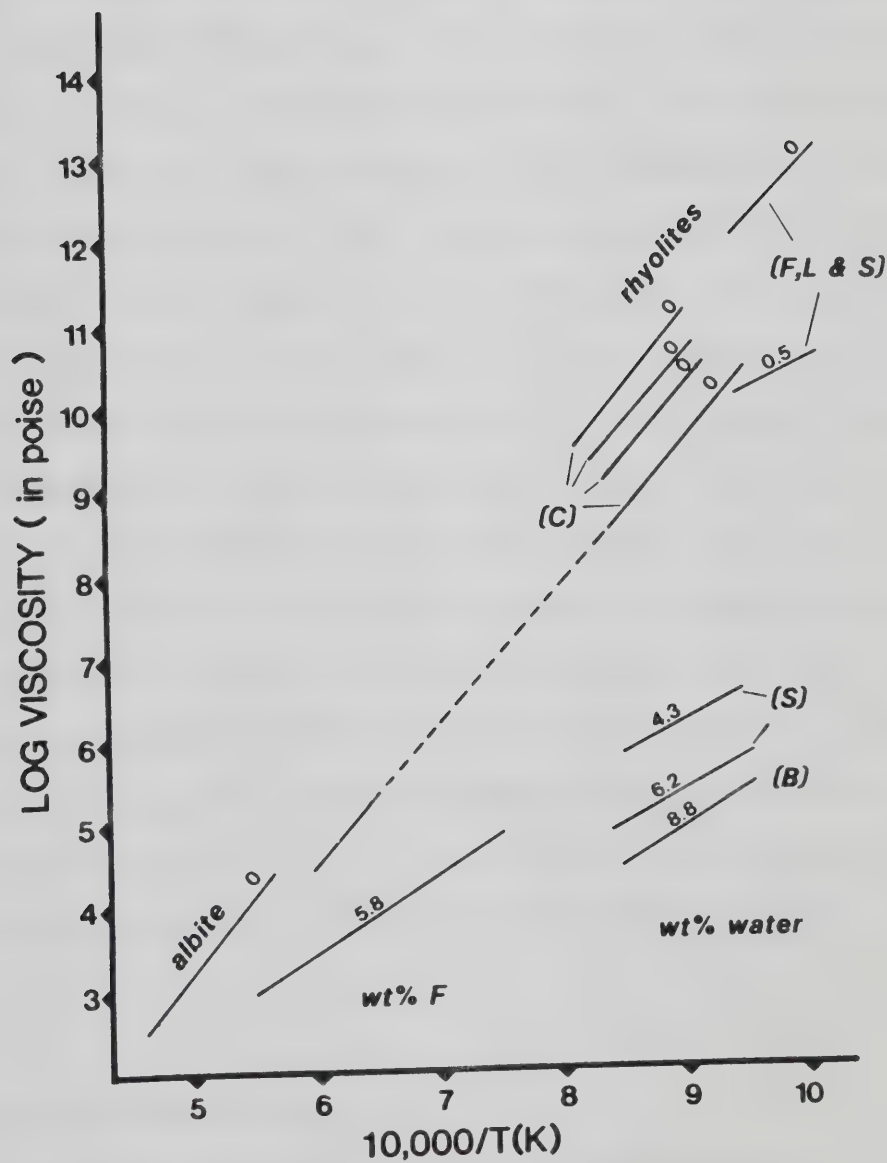
### Comparison with water

Water has a strong influence on the viscosity of silicate melts (Shaw, 1963; Friedman *et al.*, 1963; Burnham, 1964; Scarfe, 1973). The similar size and charge of  $\text{F}^-$  and  $\text{OH}^-$  ions encourage comparison of their effects. We would prefer to compare the influences of water and fluorine on identical melt compositions; however, the data do not exist. Figure 7 contains viscosity-temperature curves for dry and wet rhyolites (Shaw, 1963; Friedman *et al.*, 1963; Carron, 1969), a wet pegmatite (Burnham, 1964), albite (Riebling, 1966) and fluorine-bearing albite (this study). Activation energies decrease similarly with addition of fluorine to albite and addition of water to rhyolite. This implies similar roles for fluorine and water in the depolymerization and resulting reduction of viscosity in these polymerized melts (Fig. 7). The magnitude of viscosity reduction is a much more difficult comparison. If we select a dry rhyolite curve to coincide with the albite curve then the reduction





Figure 7. Comparison of the effects of water and fluorine on polymerized melt viscosities. Numbers on curves refer to wt.% of fluorine or water. See text for data sources. (S=Shaw, 1963; B=Burnham, 1964; F,L & S=Friedman, Long and Smith, 1963)





of viscosity (normalized on a weight percent or mole percent basis of added water or fluorine) is slightly greater for the addition of water to rhyolite than for the addition of fluorine to albite. However, recalling the positive relationship between  $\text{SiO}_2$  content and the viscosity-reducing power of fluorine (Fig. 5), it is likely that comparison of two rhyolites rather than albite and rhyolite would remove this discrepancy (note that converting from weight to mole percent does not significantly alter comparisons between fluorine and water as their molecular weights are 19.0 and 18.0 grams/mole, respectively). Therefore, the conclusion from comparison of water and fluorine is that one mole of fluorine is structurally analogous to one mole of water in depolymerizing highly polymerized melts. The equivalence of the viscosity reductions strongly implies that  $\text{H}_2\text{O}$  and fluorine disrupt an equivalent number of oxygen bridges when incorporated in highly polymerized melts. The effect of fluorine on hydrous melt viscosities cannot be discussed at this time because, with the exception of the Harding pegmatite (0.33 wt.% F, 8.8 wt.%  $\text{H}_2\text{O}$ ), there are no data on the viscosities of fluorine-bearing hydrous melts.

### Geological applications

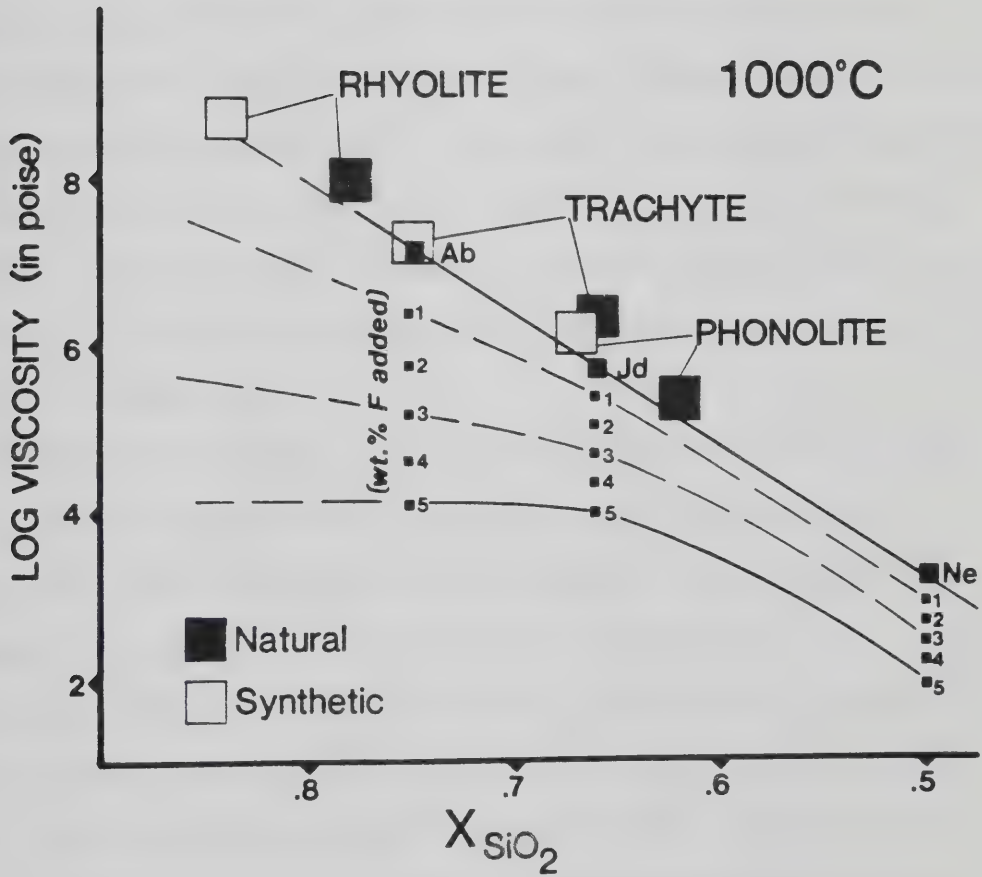
Many volcanic rocks have anhydrous chemical compositions very close to the compositional plane  $\text{KAlSiO}_4\text{-NaAlSiO}_4\text{-SiO}_2$ . In particular, "average" compositions



of phonolites, trachytes and rhyolites (Cox *et al.*, 1979, p.401) have values of  $K_2O+Na_2O+Al_2O_3+SiO_2$  near 90 weight percent. Thus the bulk physical properties of melts in the system  $K_2O-Na_2O-Al_2O_3-SiO_2$  closely resemble the properties of these natural melts. Also, the molar effects of  $K_2O$  and  $Na_2O$  on melt viscosities are similar and  $K_2O+Na_2O$  (molar) is a single parameter in Shaw's (1972) scheme for calculation of natural melt viscosities. The molar equivalence of  $Na_2O$  and  $K_2O$  means that the system  $K_2O-Na_2O-Al_2O_3-SiO_2$  may be effectively reduced to the simpler system  $Na_2O-Al_2O_3-SiO_2$  that is used as a basis for this investigation. These arguments allow application of these results to natural melts. In the previous discussion, the importance of  $SiO_2$  content in determining the ability of fluorine to reduce viscosities was discussed. The observation that the magnitude of the reduction in viscosity is positively correlated with  $SiO_2$  is illustrated in Figure 8, where  $\log_{10}$  viscosity is plotted versus mole fraction  $SiO_2$  for several compositions. Rather than plot a mixture of experimental and calculated viscosities in Figure 8, all viscosities were calculated using the method of Shaw (1972). Figure 8 contains melt compositions expressed in terms of their mole fraction of  $SiO_2$ . All natural and synthetic melts were cast into desilicated norms (composed of  $SiO_2$ ,  $NaAlO_2$ ,  $CaAl_2O_4$ ,  $FeO$ ,  $MgO$ , etc.) from which mole fractions of  $SiO_2$  ( $SiO_2/(SiO_2+NaAlO_2+KAlO_2+CaAl_2O_4, \text{etc.})$ ) were obtained. The synthetic phonolite, trachyte and rhyolite are anhydrous



Figure 8. Application of experimental results to synthetic and natural melts. The effect of fluorine content on melt viscosity for rhyolites, trachytes and phonolites at eruption temperatures near 1000°C. See text for explanation.







projections of the 1 kbar thermal minima in the system  $\text{KAlSiO}_4\text{-NaAlSiO}_4\text{-SiO}_2\text{-H}_2\text{O}$  (Tuttle and Bowen, 1958; Hamilton and MacKenzie, 1965) and the three natural compositions are "averages" from Cox *et al.*, (1979). The lines labelled 1, 2, 3, 4 and 5 represent viscosity decreases with weight percent additions of fluorine that are derived from linear interpolation of the data of this study. At an eruption temperature of 1000°C the viscosities of phonolites, trachytes and rhyolites containing 1 weight percent fluorine will be approximately 0.25, 0.5 and 1 orders of magnitude lower than the viscosities of equivalent fluorine-free melts. In comparison, strongly peraluminous or peralkaline melts will experience a smaller influence of fluorine on their viscosities.

The most dramatic effects of fluorine addition will be felt in relatively dry, fluorine-rich, high-silica rhyolites. Pre-eruption water contents of many silicic magmas may be lost during degassing immediately prior to eruption (Sparks, 1978). Due to a high melt/fluid partition coefficient (Hards, 1978), fluorine will be retained in the melt. Fluorine remaining in erupted lavas will maintain low viscosities. In certain cases fluorine may significantly influence eruptive style enhancing fluid flow and strongly reducing the pyroclastic component of a given eruption. Fluorine-rich topaz rhyolites exhibit just such features (Christiansen *et al.*, 1983).



Fluorine-rich intrusive rocks occur in a wide variety of settings. The rates of crystal settling and bubble ascent in such intrusions will be enhanced by high fluorine contents. The relatively dry magmas which form fluorine-rich alkalic intrusives will experience reduced viscosities as outlined above. The water-saturated emplacement of fluorine-rich melts such as Li-F leucogranites and associated pegmatites (Bailey, 1977; Manning, 1981) may be significantly more fluid due to an additive effect of fluorine and water on the viscosities of such melts. At the greater depths and lower temperatures associated with water-saturated emplacement of leucogranitic melts the distinction between low viscosity fluorine-rich, water-saturated melts and coexisting fluids may be diminished. This distinction is the subject of considerable controversy regarding the magmatic or hydrothermal origin of certain late-stage fluorine- and water-rich cupolas and dykes (e.g. Kovalenko, 1973; Eadington and Nashar, 1978).

#### **E. Summary and conclusions**

It has been shown that the addition of fluorine to melts in the system  $\text{Na}_2\text{O}-\text{Al}_2\text{O}_3-\text{SiO}_2$  strongly reduces viscosities and activation energies. Viscosities of fluorine-bearing aluminosilicate melts are Arrhenian functions of temperature. The viscosity-lowering effect of fluorine increases with increasing  $\text{SiO}_2$  content along the join  $\text{NaAlO}_2-\text{SiO}_2$  and is a maximum at or near Na/Al (molar)



=1 for melts containing 75 mole %  $\text{SiO}_2$ . The most probable explanation for viscosity decrease is depolymerization of melts by replacement of  $\text{Si-O-(Si,Al)}$  bridges with  $\text{Si-F}$  bonds. When the effects of water and fluorine are compared, similar reductions in viscosities and activation energies suggest similar mechanisms of melt depolymerization. The most important implications of this work concern relatively dry, crystal-poor, magmas of phonolite, trachyte and rhyolite composition and their intrusive equivalents, both wet and dry. Due to the activation energy decreases, the viscosity-lowering effect of fluorine will be greater at the lower temperatures associated with water-saturated emplacement of igneous melts at depth. It is possible that the effects of fluorine and water might be additive, resulting in extremely large viscosity reductions for certain melts.





### III. High pressure diffusion

#### A. Introduction

A knowledge of the transport properties of melts of geologic interest is required in order to model their behavior during petrogenetic processes. In particular, cationic and anionic diffusivities in silicate melts allow us to relate time, temperature, and physical scale in processes where diffusion is the rate-limiting step. Examples of such igneous processes include both melt-vapor and melt-crystal interactions (e.g. growth of zoned minerals, vapor phase transport of dissolved metals during magma degassing, crustal assimilation) and intra-melt processes such as thermogravitational diffusion and double-diffusive convection.

Fluorine, like water, has a considerable effect on many properties of silicate melts including viscosities (chapter 1), phase equilibria (Manning *et al.*, 1980), melt-vapor partitioning (Hards, 1978), and, as discussed below, component diffusivities in the melt. The occurrence of fluorine-rich amphiboles and micas in the lower crust and upper mantle (Smith *et al.*, 1981; Valley *et al.*, 1982) and the suggestion that many relatively dry, fluorine-rich, melts originate from these regions (Harris and Marriner, 1980; Burt *et al.*, 1982) indicate the need for a better understanding of the role of fluorine in melts at high



pressures. Such considerations, along with the potential for insights into the structure of F- and H<sub>2</sub>O-bearing melts, prompted this study. Jadeite melt was chosen for this study because it has been used as a model for polymerized silicate melts in several studies (e.g. melt viscosity, Kushiro (1976); oxygen diffusivity, Shimizu and Kushiro (1984); cationic diffusivities, Kushiro (1983); Raman spectra, Sharma *et al.* (1979), Seifert *et al.* (1982); fluorine-bearing melt viscosity, chapter 1).

## B. Experimental method

The starting materials were (1) fluorine-bearing jadeite glass prepared from reagent-grade sodium carbonate, alumina, aluminum fluoride and purified quartz sand and (2) jadeite glass prepared from a gel, dehydrated at 800°C for two hours. These starting glasses were analyzed for Na, Al and Si by energy dispersive analysis using an ARL SEMQ microprobe fitted with an EEDS-ORTEC energy dispersive spectrometer. Operating conditions were 15 kV accelerating voltage, 4 nA sample current and 240 sec counting time. The fluorine content of the fluorine-bearing starting glass was determined by neutron activation analysis as described in chapter 1. Analyses of the starting glasses are presented in Table 3.

The diffusion couple technique of Kushiro (1983) was used for this study. Glasses were ground in an agate mortar



Table 3 . Analyses of starting glasses\*

Element	Jadeite	Fluorine-bearing Jadeite	Stoichiometric Jadeite
Na	11.15	11.17	11.33
Al	13.34	12.75	13.34
Si	27.92	26.72	27.79
O	47.56	43.00	47.54
F	-	6.3	-
TOTAL	99.97	99.94	100.00

a, Al and Si determined by electron microprobe; F determined by neutron activation analysis; O by stoichiometry.  
 errors for microprobe data expressed as percent of the amount present  
 3 standard deviations: Na (4.3%), Al (2.0%), Si (1.0%).  
 errors in fluorine analysis are  $\pm 0.1$  wt% F at 1 standard deviation.



and packed into (5 mm diameter by 8-10 mm length) platinum capsules using a tight-fitting, stainless steel tool. The denser, fluorine-free powder was packed into the capsules first and occupied the lower end of the vertical diffusion couple in all experiments. Packed and crimped capsules were dried at 800°C for 10 minutes and immediately welded. Sealed capsules were packed with hematite powder into 3/4 inch furnace assemblies with tapered graphite heaters, which reduce the temperature gradient along the 10 mm capsule to 15°C (Kushiro, 1976). The hematite acts as a trap for any water diffusing into the charge from the assembly. The assemblies were stored in a drying oven at 110°C prior to use.

Temperatures were monitored with a Pt/Pt13Rh thermocouple without any correction for pressure, and are believed accurate to better than  $\pm 10^\circ\text{C}$ . Pressures were monitored continuously with a Heise gauge and were accurate to within  $\pm 0.5$  kbars. Pressure calibrations (by DTA) were performed using the melting curve of NaCl (Clark, 1959) and a pressure correction of -7% was applied to all runs.

Run durations were one hour with the exception of a zero-time experiment and one 1/2 hour experiment (run numbers 12 and 10 (Table 2), respectively). The zero-time experiment provided confirmation of an initially flat interface. Runs were quenched by switching off the power to the heater resulting in quench rates of approximately 125°C/sec. Quenched runs (encased in coarsely recrystallized





specular hematite) were set in epoxy and sliced in half longitudinally. The platinum capsules preserved their cylindrical form with only minor necking during the run. Thin sections of the charges were examined optically revealing colorless, transparent glasses with no crystals (even for one run conducted below the liquidus of jadeite at 1200°C and 15 kbars). The melt couple interfaces were optically invisible.

The charges were analyzed after each experiment for Na, Al and Si by the energy dispersive technique described above and for fluorine by wavelength dispersive analysis. Fluorine analyses were standardized to a sample of the original fluorine-bearing jadeite glass. This glass had been analyzed against NBS opal glass SRM #91 by neutron activation analysis (chapter 1). The use of a fluorine standard with the same matrix composition as the analyzed samples minimizes errors associated with poor ZAF correction factors for fluorine.

Wavelength dispersive analysis for fluorine required a sample current of 40 nA to achieve reasonable count rates (approximately 40 cps/wt% F). Therefore, in order to avoid significant volatilization during fluorine analysis two techniques were employed. In the first case, a point beam was moved continuously, perpendicular to the profile, covering a distance of 50 micrometers in 100 seconds. In the second case, the beam was rastered over a 10 x 10 micrometer area for 100 seconds. The fluorine totals normalized to the



standard were identical for both techniques and chart recordings showed that no significant volatilization of fluorine occurred during the stationary analyses. Fluorine (WDA) and Na, Al and Si (EDA) spectra were combined and reduced using EDATA2 (Smith and Gold, 1979).

### C. Results

This study involves chemical diffusion. Therefore, before the data are discussed and comparisons are made, we must distinguish between three categories of diffusion, namely, tracer, self and chemical diffusion. Self-diffusion is the diffusion of a single chemical species in the absence of a chemical gradient. This type of diffusion is usually investigated by labelling some of the diffusing atoms with an isotopic tracer (e.g. Shimizu and Kushiro, 1984). Tracer diffusion is the diffusion of an individual species in the presence of a small but finite chemical gradient. The tracer is usually a radioisotope (e.g. Watson, 1979) and the tracer concentration is so small that no significant concentration gradients result for any of the other melt components. Chemical diffusion is the diffusion of two or more species in response to a chemical activity gradient (e.g. Kushiro, 1983). Tracer and self-diffusion are practically equivalent for natural melts and usually represent minimum diffusivities for the components being studied because there is no large chemical activity gradient to serve as a driving



force for diffusion. The similarity of tracer and self-diffusion is evidenced by the fact that they are both described mathematically by the single component form of Fick's first and second laws (Crank, 1975; Hofmann, 1980). In a general sense, chemical diffusion is a multicomponent phenomenon, but it may be approximated to a binary interdiffusion process when the chemical activity gradient for all other species (and the resulting diffusion of these species) is insignificant. For such cases, an effective binary diffusion coefficient (EBDC) may be obtained (Cooper, 1968) and we may talk in terms of a binary interdiffusion coefficient.

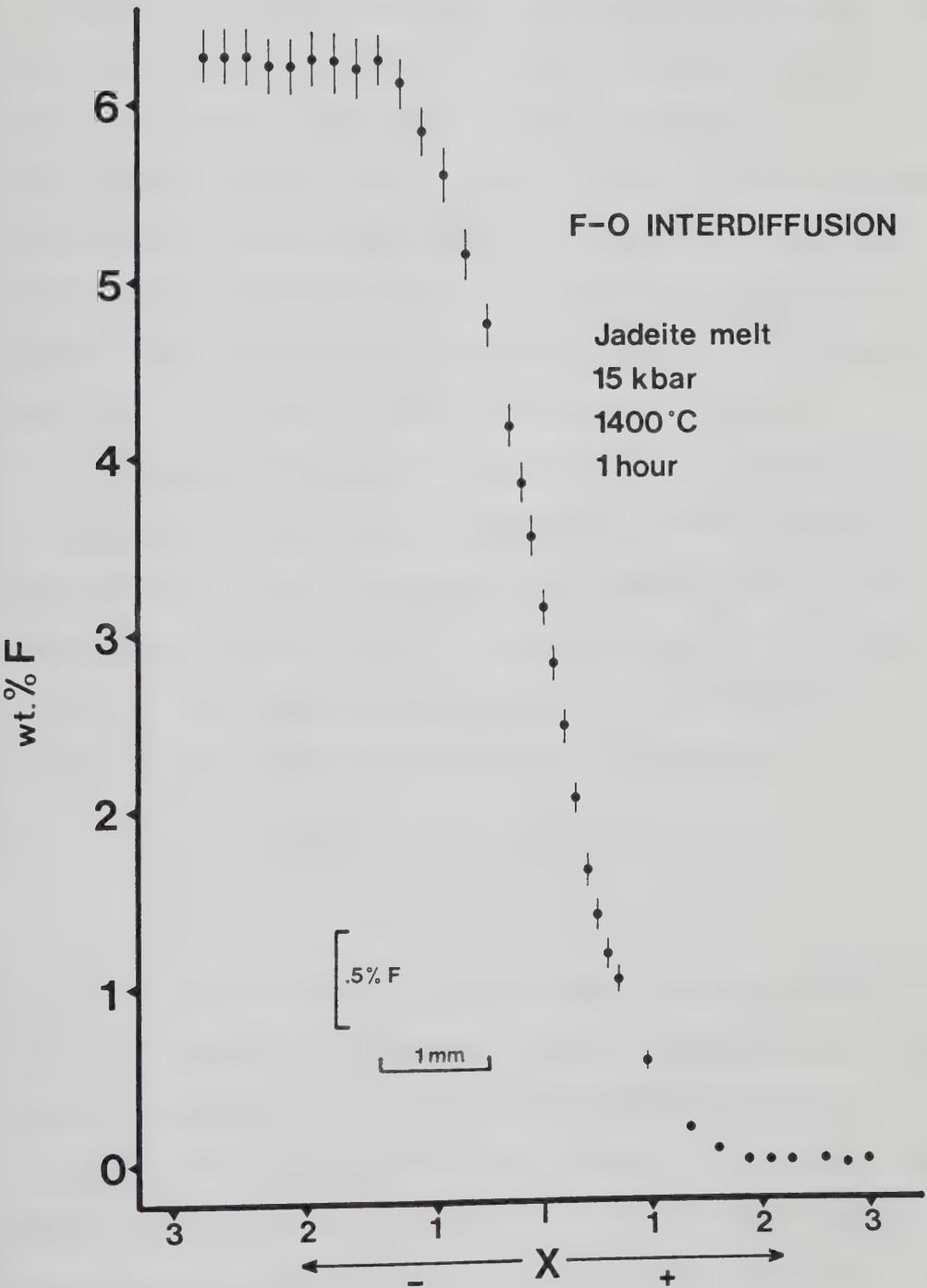
In the present study, quantitative analyses for Na, Al and Si revealed no concentration gradients for these elements, indicating that the diffusion process could be approximated by binary interdiffusion of fluorine and oxygen. Therefore, diffusion profiles of fluorine (Fig. 9) were fitted to the following form of equation (Crank, 1975):

$$\frac{x}{2\sqrt{Dt}} = \text{erf}^{-1} \left[ \frac{2C - (C_1 + C_2)}{C_1 - C_2} \right]$$

where  $D$  is the interdiffusion coefficient ( $\text{cm}^2/\text{sec}$ ),  $t$  is time (seconds) and  $C$ ,  $C_1$  and  $C_2$  are the concentration at distance  $x$ , the maximum and the minimum concentrations of fluorine, respectively.  $\text{Erf}^{-1}$  is the inverse of the error function. The interface ( $x=0$ ) was optically invisible and, therefore, the half maximum of the diffusion profile was



Figure 9. Diffusion profile of fluorine in jadeite melt.







chosen to represent the interface. This choice was confirmed by the fit of the error function (Fig. 10). Identical diffusion profiles at several locations across each charge ruled out the possibility of significant deformation of the interface during individual runs. Plotting  $\text{erf}^{-1}((C-(C_1+C_2))/(C_1-C_2))$  vs.  $x$  (Fig. 10) yields linear plots whose slopes equal  $1/2\sqrt{Dt}$ . A linear dependence of  $\text{erf}^{-1}((C-(C_1+C_2))/(C_1-C_2))$  on  $x$  indicates that the diffusion process is independent of concentration. The values of  $D$  obtained from each run are presented in Table 4.

The data of Figure 11 show increasing diffusivity of fluorine with increasing temperature. If we assume a linear dependence of  $\log D$  on reciprocal temperature, we may fit the data of Table 4 to an Arrhenius equation for each pressure. The temperature dependence of diffusion is represented by the following form of equation:

$$\log_{10} D = \log_{10} D_0 - E_a/2.303RT$$

where  $D$  is the diffusion coefficient at temperature  $T$  (K),  $D_0$  is the Arrhenius frequency factor,  $R$  is the gas constant and  $E_a$  is termed the Arrhenian activation energy of diffusion. The results of least squares fits to the data in Table 4 are presented in Table 5. F-O interdiffusion activation energies range from 36 to 39 kcal/mole.

The pressure dependence of diffusion may be linearly approximated by an Arrhenius equation of the



Figure 10. Reduced diffusion profile using equation (1) and data from fluorine-rich (triangles) and fluorine poor (inverted triangles), limbs of the diffusion profile. The slope corresponds to  $1/2\sqrt{Dt}$  (Data from run no. 3).

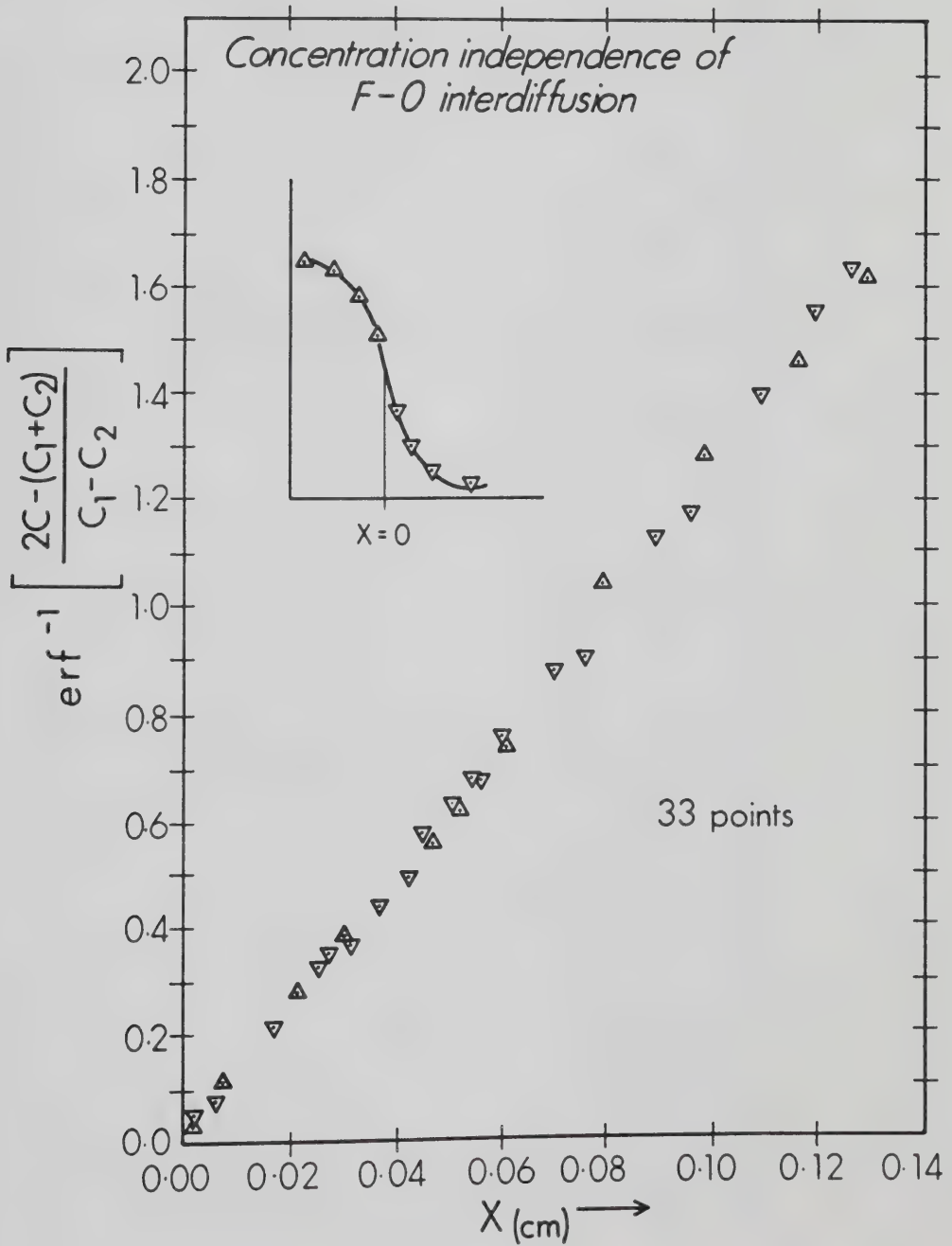




Figure 11. Diffusion data for 10, 12.5 and 15 kbars and computed Arrhenius parameters.

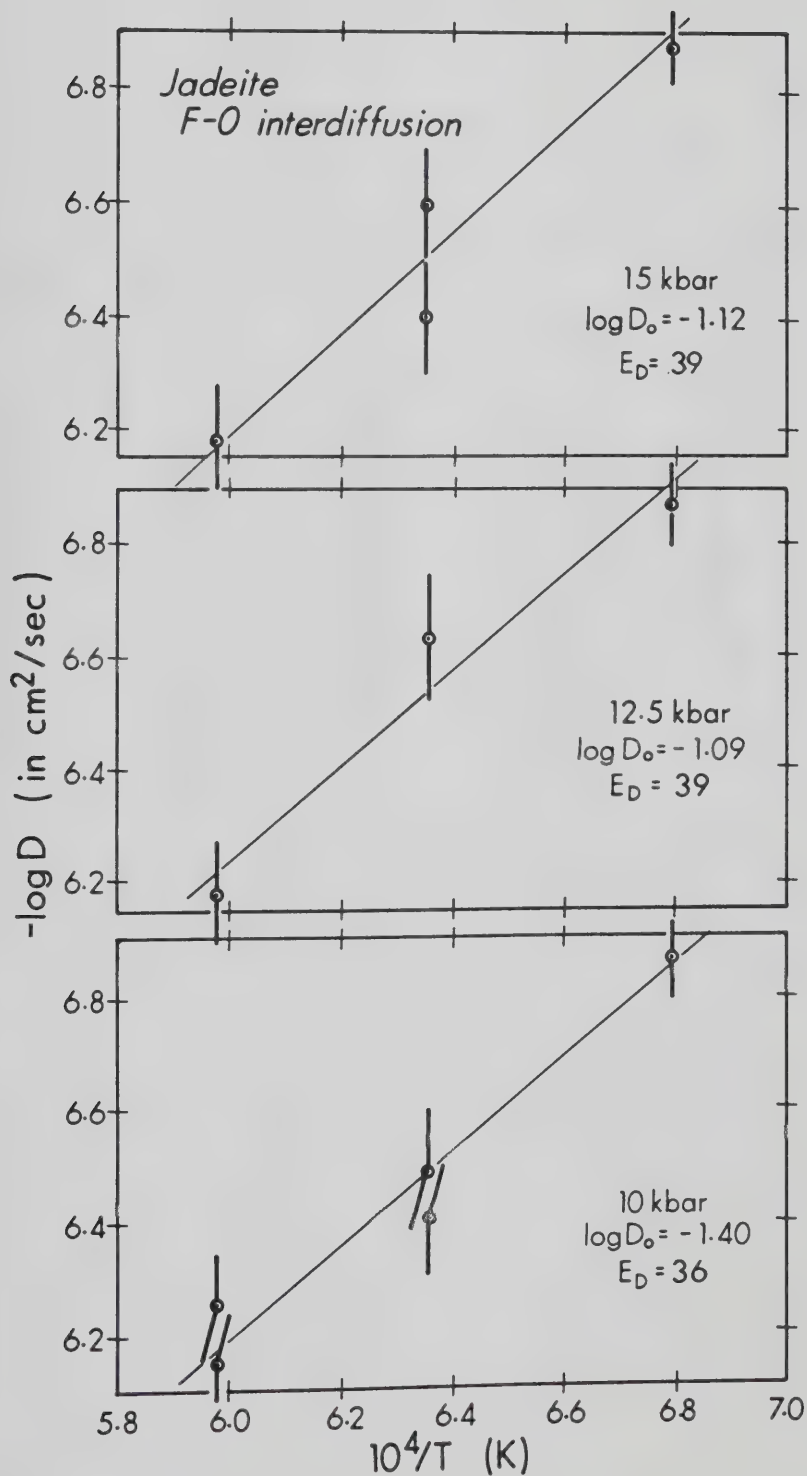




Table 4. Experimental conditions and results

Run	Temperature (°C)	Pressure (kbars)	Duration (sec)	$\log D_T$ (cm <sup>2</sup> /sec)	# of points
1	1400	15	3600	-6.18±.04	16
2	1200	15	3600	-6.87±.03	25
3	1300	15	3600	-6.39±.01	33
4	1400	10	3600	-6.15±.03	20
5	1200	10	3600	-6.87±.02	14
6	1300	10	3600	-6.49±.02	18
7	1300	12.5	3600	-6.60±.04	17
8	1400	12.5	3600	-6.18±.01	9
9	1200	12.5	3600	-6.87±.05	9
10	1300	10	1800	-6.41±.06	11
11	1400	10	3600	-6.27±.02	11
12	1300	10	0	-	-
13	1300	15	3600	-6.62±.03	10

uncertainties in  $\log D$  are quoted at 1 standard deviation.





Table 5 . Arrhenius parameters

Pressure (kbars)	Ea (kcal/mole)	log $D_0$	# of points
10	36±2	-1.46±.3	5
12.5	39±2	-1.18±.2	3
15	39±4	-1.12±.6	4
Temperature (°C)	Va (cm <sup>3</sup> /mole)	log $D_0$	# of points
1200	0.0	-6.87	3
1300	-1.4±.9	-6.36±.09	5
1400	0.9±1	-6.27±.09	4

uncertainties quoted at 1 standard deviation



form:

$$\log_{10} D = \log_{10} D_0 - V_a P / 2.303 RT$$

where  $P$  is the pressure (dyne/cm<sup>2</sup>) and  $V_a$  is the Arrhenius activation volume (cm<sup>3</sup>/mole). Calculated values of  $V_a$  obtained from the least squares fits to the data for 1200, 1300 and 1400°C are presented in Table 5. The activation volumes are small, with large uncertainties, reflecting the extremely small pressure dependence of F-O interdiffusion. Therefore, a mean activation volume of -0.33 cm<sup>3</sup>/mole was calculated (based on all twelve data points) assuming temperature-independence of the activation volume.

#### D. Discussion

##### Comparison with oxygen diffusion

Shimizu and Kushiro (1984) have measured oxygen self-diffusivity in jadeite melt from 5 to 15 kbars and 1400 to 1610°C. They have reported self-diffusivities ranging from  $6.87 \times 10^{-10}$  to  $4.72 \times 10^{-10}$  cm<sup>2</sup>/sec. These values are three orders of magnitude lower than the F-O interdiffusivities at the same pressure and temperature and this difference shows that the presence of anionic chemical activity gradients can result in a large increase in oxygen diffusivity.



### Comparison with tracer diffusion

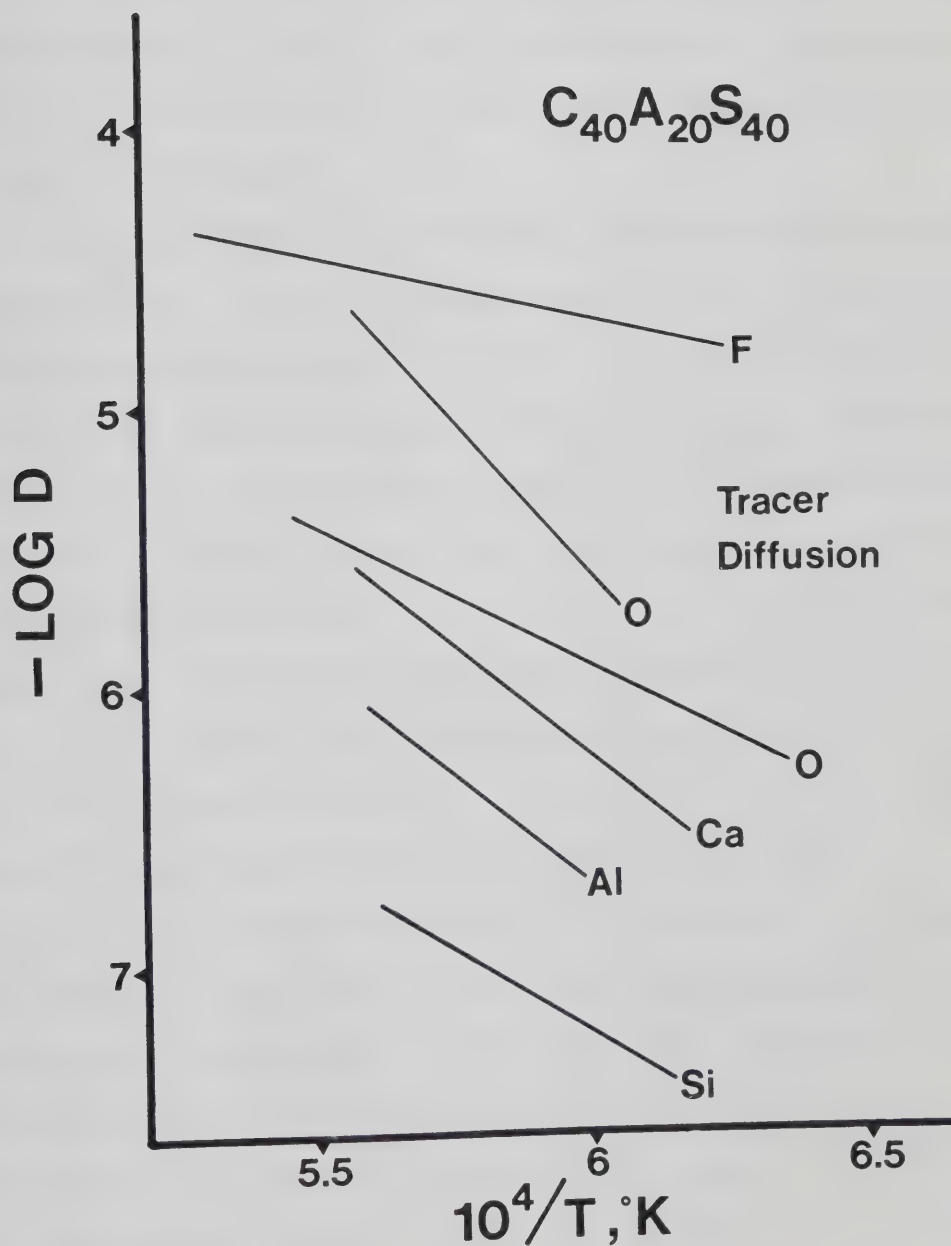
Tracer diffusion of fluorine has been studied by Johnston *et al.* (1974) in a eutectic composition in  $\text{CaO-Al}_2\text{O}_3\text{-SiO}_2$  that contains approximately 40wt% CaO, 20wt%  $\text{Al}_2\text{O}_3$  and 40wt%  $\text{SiO}_2$ , ( $\text{Ca}_{40}\text{Al}_{20}\text{Si}_{40}$ ). The results of this study are useful for a discussion of fluorine diffusivity because  $\text{Ca}_{40}\text{Al}_{20}\text{Si}_{40}$  represents a depolymerized melt which has been well-studied in the glass literature, and the diffusivities of Ca, Al, Si, and O have been measured. Figure 12 presents the results of tracer diffusion studies on Ca (Towers and Chipman, 1957), Al (Henderson *et al.*, 1961), Si (Towers and Chipman, 1957), and O (Koros and King, 1962; Oishi *et al.*, 1975) in  $\text{Ca}_{40}\text{Al}_{20}\text{Si}_{40}$  melt. It is clear from Figure 12 that fluorine diffuses faster than any of the other species studied. Also, fluorine tracer diffusivity has the lowest activation energy of any of the elements studied. As stated above, chemical diffusivities are usually larger than tracer diffusivities; however, the magnitude of tracer diffusivity in  $\text{Ca}_{40}\text{Al}_{20}\text{Si}_{40}$  melt is remarkably large. The observation that tracer diffusion in  $\text{Ca}_{40}\text{Al}_{20}\text{Si}_{40}$  melt is faster than chemical diffusion in jadeite melt implies a strong composition dependence of fluorine diffusivity.

### Comparison with Si-Ge and Al-Ga interdiffusion

Kushiro (1983) has investigated Si-Ge and Al-Ga interdiffusion in jadeite melt from 6 to 20 kbars at 1400°C.



Figure 12. Tracer diffusivities of various ions in lime-aluminosilicate melt (see text for data sources; higher oxygen diffusivity data is from Koros and King, 1962).





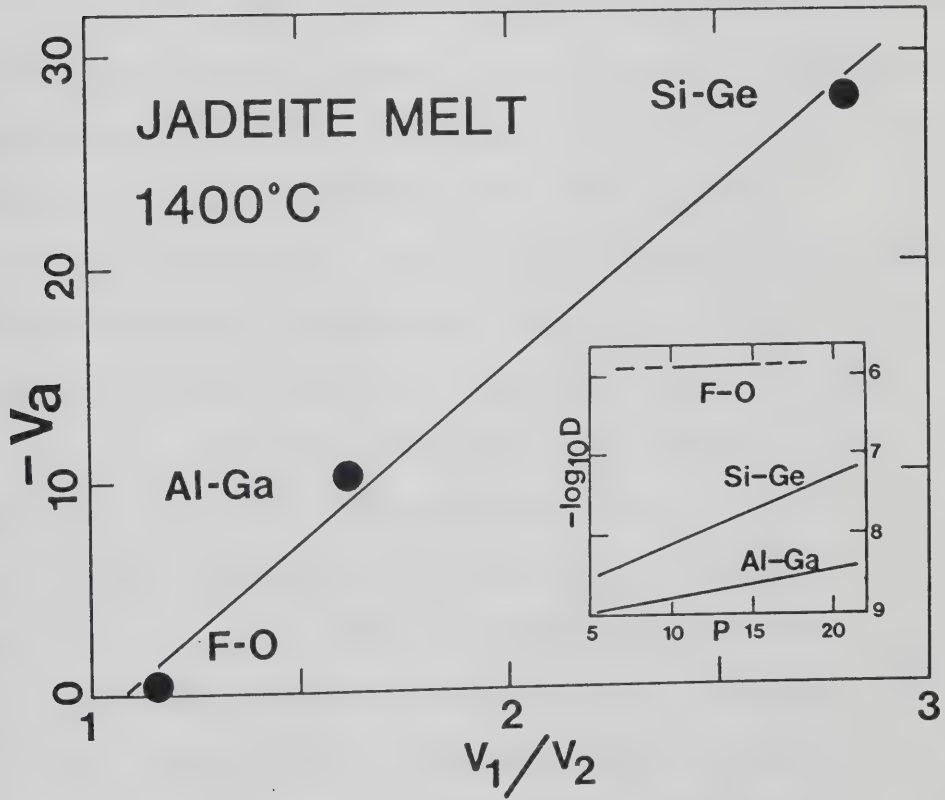


A marked asymmetry is observed in Si-Ge and Al-Ga interdiffusion profiles indicating a strong dependence of Si-Ge and Al-Ga interdiffusivities on  $\text{Si}/(\text{Si}+\text{Ge})$  and  $\text{Al}/(\text{Al}+\text{Ga})$ , respectively (Kushiro, 1983). Comparison of these interdiffusion data with the data for F-O interdiffusion at  $1400^\circ\text{C}$  and 15 kbars shows, as expected, that F-O interdiffusion is much faster than either Si-Ge or Al-Ga interdiffusion.

Kushiro (1983) did not investigate the temperature dependence of cationic interdiffusion, but he showed that the pressure dependence of Si-Ge interdiffusion was much larger than the pressure dependence of Al-Ga interdiffusion. Figure 13 is a plot of the Arrhenius activation volume,  $V_a$  ( $\text{cm}^3/\text{mole}$ ), versus the ratio of the ionic volumes of the interdiffusing species. The ionic volumes were calculated using ionic radii from Whittaker and Muntus (1970) for O, F, Al, Si, Ga, and Ge. The  $V_a$  data are least squares fits to the  $1400^\circ\text{C}$  data from Kushiro (1983) for Si-Ge and Al-Ga interdiffusion and the mean value of  $V_a$  for F-O interdiffusion from this study. It is apparent in Figure 13 that the relative sizes of the interdiffusing species are a large factor in determining the pressure dependence of interdiffusion. Therefore, it is anticipated that the pressure dependence of interdiffusion contains little, if any, information on the pressure dependence of self-diffusion.



Figure 13. Pressure dependence of F-O, Al-Ga and Si-Ge interdiffusion. Activation volume ( $V_a$ ) versus the ratio of ionic volumes of the interdiffusing species (symbol size corresponds to 1 standard deviation uncertainty in the  $V_a$  data for F-O interdiffusion). Inset. The relative pressure dependence of F-O, Al-Ga and Si-Ge interdiffusion (Al-Ga and Si-Ge data from Kushiro, 1983).





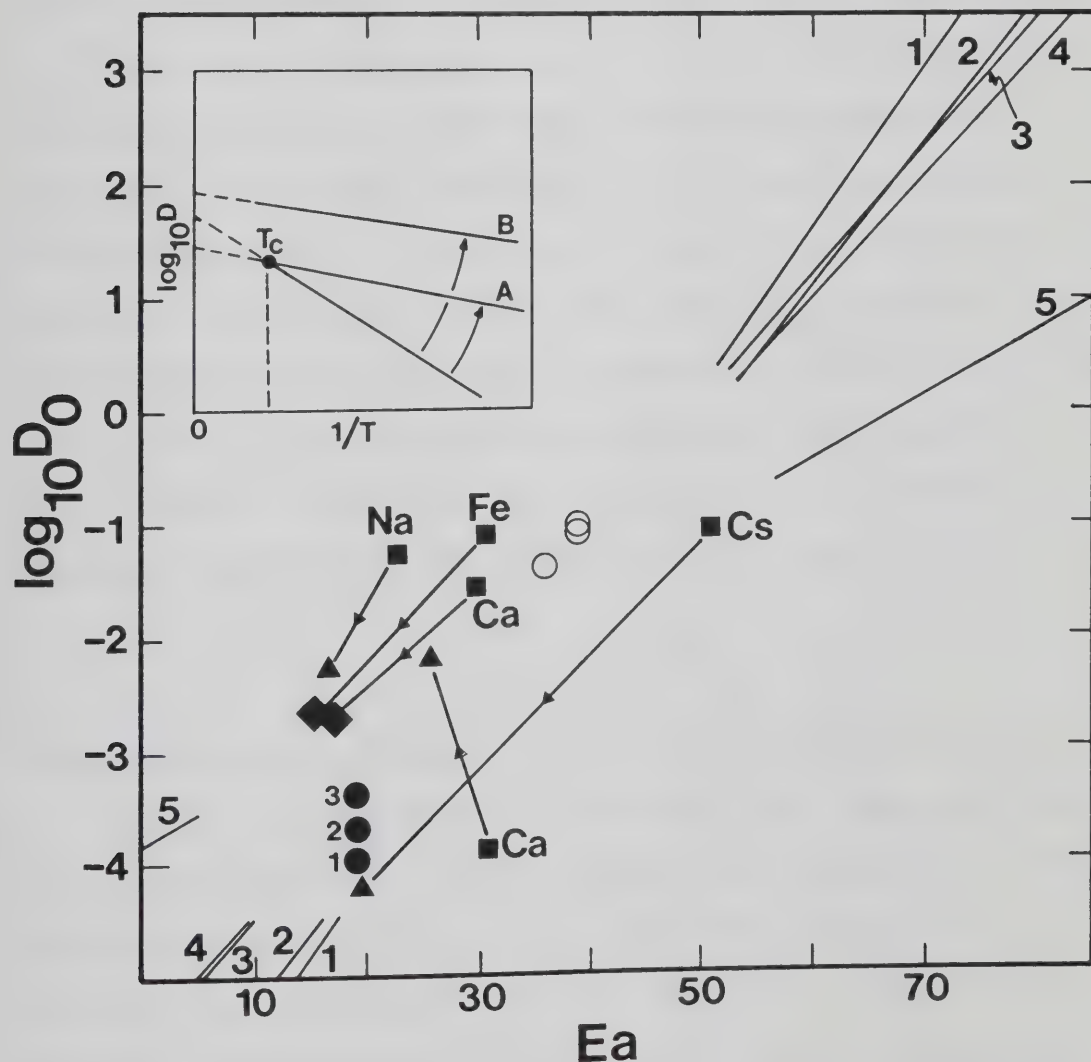
## Compensation relationships

Figure 14 is a plot of the frequency factor versus the activation energy of diffusion. Figure 14 will be used for two purposes; firstly, for a discussion of the correlation between frequency factors and activation energies (i.e. compensation) and secondly, to illustrate the effects of fluorine and water on cationic diffusivities in silicate melts. For the discussion of compensation reference will be made to the lines labelled 1 through 5 and the data for F-O interdiffusion (open circles) and H<sub>2</sub>O chemical diffusion (solid circles). The inset and cationic diffusivity data in Figure 14 will be discussed in the next section.

Winchell and Norman (1969) first showed a positive correlation between the frequency factors and activation energies of various cationic diffusivities in Ca<sub>40</sub>Al<sub>20</sub>Si<sub>40</sub> melt (Fig. 14; line 2). From this correlation they defined a compensation "law" for silicate melt diffusivities which Winchell (1969) extended to other synthetic melt compositions. Hofmann (1980) proposed an equivalent relationship for basalt and obsidian melts incorporating cationic and oxygen diffusivity data (line 4). Hart (1981) distinguished two separate compensation laws, one for basalt melts (line 1), and one for obsidian melts (line 5), and finally, Dunn (1982) proposed a compensation law for various synthetic silicate melts based on oxygen diffusivities (line 3). The most important physical implication of compensation in silicate liquids is that all melt diffusivities converge



Figure 14. Compensation plot for silicate melt diffusivities showing 1) data for  $H_2O$  chemical diffusion (Karsten et al., 1982; solid circles) and F-O interdiffusion (this study; open circles) 2) compensation laws (solid lines) 3) cationic diffusivities in dry, fluorine free melts (squares); in hydrous melts (triangles); and in fluorine-bearing melts (diamonds).







at a unique temperature ( $T$  critical or  $T_c$ ), which may or may not be attained in nature. The implications of such behavior are discussed at length by Hart (1981). Also, compensation plots provide a test of the consistency of diffusion data for a given melt composition. Figure 14 is a compensation plot which includes the results of this study for the chemical diffusion of fluorine and the results of Karsten *et al.* (1982) and Delaney and Karsten (1981) for the chemical diffusion of water. It is clear in Figure 14 that the fluorine data of this study may be included equally well within any of the compensation law relationships except the obsidian curve of Hart (1981). The same conclusion is evident for the  $H_2O$  data. The agreement of the fluorine and water data with the compensation laws for depolymerized melts (lines 1 to 4) suggests that water and fluorine depolymerize obsidian and jadeite melts, respectively.

#### Effect of water and fluorine on cationic diffusivities

Figure 14 emphasizes a second and very important aspect of fluorine and water in silicate melts. Included in Figure 14 are data on the effects of water on Ca, Na and Cs diffusivities (Watson, 1981) and fluorine on Ca and Fe diffusivities (Johnston *et al.*, 1974). The influences of water and fluorine on cationic diffusivities are large. All cationic diffusivities investigated increase when either water or fluorine is added to the silicate melt. In most



cases, the increased diffusivity yields a lower activation energy and frequency factor ( $\log_{10} D_0$ ) and, in these cases, the Arrhenius relationship for cationic diffusivity describes a line which rotates about a critical temperature,  $T_c$  (Fig. 14, inset, case A). This behavior produces a trend on the compensation plot which is sub-parallel to the various compensation relationships. In Figure 14, several cationic diffusivities are affected in this manner (e.g. increases in Ca and Fe diffusivities in fluorine-bearing melt and increases in Cs and Na diffusivities in hydrous melts). The behavior of Ca in hydrous melt is somewhat anomalous because the increase in Ca diffusivity takes the form of a bulk translation of the Arrhenius line (Fig. 14, inset, case B) yielding a lower activation energy but a higher frequency factor. However, the trends of Ca and  $H_2O$  diffusivity with increasing water content are similar (Fig. 14). Regardless of the mechanisms responsible, increased diffusivity of cations with addition of fluorine or water to silicate melts has significant implications for the roles of fluorine and  $H_2O$  in establishing chemical equilibrium during igneous processes.

### Geological applications

Jadeite melt has a highly polymerized structure similar to natural melts whose compositions are approximated by the system nepheline-kalsilite-silica (Seifert *et al.*, 1982).



Relatively dry, rhyolitic, trachytic and phonolitic melts often contain up to 1 wt% fluorine (Carmichael *et al.*, 1974; Bailey, 1977; Christiansen *et al.*, 1983). The present diffusion data provide information on a very important aspect of the petrogenesis of relatively dry, felsic melts. It has been observed experimentally that dry or water-undersaturated melts of rhyolitic and feldspathic composition have extremely slow equilibration rates due to low diffusivities in the melts (Schairer, 1950; Piwinskii, 1967; Whitney, 1975). Johannes (1978, 1980) has proposed that even water-saturated granitic melts have equilibration rates, below 700°C, which are low enough to yield metastable melt compositions in nature. Considering the dramatic effect of fluorine on diffusivities in silicate melts, the presence of fluorine in dry rhyolitic melts could be a crucial factor in determining the rate of establishment and the physical extent of chemical equilibrium during anatexis in the lower crust.

Fluorine increases cationic diffusivities in depolymerized melts (such as  $\text{Ca}_{40}\text{Al}_{20}\text{Si}_{40}$ ; Johnston *et al.*, 1974). Therefore, perhaps fluorine is capable of increasing diffusivities in melts which are already depolymerized due to dissolved water. This potential additive effect of fluorine and water on the diffusivities of various cations in late-stage, water-saturated, granitic melts may yield exceptionally high melt diffusivities.



## E. Summary and conclusions

The chemical diffusion of fluorine in a jadeite melt involves binary interdiffusion of fluorine and oxygen. This interdiffusion is concentration independent, in contrast to Si-Ge and Al-Ga interdiffusion in jadeite melt. High temperature fluorine diffusion, both chemical and tracer, is equal to, or greater than both cationic and oxygen diffusion in fluorine-free melts. The chemical diffusivity of fluorine in jadeite melt is similar in magnitude to the chemical diffusion of water in obsidian melts; however, melt compositional dependence of fluorine diffusivity precludes a direct comparison of water and fluorine diffusivities at this time. The chemical diffusion of fluorine has an Arrhenius activation energy of 36-39 kcal/mole compared with 19 kcal/mole for chemical diffusion of water in obsidian melts and for tracer diffusion of fluorine in  $\text{Ca}_{40}\text{Al}_{20}\text{Si}_{40}$  melt. The results fit several of the compensation "laws" which have been proposed for quantification of cationic and anionic diffusivities in depolymerized silicate melts. A significant effect of fluorine on melt diffusivities is that cationic diffusivities are enhanced by the addition of fluorine to silicate melts. This behavior is also observed when water is added to silicate melts. The effect of fluorine on melt diffusivities may be an important factor in the chemical equilibration of dry, igneous melts.





## IV. One atmosphere diffusion

### A. Introduction

In chapter 2, the comparison of fluorine diffusivity in the lime-aluminosilicate melt and jadeite melt indicated that the value of fluorine diffusivity may be strongly dependent on melt composition. The experiments in this chapter were conducted to 1) investigate the melt compositional dependence of F-O interdiffusivity, 2) further investigate the pressure dependence of F-O interdiffusion in jadeite melt and 3) compare the chemical diffusivities of water in obsidian and fluorine in albite at low pressure.

The volatilization of fluorine from silicate melts has been investigated by several workers using weight loss and bulk chemical analysis techniques (Kumar *et al.*, 1961; Barlow, 1965; Kogarko *et al.*, 1968; Al-Dulaimy, 1978). The present study uses the relatively high volatility of fluorine in melts in the system  $\text{Na}_2\text{O}-\text{Al}_2\text{O}_3-\text{SiO}_2$  to investigate fluorine diffusion.

### B. Experimental method

The starting materials for this study were the glasses used for the viscometry work in chapter 1. Chips of glass were ground into spheres (2-4 mm in size) using the technique of Bond (1951). Spheres of glass were suspended (with white glue) from platinum loops in an electrically-heated vertical tube furnace, equipped with a



gas-tight alumina muffle tube. An "infinite"  $O_2$  gas reservoir was maintained during the experiments by flowing oxygen gas through the furnace at a linear flow rate of 0.10 cm/sec. Temperatures were controlled using a Pt-Pt13Rh thermocouple which was suspended close to the spheres. Three spheres were run at each temperature for each composition. The experiments ranged in duration from 1200 to 19,200 sec. and melt spheres were quenched in air by removal from the furnace. Quenched melt (glass) spheres were removed from the ceramic hanger, ground in half, mounted in epoxy and polished for electron microprobe analysis. In rare cases where the glass beads deformed from spherical shape, due to improper loop size or mounting, the runs were discarded. Generally, spherical shape was extremely well-preserved. Some runs exhibited surface bubbles, presumably due to vapor formation near the melt- $O_2$  interface. These bubbles did not interfere significantly with the following analysis because the bubbles were restricted to a thin surface layer (see below).

Analyses of the concentration profiles were performed using an ARL-SEMQ electron microprobe. Operating conditions for the scans of Na, Al and Si were a 15kV accelerating voltage and a 4 nA sample current with the beam rastered over a 10 by 10 micron area. Fluorine scans and step analyses required a sample current of 40 nA to achieve reasonable count rates (approx. 40cps/wt% F). The quantitative analyses for fluorine were 100 sec counts using



a rastered beam as for Na, Al and Si.

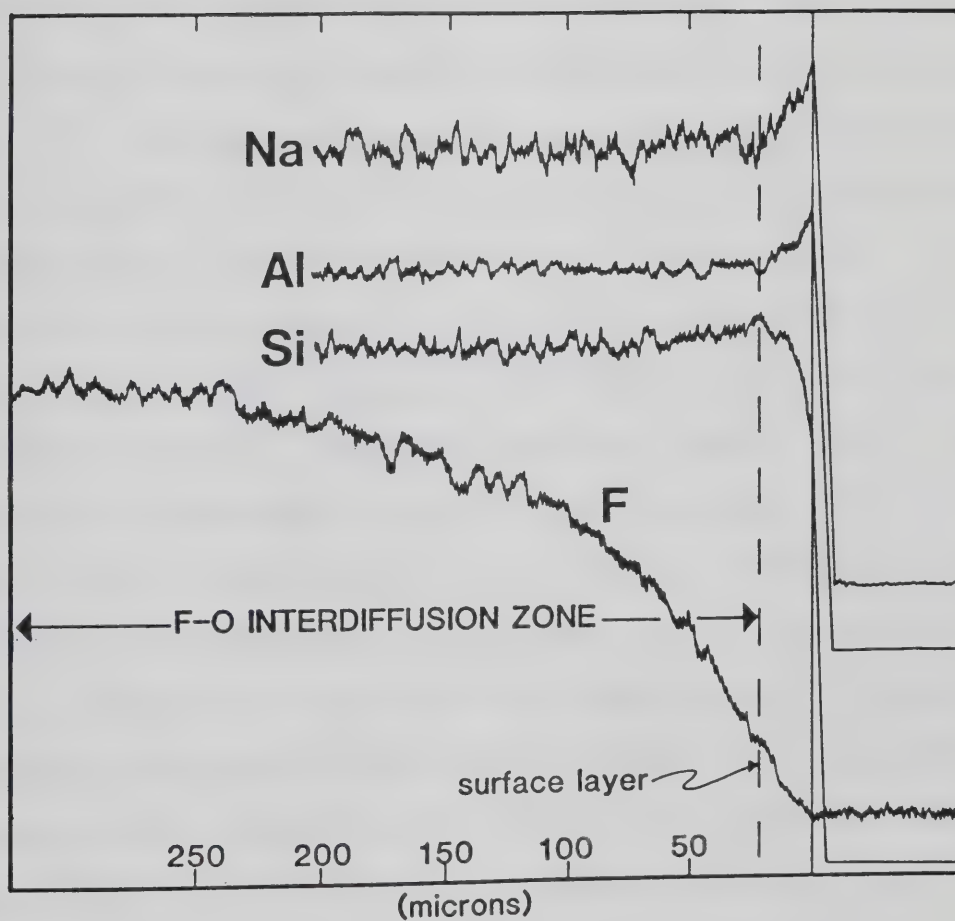
Wavelength dispersive scans for Na, Al, Si and fluorine (Fig. 15) show two basic features. Firstly, the concentration profile of fluorine extends (over several hundred microns) from essentially zero concentration at the sphere edge to a plateau corresponding to the original undepleted fluorine concentration of the melt. Secondly, the concentrations of Na, Al and Si are constant over almost the entire fluorine depletion zone except within 30-50 microns of the sphere edge.

Quantitative analyses of fluorine content were obtained by standardizing the raw counts from step scans across each sphere to the undepleted central zone of the sphere. The exchange of up to 6 wt.% fluorine for oxygen has no effect, within error, on the fluorine ZAF correction. Consequently, after background correction, raw counts from step traverses to the edge of each sphere could be normalized to the counts from the center of each sphere to obtain quantitative fluorine analyses.

The 30-50 micron wide "surface layer" of Si depletion and Na+Al enrichment strongly suggests the escape of fluorine from the melt surface is as  $\text{SiF}_4$  gas. This observation is corroborated by previous studies of fluorine volatility in dry systems at 1 atmosphere (Kumar *et al.*, 1961; Barlow, 1965; Al-Dulaimy, 1978).



Figure 15. Microprobe scans for Na, Al, Si and fluorine across sphere edge.







### C. Data reduction

The constant levels of Na, Al and Si inside the surface layer mean that bulk diffusion of fluorine to this layer may be treated as binary F-O interdiffusion. The mathematical treatment of diffusion for these experiments is for a one-dimensional semi-infinite medium (Crank, 1975; p.35-38). The chemical activity gradient which serves as the driving force for chemical diffusion is quantified by the "reduced concentration" term  $(C-C_1)/(C_0-C_1)$  where  $C$  is the measured concentration along the profile,  $C_1$  is the initial concentration in the melt, and  $C_0$  is the concentration in the gas phase. This equation holds equally well for the case of absorption into a semi-infinite melt medium from a gas phase (e.g. the hydration experiments of Shaw, 1974) as it does for the present case of desorption or volatilization. In these volatilization experiments,  $C_0 = 0$ , because the gas phase is essentially pure  $O_2$  gas. Therefore, the reduced concentration term simplifies to  $1 - C/C_1$ . In the case of concentration-independent diffusion, the equation relating the diffusion coefficient ( $D$ ), distance ( $x$ ), and time ( $t$ ) is as follows:

$$\frac{x}{2\sqrt{Dt}} = \text{erf}^{-1}(C/C_1)$$

where  $\text{erf}^{-1}$  is the inverse of the error function and  $x$  is the distance from the melt-vapor interface. In practice, plots of  $\text{erf}^{-1}(C/C_1)$  vs.  $x$  yield straight lines whose slopes



equal  $1/(2\sqrt{Dt})$ . A typical plot is shown in Figure 16.

#### D. Results

The experimental results are summarized in Table 6 and plotted versus reciprocal temperature in Figure 17. The temperature dependence of F-O interdiffusion is fitted to Arrhenius equations of the form:

$$\log_{10} D = \log_{10} D_0 - E_a/2.303RT$$

where  $D$  is the diffusivity at temperature  $T$ ,  $D_0$  is the pre-exponential or "frequency factor",  $R$  is the gas constant and  $E_a$  is termed the activation energy of F-O interdiffusion. The Arrhenius parameters,  $\log_{10} D_0$  and  $E_a$ , for each melt composition are listed in Table 7.

The interdiffusion of fluorine and oxygen in the system  $\text{Na}_2\text{O}-\text{Al}_2\text{O}_3-\text{SiO}_2$  is strongly dependent on melt composition. At  $1400^\circ\text{C}$ , F-O interdiffusion increases over two orders of magnitude in melts along the join  $\text{NaAlO}_2-\text{SiO}_2$  from albite ( $\log_{10} D = -8.46$ ) to nepheline ( $\log_{10} D = -6.26$ ). F-O interdiffusivity also varies strongly with alkali/aluminum ratio. At  $1200^\circ\text{C}$  and 75 mole %  $\text{SiO}_2$ , the diffusivity of fluorine in albite is slower than in the peralkaline and peraluminous melts.

The activation energy of F-O interdiffusion increases along the join  $\text{NaAlO}_2-\text{SiO}_2$  from albite (29 kcal/mole) through jadeite (34.4 kcal/mole) to nepheline (42.4



Figure 16. Results of the time series experiments on jadeite melt at 1200°C.

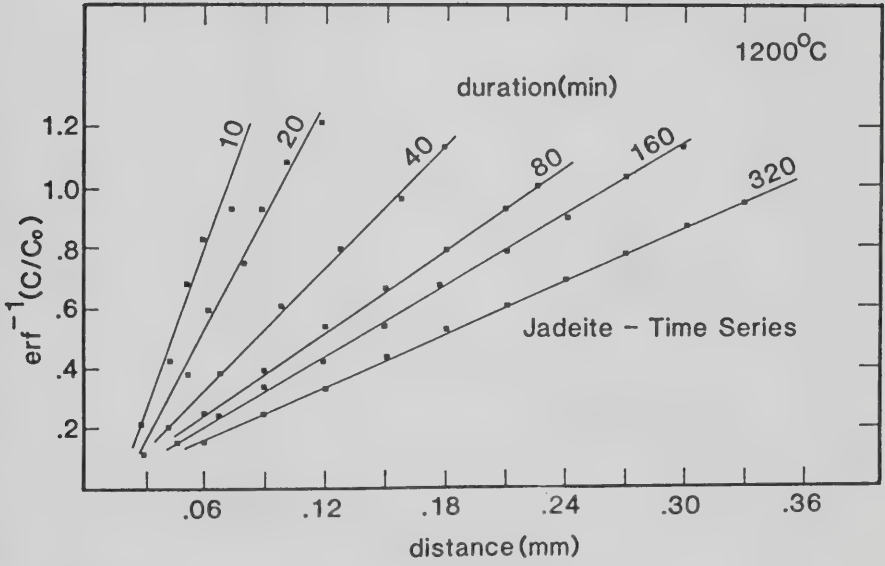




Figure 17. Results of the 1 atm diffusion experiments (asterisk denotes experiments conducted below the liquidus of the fluorine-free melts; square symbol denotes data for the peralkaline melt).

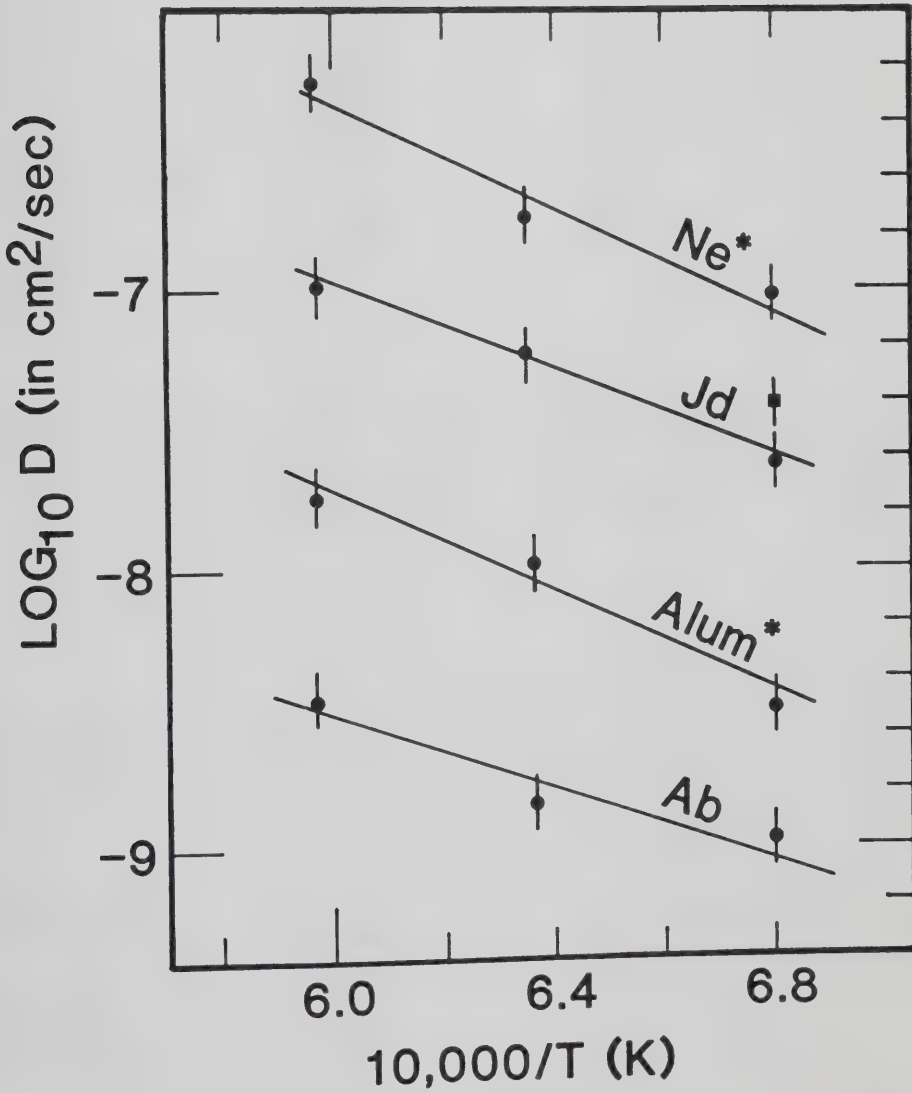






Table 6 : Experimental conditions and results

Composition	Temperature (Celsius)	Duration (min)	$-\log_{10}D$ ( $\text{cm}^2/\text{sec}$ )	# of expts.
Jadeite	1200	10-320*	7.62	7
	1300	3600	7.24	3
	1400	1860	7.01	3
Albite	1200	6900	8.98	3
	1300	7680	8.84	3
	1400	7200	8.46	3
Nepheline	1200	1920	7.02	3
	1300	1380	6.74	3
	1400	1140	6.26	3
Peraluminous	1200	11280	8.50	3
	1300	7560	7.98	3
	1400	7680	7.74	3
Peralkaline	1200	4260	7.40	3

\* Results of a time series of seven experiments (see figure 16) -uncertainty in  $-\log_{10}D$  is estimated to be  $\pm 0.1 \log$  units based on the standard deviation of the seven time series experiments in jadeite at  $1200^\circ\text{C}$ .

Table 7 : Arrhenius parameters for 1 atmosphere F-O interdiffusion

Composition	$\log_{10}D_0$ (in $\text{cm}^2/\text{sec}$ )	$E_a$ (kcal/mole)
Albite	-4.74	28.9
Jadeite	-2.50	34.4
Nepheline	-0.77	42.4
Peraluminous	-2.09	43.0



kcal/mole). If the trend of decreasing diffusivity with  $\text{SiO}_2$  content extends beyond albite along the join  $\text{NaAlO}_2\text{-SiO}_2$ , then the F-O interdiffusivity measured for albite may be taken as an upper limit on F-O interdiffusivity in obsidian melts.

## E. Discussion

### Comparison with viscosity data

The suggestion that similar mechanisms and species may control the viscous flow and diffusivities in silicate melts has led several investigators to examine the validity of the Stokes-Einstein equation which inversely relates viscosity and diffusivity (Watson, 1979; Hofmann, 1980; Jambon, 1982; Burnham, 1983; Shimizu and Kushiro, 1984). It is:

$$Dn = K_b T / 6\pi r$$

where  $K_b$  is the Boltzmann constant and  $r$  is the radius of the diffusing species. This form of equation predicts a linear inverse correlation between  $\log D$  and  $\log n$ . It has been generally concluded that the Stokes-Einstein relationship is qualitatively invalid in relating viscosity and network-modifying cationic diffusivities in silicate melts (Winchell and Norman, 1969; Magaritz and Hofmann, 1978; Watson, 1979; Hofmann, 1980; Jambon, 1982; Angell *et al.*, 1983). However, for the case of oxygen diffusion,



and Kushiro (1984) have stated that an inverse correlation with viscosity is well approximated by the Eyring form of the Stokes-Einstein equation. The success of any equation which inversely relates viscosity and oxygen diffusivity strongly implies that the same structural unit and mechanism are involved in both transport processes. Dunn (1983) has recently shown that  $O^{2-}$  is probably the dominant species involved in oxygen diffusion in basaltic melts and Shimizu and Kushiro (1984) argue that the viscous flow of jadeite and diopside melts is controlled by the diffusion of individual  $O^{2-}$  ions.

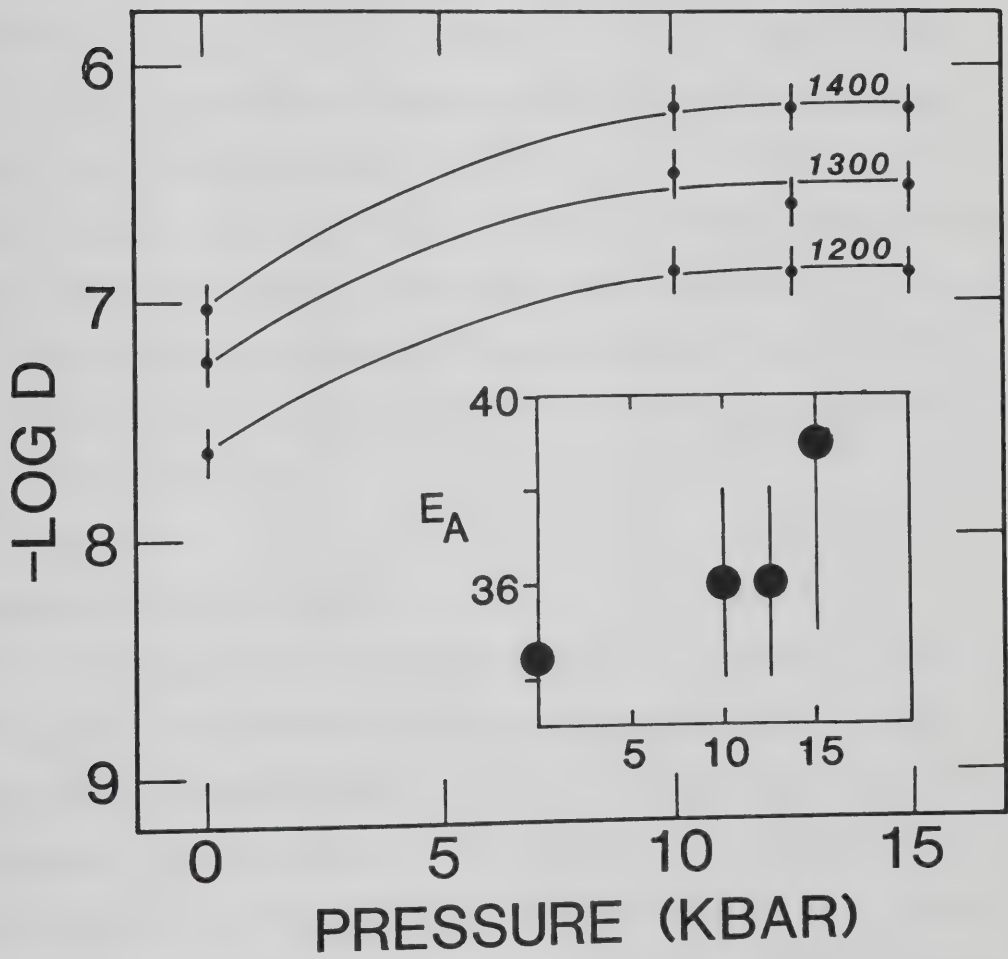
The conclusions of this study regarding the application of the Stokes-Einstein equation to F-O interdiffusivity are negative. Correlation of  $\log \eta$  versus  $\log D$  is very poor. Qualitatively, we would expect this result because the viscosity of these melts is a strong function of fluorine content but the F-O interdiffusivity is not. There is even an increase in F-O interdiffusivity with increasing viscosity from the albite to the peraluminous melt. Clearly the presence of fluorine in these melts removes the applicability of the Stokes-Einstein equation to the diffusion of oxygen.

#### **Pressure dependence of F-O interdiffusion in jadeite melt**

The results of this study for jadeite melt are compared with the high pressure data of chapter 2 in Figure 18. F-O interdiffusivity clearly increases with pressure from 0.001



Figure 18. Pressure dependence of fluorine diffusion in jadeite melt. Inset: Pressure dependence of activation energy for F-O interdiffusion.







to 10 kbars, as does oxygen self-diffusion (Shimizu and Kushiro, 1984). The lines are interpolations based on the assumption of a smoothly decreasing pressure dependence with increasing pressure. In fact, Dunn (1983) has shown that the pressure dependence of oxygen chemical diffusivity in basaltic melts is discontinuous in the pressure range of 1 to 10 kbars whereas, Shimizu and Kushiro (1984) show a smoothly increasing self-diffusivity of oxygen in jadeite melt in the pressure range of 5 to 20 kbars. This contrast may result, in part, from comparison of chemical and self diffusivities and thus the pressure dependence of F-O interdiffusion in jadeite melt is difficult to discuss in structural terms.

### Comparison with water

The comparison of the chemical diffusion of fluorine and water is interesting for two reasons. Firstly, the geological significance of fluorine in natural melts was discussed in chapter 2. It is clear that relatively dry, fluorine-rich geological melts do exist and their kinetic behavior requires investigation and comparison with that of wet melts. Secondly, the structural comparison of fluorine and water in chapter 1 led to the conclusion that the depolymerizing influences of fluorine and water have very similar effects on the viscosity of silicate melts.

Chemical diffusion of water in natural silicate melts has been investigated by several workers (Shaw, 1974;

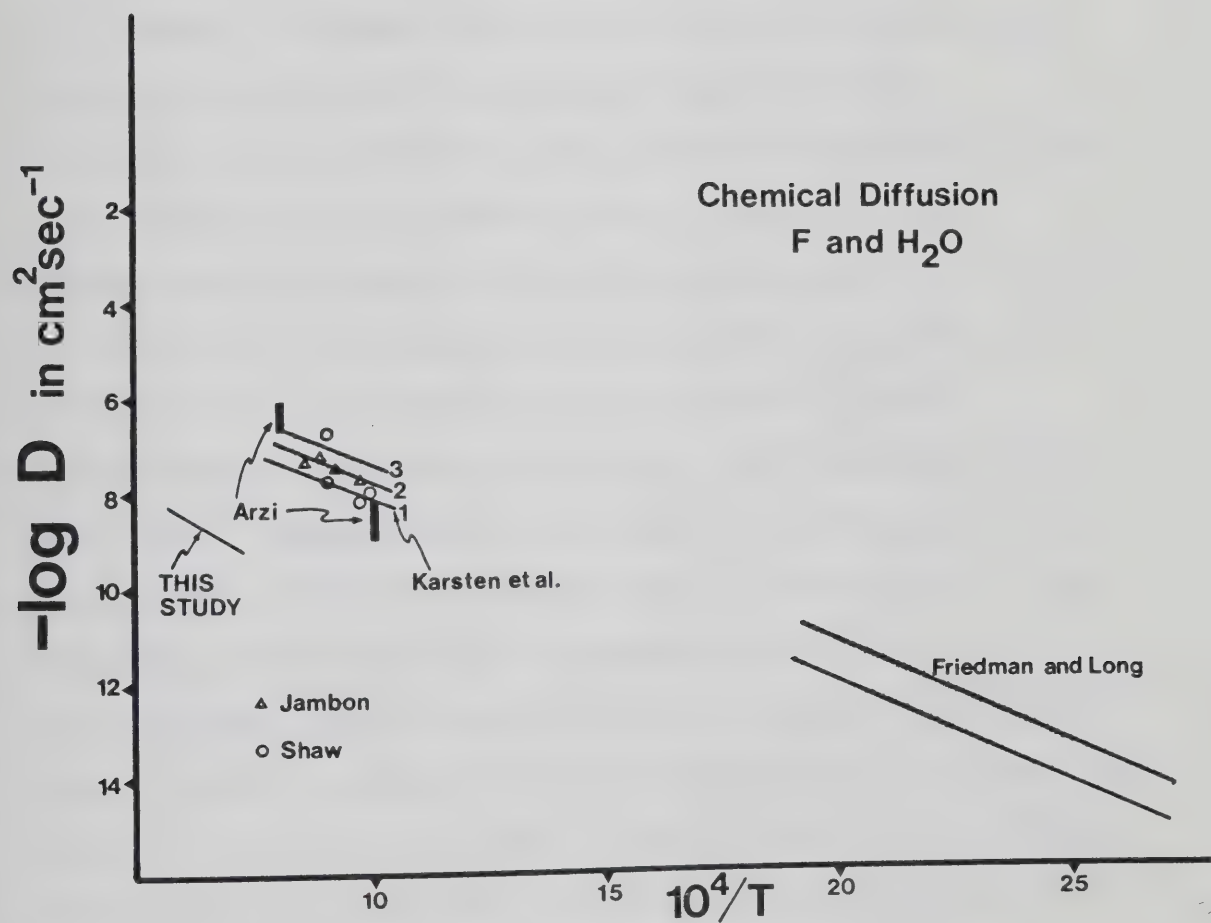


Friedman and Long, 1976; Arzi, 1978; Jambon *et al.*, 1978; Delaney and Karsten, 1981; Karsten *et al.*, 1982). In Figure 19, the data for the chemical diffusion of fluorine in albite melt are compared with the available data for the chemical diffusion of water in obsidian melts. Although the comparison of data in Figure 19 involves melts of albite and obsidian composition both represent relatively polymerized melts with alkali/aluminum (molar) ratios at or near 1:1. The comparison of Figure 19 uses 1 atmosphere data for fluorine and 0.1 - 2.0 kbar data for water diffusion. With these provisions in mind, this comparison is discussed below.

The chemical diffusivity of fluorine in albite melt is approximately two orders of magnitude less than that of water in obsidian melt. Considering the composition dependence of fluorine diffusivity observed from nepheline melt to albite melt (Fig. 17), the difference between fluorine and water diffusivities in obsidian is probably even larger. The temperature dependence of fluorine diffusivity yields an activation energy of 29 kcal/mole in albite melt compared with an activation energy of 19 kcal/mole for water diffusion in obsidian (Delaney and Karsten, 1981). Such differences in diffusivity and activation energy may result from different mechanisms of diffusion for water and fluorine in these polymerized melts. Qualitatively, these differences imply that if  $F^-$  is the principal diffusing species, as is suggested by the binary



Figure 19. Chemical diffusivities of fluorine in albite melt and  $\text{H}_2\text{O}$  in rhyolitic melts. (see text for data sources)





nature of interdiffusion of fluorine and oxygen, then water is probably not transported principally as  $\text{OH}^-$ , the monovalent anion of similar size. Conversely, if the diffusion of water is as  $\text{OH}^-$ , then the species involved in fluorine diffusion might be a larger complex such as  $\text{AlF}_6^{3-}$  (Manning *et al.*, 1980).

Perhaps the most significant difference between the diffusive behavior of fluorine and water is the concentration dependence of the chemical diffusion of water in obsidian melt contrasted with the concentration independence of fluorine diffusion in all melts investigated in this study. The concentration dependence of water diffusivity in obsidian melt has been most recently investigated by Delaney and Karsten (1981) and Karsten *et al.* (1982). These workers state that the activation energy of chemical diffusion of water remains constant while the frequency factor ( $\log D_0$ ) increases with water concentration. This increase has been interpreted (Karsten *et al.*, 1982) to result from an increase in the average jump distance associated with the diffusive mechanism. Karsten *et al.* (1982) further propose that the concentration dependence of water diffusion results from the occurrence of at least two distinct solution sites for water in obsidian melt whose relative occupancies change with water concentration.

In addition, the concentration dependence of water diffusivity, combined with the effect of water on melt viscosity, permits application of the Stokes-Einstein





equation to melts of constant composition and varying water contents (Burnham, 1983). The concentration independence of fluorine diffusion contrasts strongly with the behavior of water and suggests that a single structural site is entirely adequate to explain the observed diffusive behavior.

### Diffusion mechanisms

From a combination of data of viscosities and diffusivities in F- and H<sub>2</sub>O-bearing melts (chapters 1,2 and above) it is apparent that the effects of fluorine and water on melt viscosity are similar, whereas their diffusivities are considerably different. The viscometry data implies similar structural roles for fluorine and water within polymerized silicate melts, probably the replacement of Si-O-(Si,Al) bridges with (Si,Al)-F and (Si,Al)-OH, respectively.

The diffusivity data, in contrast, highlight several differences in the transport of fluorine and water in these melts. Fluorine exchanges with oxygen via a mechanism which is independent of concentration and strongly dependent on melt composition. The exchange is effectively binary, probably without the involvement of any cations.

Water, in contrast, diffuses in polymerized melts at a rate which varies with water concentration. Karsten *et al.* (1982) have reported preliminary evidence of K and possibly Na concentration gradients produced during chemical diffusion of water. These alkali concentration gradients

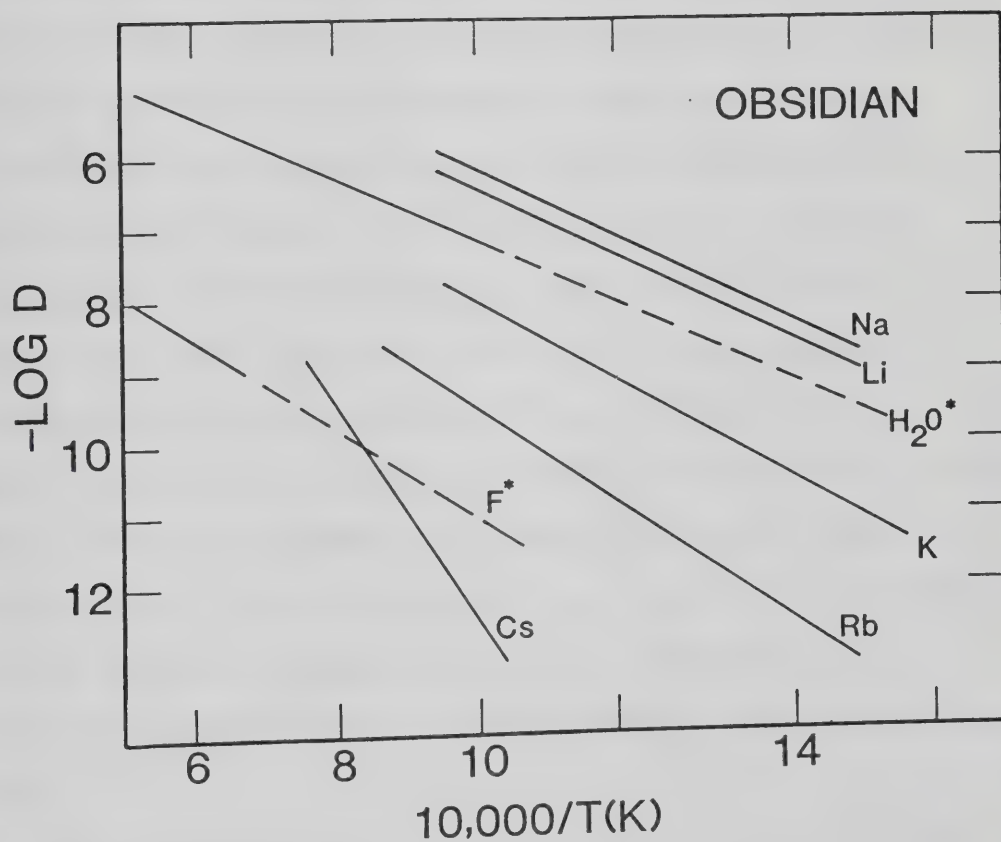


suggest that interaction of water and alkalies may be an essential characteristic of chemical diffusion of water in these melts. The albite-H<sub>2</sub>O water solubility model of Burnham (1975, 1979) does predict alkali transport during the solution of water in albite melt.

Figure 20 presents tracer diffusion data for Li, Na, K, Rb and Cs (Jambon, 1982) and chemical diffusion data for water (Fig. 6 in Hofmann, 1980) in obsidian melts, as well as chemical diffusion data for fluorine in albite melt (this study). The diffusivity of alkalies in obsidian melt increases smoothly with decreasing ionic radius from Cs to Na. However, Li diffuses at essentially the same rate as Na. Jambon (1982) has interpreted the equivalence of Na and Li diffusivity to result from the control of Li diffusivity by the structure and mobility of the matrix or neighbouring cations with which Li will interdiffuse. Thus, in obsidian melt, the diffusion of Li may be controlled by the mobility of Na (Jambon, 1982). In Figure 20, it is evident that the chemical diffusivity of water, unlike that of fluorine, is very similar to the tracer diffusivity of Na (and Li). Perhaps the diffusion of hydrogen-bearing species in obsidian is controlled by the mobility of Na via an alkali exchange reaction similar to that described by Burnham (1975) for water solubility.



Figure 20. Alkali tracer diffusivities in obsidian melt compared with chemical diffusivities of fluorine and water.





## V. Water solubility

### A. Introduction

The solubility of water in granitic liquids of various compositions is a crucial property influencing the petrogenesis of intrusive and extrusive silicic rocks (e.g. Wyllie, 1979; Burnham, 1979). The dependence of solubility on melt composition is especially important during crystallization of granitic intrusions. Saturation of residual melts results in boiling phenomena closely associated with Cu-Mo porphyry systems and various pegmatites. The explosive eruption of magmas may be triggered by energy released during the expansion of a vapor phase evolved from melts (e.g. Sparks *et al.*, 1977; Harris, 1981b). Numerical models for the evolution of vapor (e.g. Wilson *et al.*, 1980) from granitic liquids at low pressures require detailed knowledge concerning the effects of composition and pressure on the solubility of water in such melts.

The solubility of water in granitic melts has been the topic of several experimental studies; however, there is no consensus on the results or their interpretation (e.g. Oxtoby and Hamilton, 1978b; Day and Fenn, 1982). These previous solubility determinations may be divided broadly into two categories: those using chemographic or phase equilibrium techniques (Burnham and Jahns, 1962; Fenn, 1973; Whitney, 1975; Voigt *et al.*, 1981) and those using a weight





loss method (e.g. Goranson, 1931, 1938; Bowen and Tuttle, 1950; Yoder *et al.*, 1957; Orlova, 1963; Oxtoby and Hamilton, 1978a). Solubility data obtained by such techniques were reviewed by Day and Fenn (1982) who discussed the assumptions and limitations associated with each method. A new capacitance manometric technique for micro-determination of  $H_2O$  evolved from vacuum fusion of glass (Harris, 1981a) affords a method for measuring  $H_2O$  released from experimentally quenched vapor-saturated melts prepared as glass wafers free of fluid-filled vesicles. By using this technique the solubility of water in haplogranitic melts in the system  $K_2O-Na_2O-Al_2O_3-SiO_2$  has been determined.

The other unique aspects of this work are : (1) the study of haplogranitic melts to bridge the gap between melts of feldspar composition and natural granitic liquids; (2) the precise measurement of water solubility at up to four pressures in the range 1-2 kbars and determination of the pressure dependence for two compositions; and (3) investigation of the effects of increasing peralkalinity on water solubility at 1 kbar. The effects of composition and pressure on the solubility of  $H_2O$  are essential for understanding the petrogenesis of silicic plutonic and volcanic rocks.



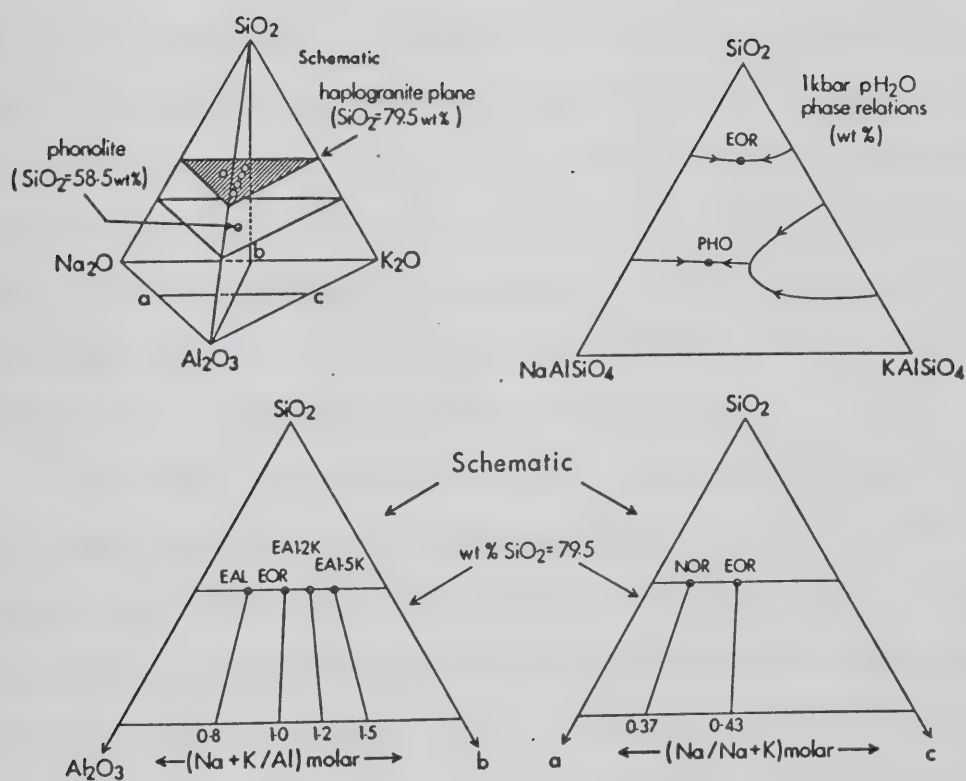
## B. Experimental and analytical procedures

The glasses used in the hydrothermal runs were synthesized from reagent grade  $\text{Na}_2\text{CO}_3$ ,  $\text{K}_2\text{CO}_3$ ,  $\text{Al}_2\text{O}_3$ , and  $\text{SiO}_2$  by using standard techniques described by Schairer and Bowen (1956). The compositions of the anhydrous glasses used as starting materials (Fig. 21) were determined by electron microprobe.

Synthetic vapor-saturated melts were produced hydrothermally. Twenty-five to fifty milligrams of powdered glass were added to 10 to 20 milligrams of triple-distilled water in 3 mm Pt capsules and welded. The capsules were checked for possible leakage by testing for weight loss after drying in an oven at  $110^\circ\text{C}$  for 15 minutes. Sealed capsules were loaded into cold-seal pressure vessels and raised to the desired run pressure by using an air-driven hydraulic pump. Pressurized capsules were heated to the run temperature ( $800^\circ\text{C}$ ) by using Kanthal-wound resistance furnaces mounted concentrically about the vessels along a vertical axis. Temperatures were monitored with Chromel-Alumel thermocouples and the actual temperatures are believed accurate to  $\pm 5^\circ\text{C}$ . Pressures were measured with Bourdon-tube gauges previously calibrated with a Heise gauge. All run durations were  $10^6$  seconds. The charges were quenched isobarically by using compressed air. Pressure was maintained during the quench by opening the vessel to the pressure line and by pumping for the duration of the quench. Owing to the response time of the pump there were slight



Figure 21. Melt compositions in the system  $\text{K}_2\text{O}-\text{Na}_2\text{O}-\text{Al}_2\text{O}_3-\text{SiO}_2$  (1 kbar phase equilibria data from Tuttle and Bowen (1958) and Hamilton and MacKenzie (1965)).





fluctuations in pressure during quenching. These fluctuations were monitored and are included in the pressure uncertainties listed in Table 8. Except for water, the compositions of the hydrated glasses were determined by electron microprobe (Table 8). All of the glass compositions, when recalculated H<sub>2</sub>O-free and normalized to 100%, are within analytical error of their respective anhydrous starting compositions.

The quenched run products consisted of vesicular glass free of microlites. The vesicles contained liquid water and an enclosed vapor bubble and indicate that the charges were fluid-saturated during the experiments. It is extremely difficult to accurately estimate the volume fraction of vesicles in the run products. This difficulty was avoided by preparation of vesicle-free glass wafers.

Polished glass wafers free of occluded fluids were prepared manually from the experimental charges. The resulting wafers were typically 40-100 micrometers thick, depending upon the sizes and locations of vesicles within the glass wafer. Absence of occluded fluid was established by transmitted light microscopy at 200X magnification. The glass wafers were liberated from the Canada balsam mounting media by using acetone. The wafers were washed ultrasonically in acetone and checked again optically for purity at 200X magnification using transmitted and reflected light microscopy.





TABLE 8  
EXPERIMENTAL DETERMINATIONS OF H<sub>2</sub>O SOLUBILITY FROM MEASUREMENTS OF H<sub>2</sub>O IN QUENCHED GLASS

Run No. Series	80 EAL2K	38 EAL2K	48 <sup>a</sup> EAL2K	43 EAL2K	85 EAL2K	44 EAL2K	36 EAK	83 EAK	37 EOR	61 NOR	60 PHO	58 <sup>a</sup> EAL
Pressure <sup>b</sup> f <sub>H<sub>2</sub>O</sub>	970 825	970 825	1160 965	1450 1175	1620 1297	1630 1305	970 825	1620 1297	970 825	970 825	970 825	970 825
Pressure and fugacity of H <sub>2</sub> O during experiments at 800°C												
Microprobe <sup>c</sup> analyses and vacuum fusion determinations <sup>d</sup> of H <sub>2</sub> O in glass												
SiO <sub>2</sub>	75.00	74.24		74.84	73.64	73.99	74.63	72.27	75.27	75.67	54.67	
Al <sub>2</sub> O <sub>3</sub>	9.80	9.73		9.74	9.66	9.57	9.19	8.93	11.20	11.15	22.82	
Na <sub>2</sub> O	4.02	4.08		4.08	3.96	4.10	4.70	4.41	3.79	4.53	10.56	
K <sub>2</sub> O	4.69	4.55		4.68	4.59	4.60	5.33	5.25	4.32	3.09	5.08	
H <sub>2</sub> O	3.38	3.29	3.72	4.36	4.67	4.55	3.44	4.98	2.88	2.74	5.01	3.46
Total	96.89	95.89		97.70	96.52	96.81	97.29	95.84	97.46	97.18	98.14	
Glass compositions recalculated to 100% totals												
SiO <sub>2</sub>	77.49	77.53	77.32	76.68	76.43	76.54	76.79	75.58	77.29	77.92	55.76	75.62
Al <sub>2</sub> O <sub>3</sub>	10.13	10.16	10.06	9.98	10.03	9.90	9.46	9.34	11.50	11.48	23.28	13.24
Na <sub>2</sub> O	4.15	4.26	4.15	4.18	4.11	4.24	4.84	4.61	3.89	4.67	10.77	3.52
K <sub>2</sub> O	4.85	4.75	4.75	4.80	4.76	4.76	5.48	5.49	4.44	3.18	5.18	4.16
H <sub>2</sub> O	3.38	3.29	3.72	4.36	4.67	4.55	3.44	4.98	2.88	2.74	5.01	3.46
Moles of cations per 100 g of melt												
Si	1.290	1.290	1.287	1.276	1.272	1.274	1.278	1.258	1.286	1.297	.928	1.259
Al	.199	.199	.197	.196	.197	.194	.186	.183	.226	.225	.457	.260
Na	.134	.138	.134	.135	.137	.137	.156	.149	.126	.151	.348	.114
K	.103	.101	.101	.102	.101	.101	.116	.117	.0942	.0676	.110	.088
H	.375	.365	.413	.484	.519	.505	.382	.553	.320	.304	.556	.384
Total	2.101	2.093	2.132	2.193	2.222	2.111	2.118	2.260	2.0522	2.0446	2.399	2.105
Na/Na + K	.565	.577	.570	.570	.568	.576	.574	.560	.572	.691	.760	.564
Na + K/Al	1.19	1.20	1.19	1.21	1.19	1.23	1.46	1.45	.97	.97	1.00	.777
Si/Al	6.48	6.48	6.53	6.51	6.46	6.57	6.87	6.87	5.69	5.76	2.03	4.84
X <sub>w</sub> <sup>m</sup> based upon solubility measurements and the model of Burnham (1979)												
X <sub>w</sub> <sup>m</sup>	.363	.356	.386	.426	.443	.437	.372	.465	.322	.308	.379	.371
X <sub>w</sub> <sup>m</sup> calculated from Burnham's (1979) paper												
X <sub>w</sub> <sup>m</sup>	.409	.409	.423	.454	.465	.465	.409	.465	.409	.409	.409	.409
MW	.293	.293	.293	.293	.293	.293	.299	.299	.289	.285	.208	.296
ln K	1.79	1.79	1.72	1.58	1.53	1.53	1.79	1.53	1.79	1.79	1.79	1.79

<sup>a</sup> Microprobe analyses of hydrous products are not available for runs 48 and 58.

<sup>b</sup> Pressure and fugacity are given in bars; pressure uncertainty is  $\pm 10$ ,  $-30$  bars. Fugacity was calculated from Burnham et al. 1969.

<sup>c</sup> Glasses were analyzed by D. B. Dingwell with the University of Alberta ARL SEMQ microprobe using 15 kV accelerating voltage and a 4 nA sample probe current in the energy dispersive mode; a beam raster of  $20 \times 20$  micrometers and a continuously moving sample were used to prevent alkali loss. Standards used were quartz, albite, and sandline and the data were reduced using EDATE2 (Smith and Gold, 1979). Analyses have the following 3 standard deviation uncertainties quoted as percentages of the amount present: SiO<sub>2</sub>, 0.69%; Al<sub>2</sub>O<sub>3</sub>, 1.78%; K<sub>2</sub>O, 2.58%; Na<sub>2</sub>O, 4.76%.

<sup>d</sup> Determinations of H<sub>2</sub>O (D. M. Harris) are duplicate means for individual experiments; reproducibility of solubility determinations is about  $\pm 0.06$  wt % (see runs 80, 38, 85, and 44).



The amount of  $\text{H}_2\text{O}$  dissolved in the glass was determined by the vacuum fusion micromanometric method described in Harris (1981a). The determinations of  $\text{H}_2\text{O}$  were made on duplicate glass wafers of different mass for each run and the amounts reported are the duplicate means. The samples of glass ranged in mass from 0.020 to 0.600 mg. Sample masses were determined with a Cahn-G electronic microbalance and are considered precise to  $\pm 0.003$  mg. The analytical precision for water can be estimated by considering the variance of the relative deviations of the individual measurements about their duplicate mean. This method provides an estimate of  $\pm 2.8\%$  of the concentration for the standard deviation of the duplicate means about their ensemble mean, if multiple pairs of determinations were made for each experimental charge. The overall reproducibility of these solubility measurements includes uncertainties due to variation of run pressures, possible variable diminution of dissolved water during the quench, and analytical errors in the determination of  $\text{H}_2\text{O}$  (e.g. incomplete extraction of  $\text{H}_2\text{O}$  during vacuum fusion of samples, or loss of  $\text{H}_2\text{O}$  due to adsorption by the walls of the vacuum system). The overall reproducibility was estimated by repetition of experiments. Two solubility determinations have been repeated (Table 8; EA1.2K at 970 bars, runs 80 and 38; EA1.2K at 1620 bars, runs 85 and 44). Both solubility determinations were within 0.06 wt%  $\text{H}_2\text{O}$  of their ensemble means, or about 1.4 % of the concentration. The precision attained in these measurements



exceeds that reported by Harris (1981a) owing to the greater precision of sample masses that were made possible in this study by using an electronic microbalance.

### C. Results

The glass compositions and solubility determinations at various pressures are given in Table 8. The effects of pressure and composition are described next.

#### Pressure dependence

The effects of pressure on the solubility of water were determined for two melts with identical Na/(Na+K) ratios (0.57) and similar Si/Al ratios but with differing (Na+K)/Al ratios. Both liquid compositions were peralkaline. The experimentally determined solubilities, expressed as weight percent H<sub>2</sub>O in the hydrous liquid, are shown in Table 8. The solubilities were recast as mole fractions by using the method of Burnham (1979) and fit (Table 9) to linear equations as functions of the square root of the water fugacity (Burnham *et al.*, 1969). The root mean square deviations from linearity are less than 1.4% (Figure 22). The equimolar solubility of water is slightly larger for the more peralkaline liquid at both 970 and 1620 bars P(H<sub>2</sub>O). Hence, the derivatives with respect to square root of fugacity differ by 5%.



Figure 22. Effect of pressure on water solubility.

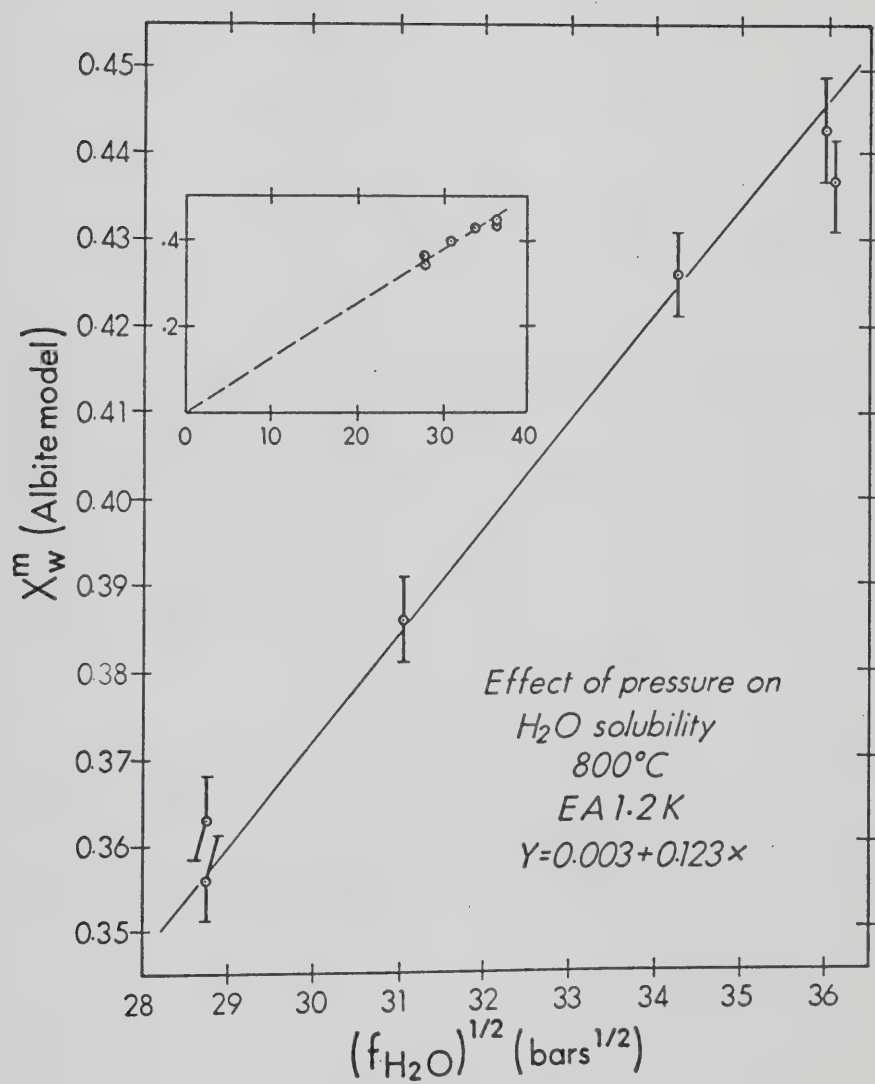






TABLE 9  
EFFECT OF PRESSURE ON THE SOLUBILITY OF H<sub>2</sub>O IN TWO LIQUIDS

Run No.	Pressure bars	$f_{\text{H}_2\text{O}}$ bars	$f_{\text{H}_2\text{O}}^{1/2}$ bars <sup>1/2</sup>	$X_w^m$ meas.	$X_w^m$ calc.	Residual
EA1.2K 970–1630 bars						
80	970	825	28.72	.363	.356	-.007
38	970	825	28.72	.356	.356	.000
48	1160	965	31.06	.386	.385	-.001
43	1450	1175	34.28	.426	.425	-.001
85	1620	1297	36.01	.443	.446	.003
44	1630	1305	36.12	.437	.447	.010
$X_w^m = 0.003 + 0.0123 (f_{\text{H}_2\text{O}}, \text{bars})^{0.5}$ r.m.s. error of fit = 0.005						
EAK						
36	970	825	28.72	.372	.371	-.001
83	1620	1297	36.01	.465	.465	.000
$X_w^m = 0.0006 + 0.0129 (f_{\text{H}_2\text{O}}, \text{bars})^{0.5}$ r.m.s. error of fit = 0.0006						

NOTES.—Solubility data and the origin were fit to linear equations by the method of least squares.



## Effects of Na-K exchange

The effects of exchanging Na and K in haplogranitic melts may reveal whether there is a notable effect of alkali cation size on the solubility of water. Two experiments (runs 37 and 61) conducted at 970 bars show that the increase of the Na/K ratio from 1.34 at the eutectic to 2.23 caused no measurable change in solubility (maximum 0.14 wt%). Further research should determine whether this is also true for other liquid compositions in the vicinity of the ternary eutectic.

## Dependence of solubility on the alkali/aluminum ratio

The equimolar solubilities of water in four liquids that differ in alkali/aluminum ratio were determined at 970 bars and are summarized in Table 10. For the range of silica-saturated compositions investigated, the equimolar solubility at 970 bars water pressure increases with increasing alkali to aluminum ratio and the root mean square deviation from linearity is about 1.4%. However, the solubility of water in the peraluminous liquid (Table 8, Run 58) does not lie on the extension of this line to the peraluminous field. This suggests the existence of minima in the solubility of H<sub>2</sub>O at (Na+K)/Al=1 for melts along joins of constant molar SiO<sub>2</sub> in anhydrous melts (Fig. 23).



Figure 23. Effect of the alkali/aluminum ratio on water solubility.

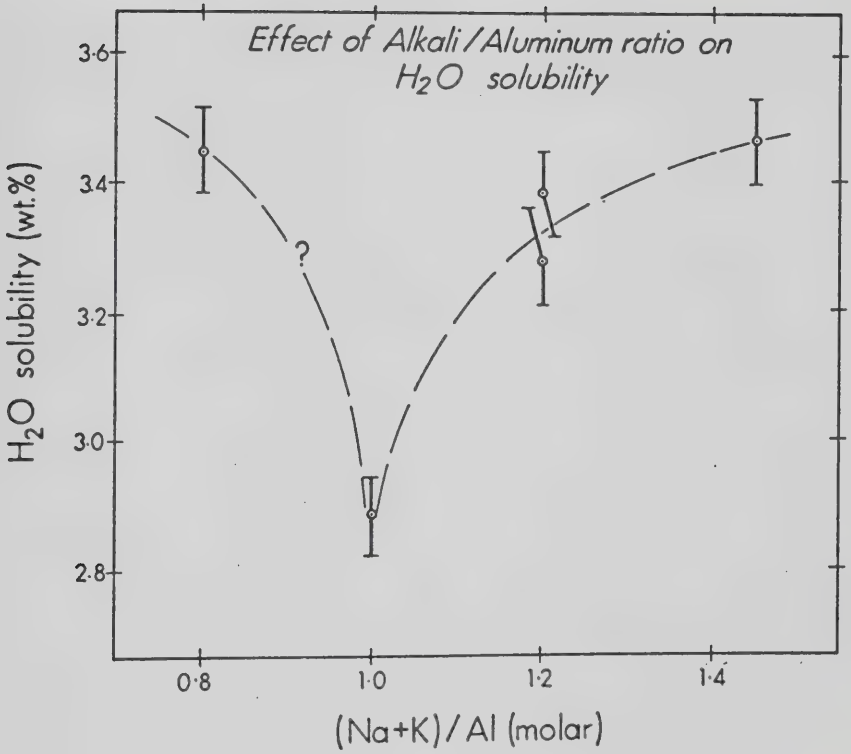




TABLE 10

DEPENDENCE OF THE EQUIMOLAR SOLUBILITY OF WATER IN MELTS ON THE ATOMIC RATIO OF TOTAL ALKALIS TO ALUMINUM AT 970 BARS H<sub>2</sub>O PRESSURE

Run	Series	SiO <sub>2</sub> wt %	(Na + K)/Al molar	X <sub>w</sub> <sup>m</sup>
61	NOR	77.92	0.97	.308
37	EOR	77.29	0.97	.322
80	EA1.2K	77.49	1.19	.363
38	EA1.2K	77.53	1.20	.356
36	EAK	77.53	1.46	.372
$X_w^m = 0.200 + 0.124 (Na + K)/Al$ r.m.s. error of fit = 0.0110				





### **Solubility in a phonolite liquid**

The 970 bar solubility of  $H_2O$  in the phonolite liquid exceeds that of all the granitic melts investigated. The phonolite composition, which has alkali/aluminum equal to 1 and very much less silica than those runs listed in Table 10, does not satisfy the linear relation obtained in Table 10.

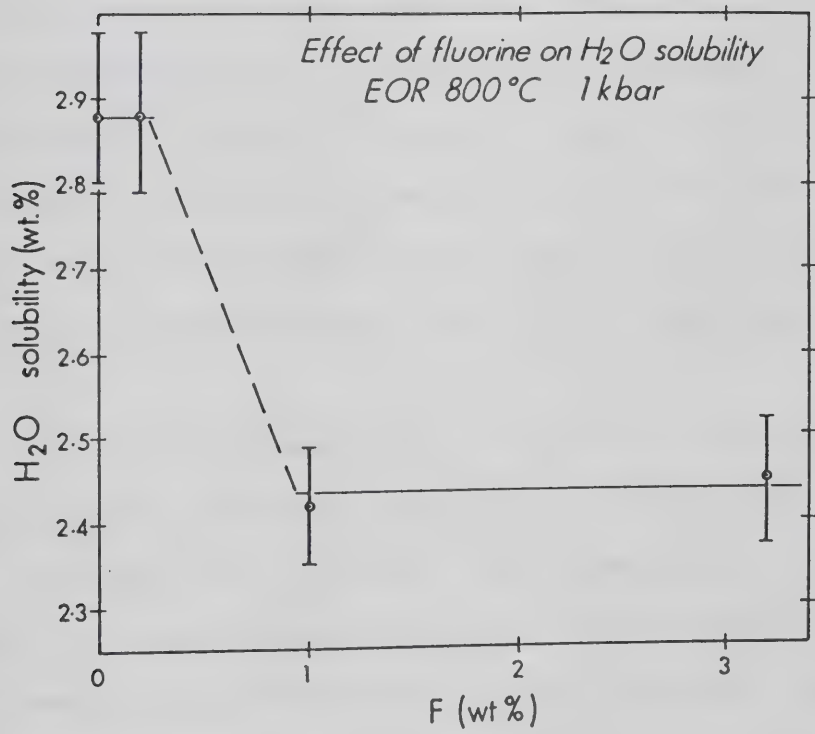
### **Effect of fluorine on solubility**

Three fluorine-bearing melts of EOR composition, whose synthesis is described in chapter 6, were analyzed for water in an effort to determine the effect of added fluorine on the solubility of water in this melt. The results of these analyses are presented in Figure 24. It is clear that fluorine added to haplogranitic melts decreases the solubility of water in these melts. These results contrast with the chemographic data of Koster van Groos and Wyllie (1968) and Wyllie (1979) which indicate enhanced water solubility in fluorine-bearing feldspar melts. The observed decrease in water solubility from this study implies that fluorine is incorporated within the silicate melt structure in a way which reduces the number of sites available for water dissolution.

If water is dissolved predominantly as hydroxyl ions coordinated by tetrahedrally-coordinated cations (Burnham, 1979, 1981) then perhaps fluorine is simply substituting for



Figure 24. Effect of fluorine on water solubility.





OH<sup>-</sup> in the depolymerized melt structure.

#### D. Discussion

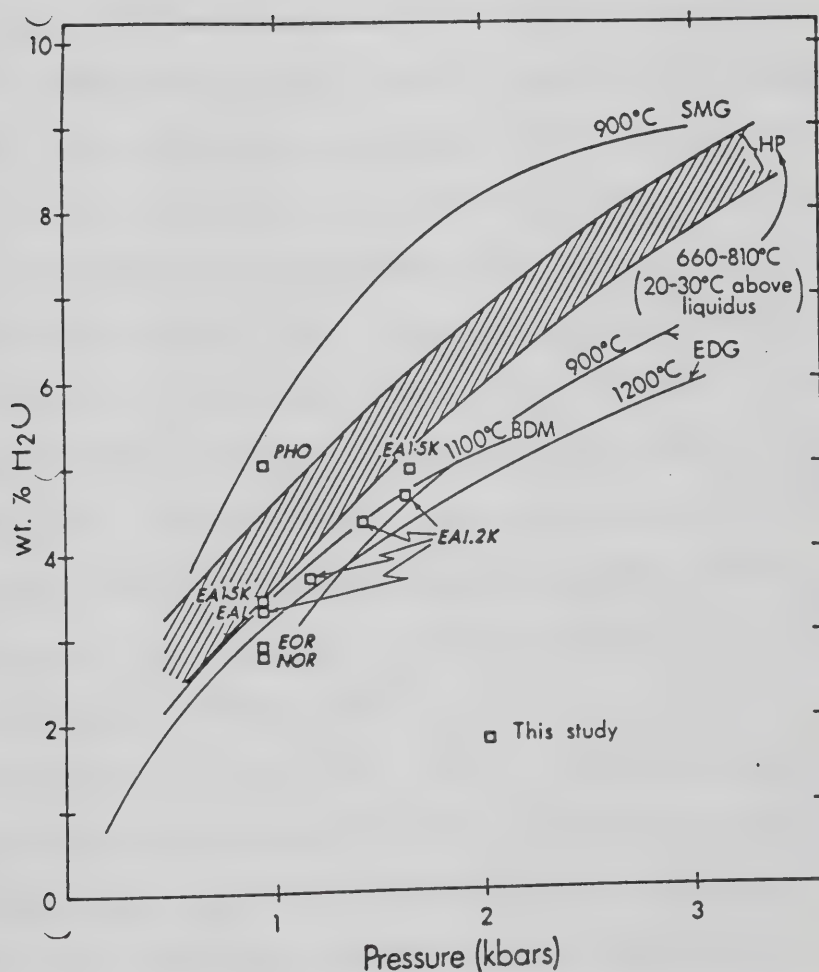
##### Comparison with earlier determinations

The determinations of water solubility in haplogranitic liquids from this study are shown (Fig. 25) in relation to other determinations at low pressures. Although the results are generally similar to those of earlier workers, the effects of pressure and composition on the water solubilities are evident in the results of this study and may help to explain some of the differences shown in Figure 25.

All previous measurements of water solubility in granitic melts (except those of Khitarov *et al.*, 1959, 1967) have employed one or both of the chemographic and weight-loss techniques. The chemographic technique involves the construction of isobaric T-X or rock-water pseudobinary phase diagrams (see Burnham and Jahns (1962) for discussion). In these diagrams the intersection of the water-saturated liquidus with the divariant L-L+V or L-L+C curve is determined. The intersection gives the concentration of water equal to the solubility limit. However, according to Day and Fenn (1982), water contents may be overestimated by as much as 1.0 wt% by using the L-L+V or 'dimple' technique. At pressures below two kbar the



Figure 25. Solubility determinations in natural and synthetic granites. (BDM, Beinn an Dubhaich granite, Oxtoby and Hamilton, 1978b; SMG, Stone Mountain granite, Goranson, 1931; EDG, El'Dzurtinskii granite, Khitarov *et al.*, 1959; HP, Harding pegmatite, Burnham and Jahns, 1962). Data from this study are for  $T = 800^{\circ}\text{C}$ .







L-L+C technique requires the careful addition of small amounts of water to experimental charges and the execution of water-undersaturated experiments on melts for which equilibrium is difficult to achieve.

In the weight-loss technique, water concentrations are obtained by comparison of the weight of  $H_2O$  added to the charge before the experiment with the weight of the post-run hydrous glass after the charge has been pierced and heated to  $110^{\circ}C$  (Hamilton *et al.*, 1964). Because the charges are generally oversaturated with  $H_2O$ , the run products, especially below 2 kbar, are vesicular and the amount of  $H_2O$  in the vesicles must be subtracted from the total  $H_2O$  determined by weight loss (Burnham and Jahns, 1962). Alternatively, if the vesicles can be ruptured by stepwise heating without loss of any  $H_2O$  from the glass (e.g., Oxtoby and Hamilton, 1978a), then it may be possible to determine the solubility from weight loss measurements during heating of vesicular glass. Uncertainties for weight loss techniques are predictably rather large.

In contrast, the experimental, sample preparation, and microanalytical techniques used in the present work permit the solubility to be determined with a variation of about  $\pm 0.10$  wt% (2 standard deviations) in replicate experiments at pressures from 1.0-2.0 kbars. The principal advantage over the previously mentioned techniques are the high precision and the fact that the measured water is wholly derived from the glass. Other significant advantages are



that the technique does not require multiple runs, precise determination of a phase boundary, or precise measurement of the amount of water added to an experimental charge.

From the comparison of the present data and previous work for granitic melts depicted in Figure 25, two major conclusions can be drawn. The first conclusion is that the results of this study at 800°C and those of Khitarov *et al.* (1959) for the El'Dzurtinski granite at 900°C are approximately similar. On the other hand the data of Oxtoby and Hamilton (1978b) on the Beinn an Dubhaich granite, although similar in magnitude, were obtained at 1100°C. The second conclusion is that the solubilities from this study are lower than those of Burnham and Jahns (1962) on the Harding pegmatite at temperatures between 660-810°C and those of Goranson (1931) on the Stone Mountain at 900°C. The Stone Mountain, El'Dzurtinskii and Beinn an Dubhaich granites are approximately similar in alkali/aluminum ratios but they vary considerably in their K/Na ratios. The Harding pegmatite is distinct in having high contents of Rb, Li and fluorine (see Burnham, 1979). Oxtoby and Hamilton (1978b; see also Voigt *et al.*, 1981) showed that the equimolar solubility of water is significantly greater in  $\text{NaAlSi}_3\text{O}_8$  melt than in  $\text{KAlSi}_3\text{O}_8$  melt. It is concluded that compositional variations and measurement techniques are causes for these differences. These problems have been reviewed recently by Day and Fenn (1982).



It is emphasized that the equimolar solubility of water is enhanced in increasingly peralkaline melts and this variation is not predicted by the model of Burnham (1979). The model of Burnham (1981) does reproduce the solubility determinations for PHO at 970 bars (wt% H<sub>2</sub>O calc. = 5.02); and EA1.2K at 1620 bars (wt% H<sub>2</sub>O calc. = 4.68) but overestimates all the other melt solubilities in Table 8. Further discussion on solubilities in feldspathic melts is outside the scope of this study which pertains to haplogranitic melts and natural granitic melts.

The fact that phonolitic melts show strongly enhanced solubility of H<sub>2</sub>O over SiO<sub>2</sub>-saturated compositions indicates the potential for a far more dramatic role for H<sub>2</sub>O in the crystallization and emplacement of phonolitic magmas. Generally, it is clear that a range of water solubilities are to be expected in granitic melts of variable composition. These differences must be taken into account in the geochemical modelling of processes such as pegmatite formation, hydrothermal activity, crystallization, volatile exsolution, and eruptive mechanisms for granitic magmas.

### **E. Geological application**

The experimentally determined solubility of water in haplogranitic melts and determinations of water in rhyolitic melt inclusions in phenocrysts may be used to estimate the minimum pressure of crystallization for the Bishop Tuff.



Druitt *et al.* (1982) determined the concentration of water in rhyolitic glass in quartz from the basal Plinian airfall unit of the Bishop Tuff to be  $4.9 \pm 0.5\%$ . A vacuum fusion gas analyser method was used. The glass contained 77.6%  $\text{SiO}_2$ , 13.3%  $\text{Al}_2\text{O}_3$ , 0.6%  $\text{FeO}$ , 0.5%  $\text{MgO}$ , 0.3%  $\text{CaO}$ , 3.9%  $\text{Na}_2\text{O}$ , and 4.6%  $\text{K}_2\text{O}$  (A. T. Anderson, personal communication). The gram molecular weight of the anhydrous melt (286 g) was calculated by the method of Burnham (1979). The  $\text{Na}/(\text{Na}+\text{K})$  and  $\text{Si}/\text{Al}$  ratios are 0.563 and 4.95, respectively, and near to or within the range investigated. The alkalies Na and K account for about 90 mole % of the exchangeable cations and the range of exchangeable cations to aluminum is 0.96. Therefore, the equimolar solubility for the stated composition is estimated to be  $X = 0.0111 \times (f(\text{H}_2\text{O}), \text{bars})$ . Accordingly, the pre-eruption fugacity of water estimated from the  $4.9 \pm 0.5\%$  in the melt inclusions at  $800^\circ\text{C}$  is  $1630 \pm 200$  bars. The pressure of water is estimated to have been  $2100 \pm 200$  bars. The implied minimum depth of origin of these phenocrysts is  $7.8 \pm 1.1$  km. The known presence in these inclusions of other components such as  $\text{CO}_2$  (A. T. Anderson, personal communication) would increase the minimum pressures and depths of crystallization. Druitt *et al.* (1982) reported a minimum concentration of water (2 wt%) in rhyolitic inclusions in quartz phenocrysts from the last erupted Mono Lobe. Our solubility measurements suggest minimum fugacities and pressures of  $\text{H}_2\text{O}$  of 480 and 530 bars, respectively. The direct measurements of pre-eruption water contents (Druitt







*et al.*, 1982) and solubility of water in related haplogranitic melts at 1-2 kbar and 800°C (this study) yield more direct estimates of pressures than are available from mineral equilibria (Hildreth, 1979).

The increase in water solubility with increasing peralkalinity observed in this work has at least one major implication for the petrogenesis of hydrous peralkaline melts. Silicic peralkaline volcanic suites often exhibit the chemical characteristic of increasing peralkalinity with increasing magmatic evolution. This effect was attributed by Bowen (1928) to the predominant crystallization of feldspar from such melts which results in residual peralkaline melts becoming more extremely peralkaline (i.e. the "plagioclase effect"). The data from this study show that one effect of increasing peralkalinity on an evolving magma system is to extend the percentage of crystallization which can occur before the residual magma becomes saturated with water.



## VI. Major element partitioning

### A. Introduction

Crystallization of hydrous granitic magmas at depth commonly results in the eventual saturation of the residual melt phase with water. Water saturation combined with further crystallization causes vesiculation of an aqueous fluid from the magma by the process of second boiling. The composition of the aqueous phase released in this manner is an important parameter in alteration of the country rocks and in the reconstruction of the chemical compositions of magmas which yield holocrystalline granitic plutons.

Chlorine-rich, magmato-hydrothermal systems are often host to economic concentrations of various metals (Burnham, 1979) and, therefore, the composition of chlorine-bearing fluids in equilibrium with granitic melts has been extensively investigated by Burnham (1967 and data in Clark, 1966). Pichavant (1981) has produced equivalent data for boron-bearing systems. Examples of fluorine-rich magmato-hydrothermal systems occur in several localities (Bailey, 1977) illustrating the need for a better understanding of their geochemistry. This study was undertaken to characterize the chemical composition of the aqueous fluid phase in equilibrium with fluorine-rich granitic melts.



## B. Experimental and analytical methods

The starting compositions chosen for these experiments are shown in Figure 26. The glass compositions are centered on the 1 kbar haplogranite minimum melting composition (Tuttle and Bowen, 1958) and represent two compositional series ; KOR - EOR - NOR along the exchange vector  $\text{KNa}_{-1}$ , and EAK1.5 - EAK1.2 - EOR - EAL0.8 - EAL0.5, along the exchange vector  $\text{Al}_2\text{Na}_{-1}\text{K}_{-1}$ . These compositions were chosen in order to evaluate the effect of melt Na/K ratio and alkali/aluminum ratio on melt/vapor partitioning.

The glasses used in the hydrothermal runs were synthesized from reagent-grade  $\text{Na}_2\text{CO}_3$ ,  $\text{K}_2\text{CO}_3$ ,  $\text{Al}_2\text{O}_3$  and  $\text{SiO}_2$  by using standard techniques described by Bowen and Schairer (1956). The compositions of the anhydrous glasses used as starting materials were determined by electron microprobe (Table 11). Experiments were conducted in cold-seal pressure vessels at 1 kbar and 800°C. Fifty milligrams of powdered glass was added to fifty milligrams of HF solution (1, 2 or 4 wt% HF) in platinum capsules. The capsules were welded and checked for possible leakage by testing for weight loss after 15 minutes in an 110°C drying oven. Leak-free capsules were loaded into the cold-seal vessels and were raised to run pressure using an air-driven hydraulic pump. Pressurized capsules were heated to run temperature by using Kanthal-wound resistance furnaces mounted concentrically about the vessels along a vertical axis. Temperatures were monitored with Chromel-Alumel thermocouples and the actual



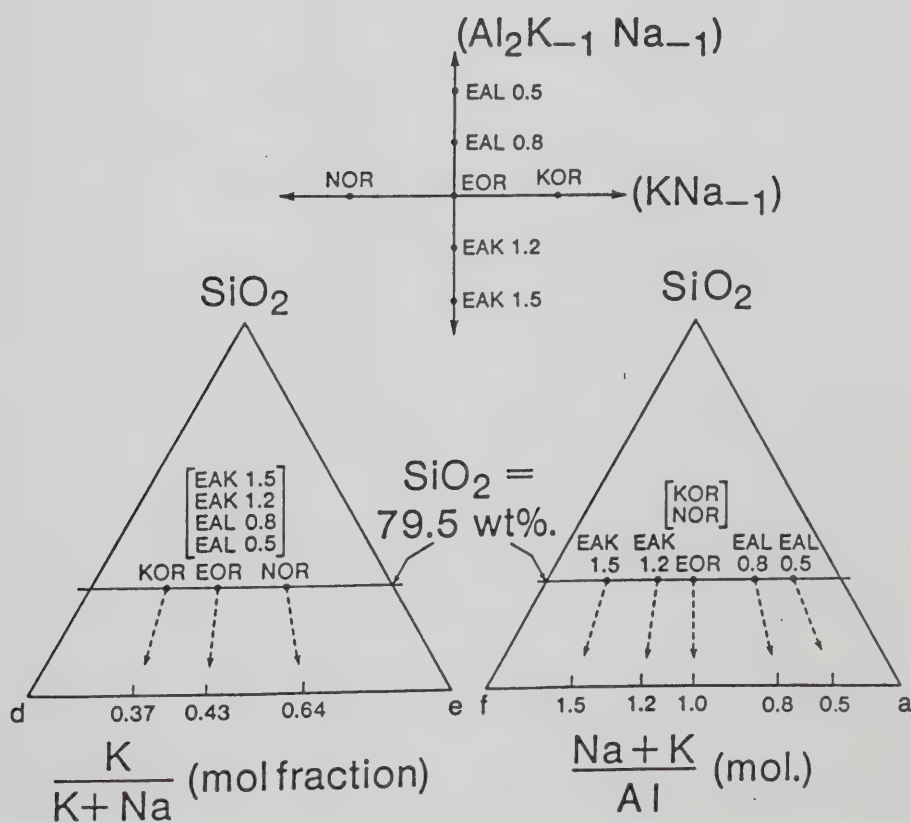
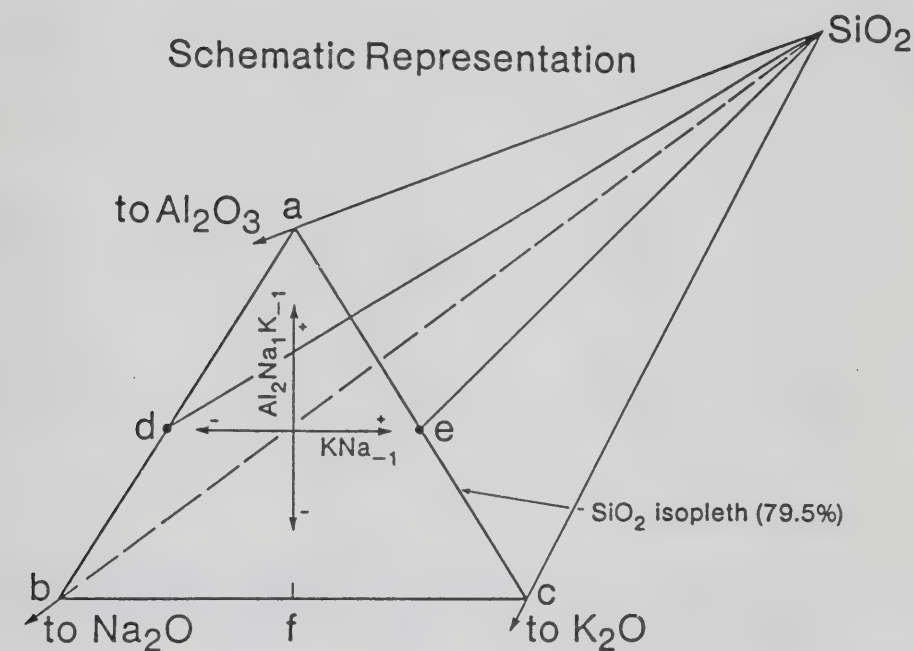
Figure 26. Starting compositions in  $K_2O$ - $Na_2O$ - $Al_2O_3$ - $SiO_2$ .





Table 11 : Microprobe analyses of starting glasses.

Glass	Na <sub>2</sub> O	K <sub>2</sub> O	Al <sub>2</sub> O <sub>3</sub>	SiO <sub>2</sub>	TOTAL
EOR	3.94	4.52	11.48	80.0	99.94
NOR	4.75	3.23	11.65	79.4	99.03
KOR	2.41	6.37	11.45	78.7	98.93
EAL0.5	2.27	2.73	12.30	81.6	98.90
EAL0.8	3.65	4.31	13.71	78.4	100.07
EAK1.2	4.41	4.91	10.51	80.2	100.03
EAK1.5	5.18	5.70	9.77	79.2	99.85

-uncertainties quoted as percent of the amount present (3 standard deviations) are as follows: SiO<sub>2</sub>,0.69%; Al<sub>2</sub>O<sub>3</sub>,1.78%; K<sub>2</sub>O,2.58%; Na<sub>2</sub>O,4.76%.



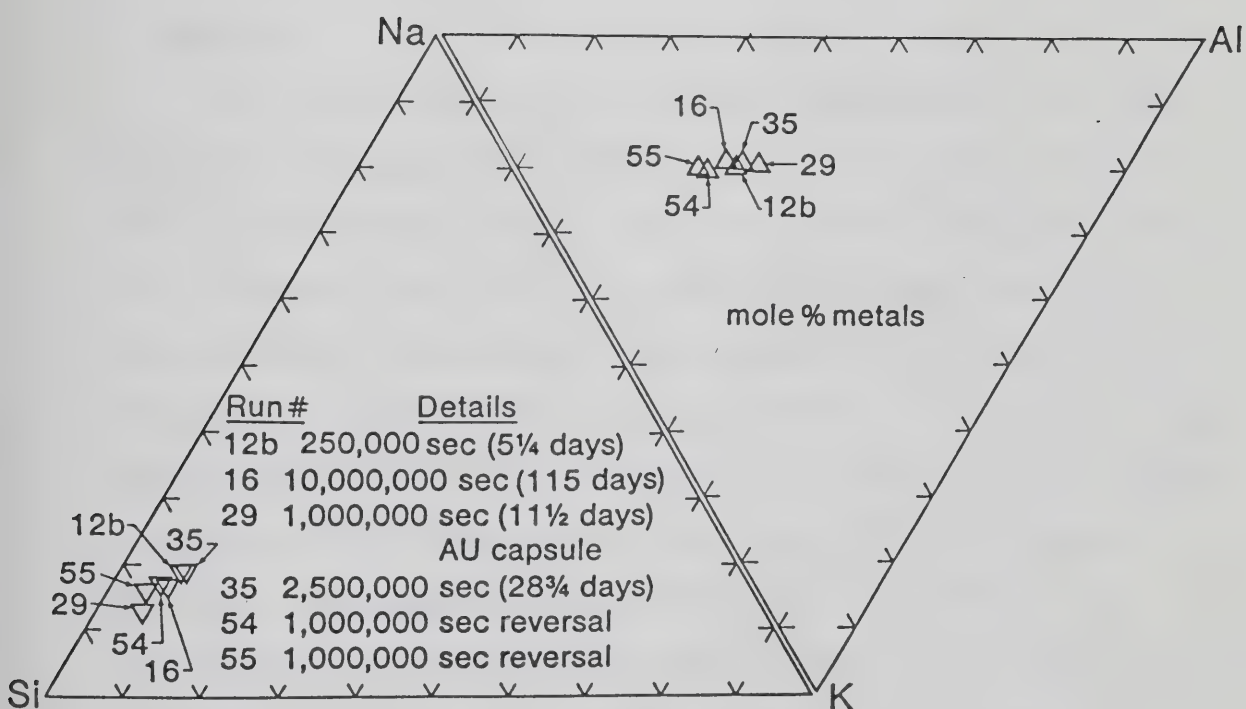
temperatures are believed accurate to  $\pm 5^{\circ}\text{C}$ . Pressures were measured with Bourdon-tube gauges previously calibrated with a Heise gauge and are accurate to  $\pm 20$  bars. Run durations were  $10^6$  seconds for all runs except those which form a time series test of equilibrium (runs 12b, 16, 27 and 35). The charges were quenched isobarically by opening the vessel to the pressure line and by pumping for the duration of the quench .

Reversal experiments were accomplished using the fluorine-bearing glasses from forwards experiments. Fluorinated glasses were ground in an agate mortar, rinsed with distilled water, and fifty milligrams of glass were added to fifty milligrams of triple-distilled water. Reversals were then run under equivalent conditions as the forwards experiments. As a check on the inert behavior of platinum in the presence of fluorine-bearing aqueous fluids at this pressure and temperature, duplicate experiments were conducted using gold capsules and equivalent results were obtained (Fig. 27).

Run capsules which suffered no weight change ( $< 1$  milligram) and no visible signs of breach during the run, were ultrasonically cleaned in acetone and frozen in liquid nitrogen prior to opening. The frozen capsules were slit longitudinally with a razor blade, immersed in triple-distilled  $2\text{N HNO}_3$ , and returned to the ultrasonic bath to help dissolve quench fluorides. Atomic absorption spectrometric analyses were carried out using the Dept. of



Figure 27. Reversals and time series experiments in molar Na-K-Al-Si space.





Geology Perkin Elmer 503 spectrophotometer. Standards for Na, K, Al and Si were prepared in  $\text{HNO}_3$  media. For certain experiments (runs 16, 20, 27 and 29) an aliquot of the remaining fluid was titrated to neutral pH by using 8% NaOH, combined with a total ionic strength buffer, and analyzed for fluorine by using an Orion fluorine specific electrode.

### C. Results

The results of Na, K, Al and Si analyses of the fluid phase are presented in Table 12. Runs # 12b, 16, 27 and 35 form a time series test for equilibrium and runs # 54 and 55 are reversals. Run # 35 is a gold-encapsulated experiment. The attainment of chemical equilibrium in the partitioning of Na, K, Al and Si between vapor and melt is evident in the results of Table 12. Figure 27 is a projection of the solute contents of the vapor phase into molar Na-K-Al-Si space. Figure 27 indicates the reproducibility obtained in the analysis of the solute, and these projections are used in subsequent figures. The largest scatter in the data is in Al and Si content due to the relatively poor precision of the atomic absorption analyses at these low levels (actual analyzed solutions contained 1-10 ppm Al and 10-50 ppm Si). The solute yields for EOR runs with 1, 2, and 4wt% fluorine and chlorine added as HF and HCl, respectively, are shown in Figure 28. Fluorine and chlorine have similar effects on the solubility of Na and K. Na and K contents increase rapidly with added F or Cl. The dissolved contents of Si, and





Figure 28. Solute yields for Na, K, Al and Si.

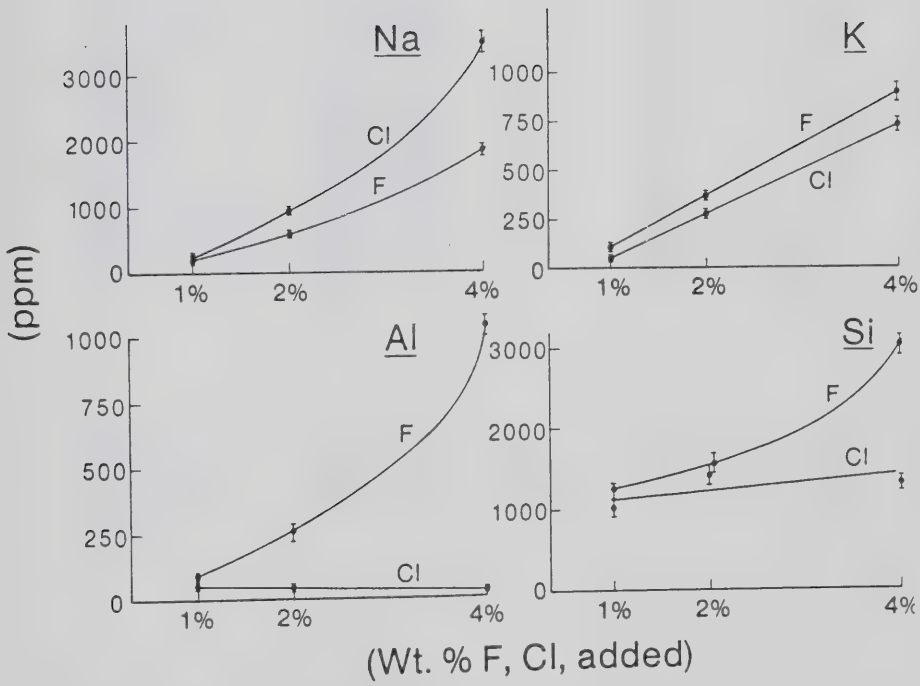




Table 12 : Na, K, Al and Si analyses of the vapor phase.

Run	Composition	Duration (sec)	Na	K	Al	Si
27	EOR2F	1,000,000	425	250	206	2153
12b	EOR2F	2,500,000	450	296	300	1870
16	EOR2F	10,000,000	443	257	208	1780
29	EOR2F*	1,000,000	366	250	288	1769
35	EOR 2F	25,000,000	490	310	350	1800
54	EOR2F**	1,000,000	393	232	194	1911
55	EOR2F**	1,000,000	373	242	119	2018
32	NOR2F	1,000,000	437	147	252	2364
33	KOR2F	1,000,000	215	298	204	2136
20	EOR4F	1,000,000	1986	921	1072	3178
23	EOR1F	1,000,000	219	106	60	1066
50	EAK1.2-2F	1,000,000	835	627	194	2552
51	EAL0.8-2F	1,000,000	528	303	417	1556
72	EAL0.5-2F	1,000,000	402	207	469	2709
74	EAK1.5-2F	1,000,000	1071	689	209	1818
15	EOR2C1	1,000,000	1940	370	40	1380
22	EOR1C1	1,000,000	250	43	60	1010
19	EOR4C1	1,000,000	3510	731	25	1270

-\* gold capsule experiment

\*\*\* reversal experiment

- all analyses quoted as ppm; uncertainties in analyses are as follows: Na and K ( $\pm 25$  ppm); Al ( $\pm 50$  ppm); Si ( $\pm 200$  ppm); F ( $\pm 200$  ppm).



especially Al, increase substantially with increasing fluorine in the vapor phase, while chlorine has little or no effect on Si solubility and an apparent negative effect on Al solubility.

Yields of fluorine from the vapor phase are presented in Figure 29. A vapor/melt partition coefficient of 0.08 holds for the range 2 to 4 wt% F.

Figure 30 presents the molar projection of melt and vapor compositions for these experiments. Tie lines join melt compositions (solid triangles) to coexisting fluid compositions (open triangles). Clearly, the vapor composition is strongly dependent on melt composition. These projections show that all vapor compositions are more sodic and alkalic than the corresponding melt compositions. The alkali/aluminum ratios of the solute are directly controlled by the melt composition.

For convenience, vapor/melt distribution coefficients may be defined as follows :

$$D(\text{Na/K}) = \frac{(X_{\text{Na}}/X_{\text{K}})_{\text{vapor}}}{(X_{\text{Na}}/X_{\text{K}})_{\text{melt}}} \quad \text{and} \quad D(\text{Ak/Al}) = \frac{(X_{\text{Na+K}}/X_{\text{Al}})_{\text{vapor}}}{(X_{\text{Na+K}}/X_{\text{Al}})_{\text{melt}}}$$

The values of these distribution coefficients for the melts studied are given in Table 13. The value of  $D(\text{Na/K})$  ranges from 1.9 to 2.4 and decreases with increasing peralkalinity, while the value of  $D(\text{Ak/Al})$  ranges from 2.3 to 5.4 and is highest for peralkaline melts.



Figure 29. Solute yields for fluorine.

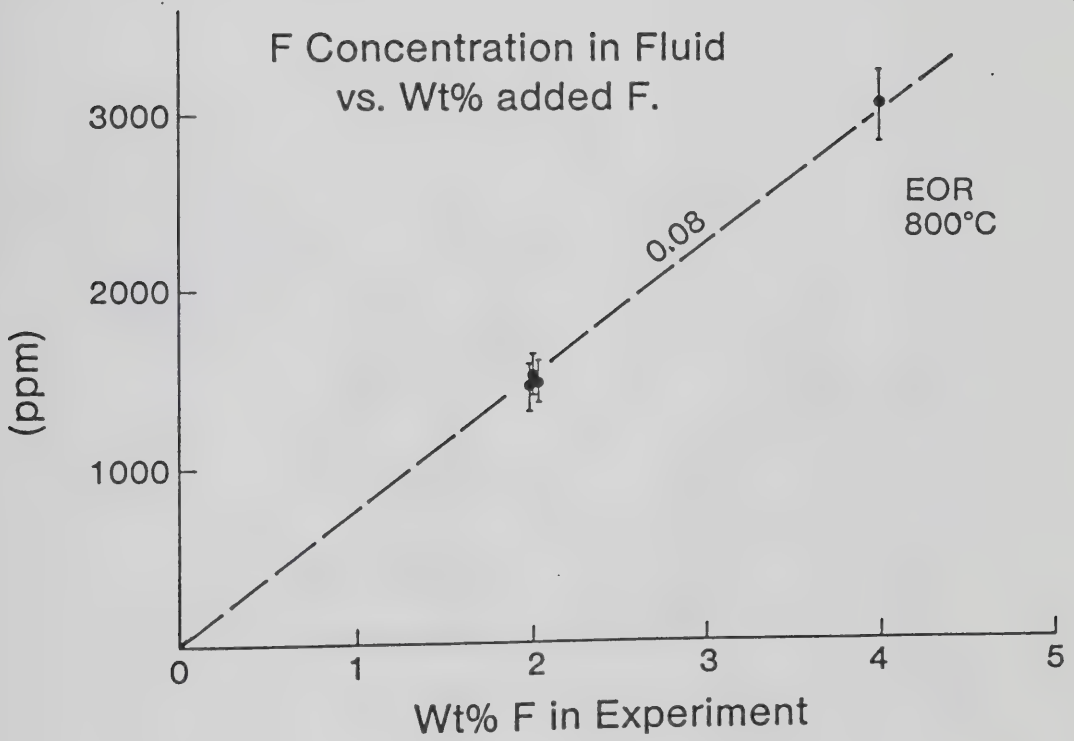






Figure 30. Experimental results of the partitioning experiments; effect of melt composition.

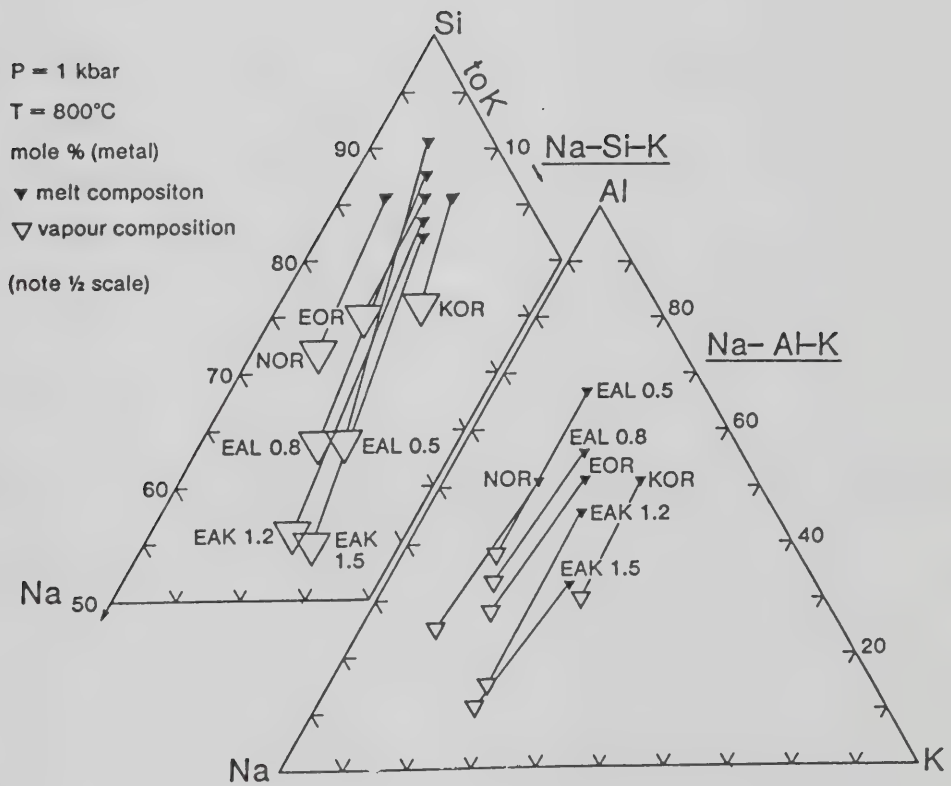




Table 13 : Melt/vapor distribution coefficients

Melt Composition	D (Na/K)	D (Ak/Al)
EAL0.5	2.4	3.0
EAL0.8	2.4	2.6
EOR	2.0	2.6
EAK1.2	1.9	4.7
EAK1.5	1.9	5.4
NOR	2.4	3.0
KOR	2.0	2.3

-uncertainties in melt/vapor partition coefficients are;  
 $D(\text{Na/K}) \pm 40\%$  ;  $D(\text{Ak/Al}) \pm 70\%$ .



## D. Discussion

Although the data presented above are not extensive enough to permit modelling of the exact stoichiometry of fluoride complexation in these fluids, the following observations are significant.

The solubility of Al is extremely sensitive to fluorine concentration, implying the existence of some form of aluminofluoride species in solution at this pressure and temperature. It cannot be concluded, however, that the Al solubility increase is due entirely to the formation of a simple Al-F complex. Increased Na, K and Si solubility with increasing fluorine concentration may be indicating the stabilization of one or more alkali-aluminofluoride complexes (cryolite-like species?) in solution. What does seem certain, however, is that fluorine does not compete with Al for a large proportion of the dissolved alkalis to the same extent as Cl. Anderson and Burnham (1983) have proposed that the low solubility of Al in hydrothermal fluids containing Cl is a direct consequence of alkali chloride complexation which decreases the amount of dissolved alkalis available for complexation in alkali-aluminosilicate complexes (feldspar stoichiometry). Decreasing Al solubility as a function of chlorine concentration in Figure 28 probably results from this effect.

Another aspect of fluoride complexation is that the effects of fluorine on hydrothermal fluids is remarkably



large for relatively low concentrations of dissolved F. At equivalent molalities of HF and HCl in these experiments, the vapor phase in chlorine-bearing experiments contains an order of magnitude more dissolved halide than the corresponding fluorine-bearing experiment, due to the different vapor/melt partition coefficients for fluorine (Hards, 1978) and chlorine (Kilinc and Burnham, 1972) .

Comparison with the data of Burnham (1967) for the Spruce Pine pegmatite melt-HCl-H<sub>2</sub>O is difficult due to the higher pressure range of Burnham's study (2-6 kbars); however, the pressure dependence of the composition of the chlorine-bearing fluid is not large (Fig. 2.7 in Burnham, 1967). Figure 31 compares the compositions of fluorine-bearing fluids coexisting with haplogranitic melts (this study) with the results of Burnham (1967) for chlorine-bearing fluids and Pichavant (1981) for boron-bearing fluids. From this comparison it is concluded that the solute contents of F-bearing fluids exhibit higher Al/(Na+K) ratios than either Cl- or B-bearing fluids while Cl-bearing fluids exhibit lower Si/(Na+K) ratios than either F- or B-bearing fluids.

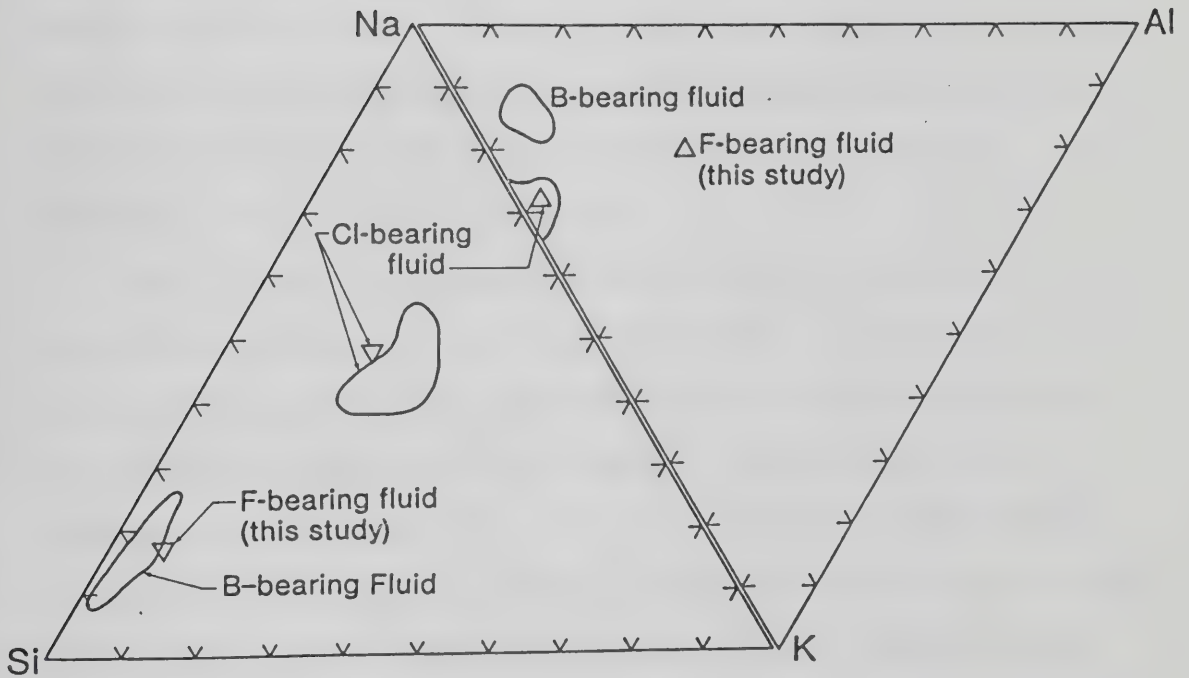
### **E. Geological implications**

The physical and chemical conditions which permit the coexistence of granitic magmas and aqueous fluids have received extensive consideration in the literature (Burnham, 1967, 1979; Holland, 1972; Burnham and Ohmoto, 1980).





Figure 31. Comparison of the compositions of fluorine-bearing, chlorine-bearing and boron-bearing fluids coexisting with granitic melts (see text for data sources).





An aqueous fluid phase may be evolved from a granitic magma in two ways; decompression and crystallization. The rapid ascent of a water-undersaturated melt is accompanied by a pressure decrease which, in turn, decreases the solubility of water in the melt and results in vesiculation. Alternatively, the crystallization, at constant total pressure, of dominantly anhydrous and water-poor phases from such a melt will also result in the water saturation of the diminishing melt volume due to the increasing proportion of dissolved water remaining in the melt (i.e., second, resurgent, or retrograde boiling).

One or both of these processes are involved in every geological situation where magmatic water forms as a separate phase. If the separation of an aqueous phase from an ascending magma occurs at depths which correspond to pressures greater than the critical region of the aqueous fluid then the immediate result of aqueous phase separation is a supercritical fluid. The present study simulates the case of a supercritical aqueous fluid which is equilibrated with such a melt.

If the aqueous phase separates at shallow, sub-volcanic depths corresponding to pressures of several hundred bars then the  $\text{H}_2\text{O}$ - $\text{NaCl}$  critical curve may intersect the solidus. In this case the aqueous phase may separate as two distinct fluid phases, a vapor and a brine, i.e. critical behavior. Evidence for the coexistence of sub-critical brine and melt is provided by Roedder and Coombs (1967). Primary boiling



also occurs if magmatic aqueous fluids produced at depth ascend into the P-T region of critical behavior, or if high temperature, low pressure fluids from more mafic, subvolcanic melts cool into this P-T region.

The formation of deep-seated, intrusion-hosted pegmatites is an example of the separation of a supercritical fluid phase and subsequent precipitation of dissolved species in the absence of boiling (Jahns and Burnham, 1969) Many pegmatitic greisens may form in this manner (Shcherba, 1970, Burt, 1981). In contrast, the fluid inclusion evidence of simple or first boiling is widespread in shallow, subvolcanic magmato-hydrothermal systems such as porphyry Cu deposits (Burnham and Ohmoto, 1980; Gustafson, 1978; Titley and Beane, 1980).

Fluorine has a high melt/fluid partition coefficient compared with chlorine (Hards, 1978; Kilinc and Burnham, 1972) . Therefore, hydrous granitic magmas, containing similar amounts of fluorine and chlorine, which become water-saturated will yield Cl-dominated aqueous fluids. Fluid inclusions often record fluid salinity and compositions which reflect post-solidus modification by primary boiling.

Despite the affinity of chlorine for aqueous fluids, evidence for mild to extreme enrichments of fluorine in certain granitic magmas and associated fluids is evidenced by petrochemical studies of silicic hypabyssal and volcanic rocks (Kovalenko, 1973; Bailey, 1977; Eadington and Nashar,



1978; Burt *et al.*, 1982; Christiansen *et al.*, 1983, 1984) and the mineral chemistry of equivalent plutons (Pauly, 1960; Gunow *et al.*, 1980; Nedachi, 1980; Czamanske *et al.*, 1981). Fluorine enrichment in such systems as deep-seated pegmatitic greisens (Burt, 1981), shallow Mo-porphyrries, stockwork Mo and vein-type Sn and W deposits (Westra and Keith, 1981; Huspeni *et al.*, 1984) and lithophysal topaz rhyolites (Burt *et al.*, 1982; Christiansen *et al.*, 1983, 1984) all clearly indicate that F-dominated magmato-hydrothermal systems can and do occur. The causes of such fluorine concentration are not clearly understood and several factors may contribute to their formation. The most crucial factor may be the early depletion of the systems in chlorine by fluid escape. Certainly, the evidence for multiple intrusion and protracted magmatic evolution of fluorine-rich systems does exist (White *et al.*, 1980). Alternatively, the magmas may have originated in Cl-poor source regions due to prior metasomatic and/or magmatic processes which resulted in chlorine depletion.

Regardless of the causes for the development of fluorine-rich systems, one of the most important considerations for the magmato-hydrothermal systems which they yield is the role of fluorine in enhancing the solubilities of dissolved metals. In most cases, fluorine is eventually partitioned into a fluid phase which is responsible for its mobility and concentration.





F-rich systems are also characterized by evidence of Al mobility, a feature absent in Cl-dominated systems (Titley and Beane, 1980; Anderson and Burnham, 1983; Rubie and Gunter, 1983). The results of this study provide an experimental confirmation of the mobility of Al in close association with fluorine-rich igneous rocks as evidenced by distal fluor-muscovite veins in fluorine-rich skarns (Barton, 1982); massive cryolite roof rocks (Pauly, 1960); topaz-lined vesicles in lithophysal rhyolites (Burt *et al.*, 1982; Christiansen *et al.*, 1983, 1984), and cryolite + fluorite + elpasolite daughter crystals in fluid inclusion of hypabyssal ongonites (Naumov *et al.*, 1971, 1977).

Unfortunately, the results presented here can only be applied qualitatively at this time because the melt-fluid system investigated is multivariant in the absence of calibrated buffer phases for all components except hydrogen. Quantification of fluorine speciation and fluoride complex stability in aqueous fluids may be measured by mineral solubility studies (Anderson and Burnham, 1967; Frantz *et al.*, 1981) and exchange mineral/fluid exchange equilibria (Orville, 1963; Barton and Frantz, 1983). The thermodynamic data from these experiments will eventually allow quantitative modelling of aqueous fluid behavior. Extension of these studies to mineral + melt + fluid systems should eventually permit further thermodynamic modelling of water-saturated natural silicate melts.



## VII. Summary and conclusions

### A. Summary of results

Various aspects of the solution of fluorine in aluminosilicate melts have been investigated in this thesis. The following is a short summary of the results.

The viscosity of polymerized melts in  $\text{Na}_2\text{O}-\text{Al}_2\text{O}_3-\text{SiO}_2$  is strongly reduced by the addition of fluorine. These viscosity reductions are similar to the effect of added water on melt viscosity. The viscosity-reducing effect of fluorine increases with  $\text{SiO}_2$  in melts along the join  $\text{NaAlO}_2-\text{SiO}_2$  and at 75 mole percent  $\text{SiO}_2$ , fluorine-bearing melts increase in viscosity from peralkaline through albite to peraluminous compositions. Due to the lower activation energy of viscous flow in fluorine-bearing melts, the viscosity reductions with fluorine addition increase with decreasing temperature.

The chemical diffusion of fluorine in these melts is much faster than the self-diffusion of oxygen but significantly slower than the chemical diffusion of water. The chemical diffusion of fluorine is a binary, concentration-independent, composition-dependent exchange with oxygen. This behavior contrasts with the chemical diffusion of water which may involve alkali exchange. Volatilization of fluorine from dry aluminosilicate melts is predominantly as  $\text{SiF}_4$  and this property has been used to



investigate fluorine diffusivity at 1 atmosphere. Fluorine increases the diffusivity of oxygen and network-modifying cations in aluminosilicate melts as does water. The pressure dependence of F-O interdiffusion is very slight in the pressure range of 10 to 15 kilobars but from 0.001 to 10 kilobars an increase in interdiffusivity is observed. F-O interdiffusivity decreases along the join  $\text{NaAlO}_2\text{-SiO}_2$  and, at 75 mole percent  $\text{SiO}_2$ , F-O interdiffusion is slower in albite melt than in peralkaline and peraluminous melts.

The solubility of water in haplogranitic melts at 1 to 2 kilobars and  $800^\circ\text{C}$  is greater in peralkaline and peraluminous melts than in the 1 kilobar granitic minimum melt. Phonolitic melts dissolve twice as much water as granitic melts. Fluorine slightly decreases the solubility of water in granitic melts.

Fluorine, in contrast with chlorine, increases the solubility of aluminum in magmato-hydrothermal fluids. The distribution of Na and K between granitic melts and coexisting aqueous fluids is controlled by the melt Na/K ratio and is similar for fluorine- and chlorine-bearing aqueous fluids. Despite the strong preference of fluorine for the melt phase, fluorine increases the aqueous solubility of each of Na, K, Al and Si in the fluid phase. The alkali/aluminum ratio of the fluid phase is influenced by the melt alkali/aluminum ratio ; however, the alkali/aluminum (molar) ratio of the fluorine-bearing aqueous fluid phase is greater than 1 in all experiments.



## B. Conclusions

### Melt structure

The dissolution of fluorine in dry aluminosilicate melts involves the replacement of oxygen in Si-O-(Al,Si) bridges by Si-F or Al-F units. Thus, fluorine depolymerizes the three-dimensional structure of polymerized melts in  $\text{Na}_2\text{O-Al}_2\text{O}_3\text{-SiO}_2$ . The viscous flow of aluminosilicate melts with added fluorine or water is similar, indicating that (Al,Si)-F and (Al,Si)-OH units within the melt have similar resistance to viscous flow. Despite this similarity, the transport of fluorine within aluminosilicate melts is unlike that of water. Fluorine transport occurs by an effective binary exchange with oxygen, whereas water diffusion probably involves alkali exchange. Failure of the Stokes-Einstein relationship to predict viscosity-diffusivity relationships in fluorine-bearing melts suggests that the mechanisms and/or species involved in viscous and diffusive transport in these melts are not equivalent.

In hydrous aluminosilicate melts, fluorine may compete directly with water for dissolution sites, thus decreasing the solubility of water in these melts. Fluorine is very effective in decreasing the activity of feldspar-forming components in hydrous aluminosilicate melts (Manning, 1981) and the decrease in water solubility with fluorine addition





may be an indirect consequence of the decrease in the activity of  $\text{NaAlO}_4$  units. The solubility of water in fluorine-free melts is strongly influenced by the alkali/aluminum ratio but not by the Na/K ratio. The behavior of water solubility as a function of alkali/aluminum ratio strongly suggests the operation of more than one mechanism of water solution. The preference of fluorine for Al-bearing species in supercritical aqueous fluids indicates that fluorine does not compete strongly with aluminum for the coordination of dissolved alkalies as is the case for chlorine.

### Geological implications

Silicic volcanic rocks which contain up to 2 weight percent fluorine are often characterized by low eruption temperatures, extensive lava flows, crystal-poor glasses, and topaz-lined lithophysae (Burt *et al.*, 1982). Such volcanics often have trace element signatures consistent with an origin involving extreme degrees of crystal fractionation (Christiansen *et al.*, 1984). The subvolcanic granites of equivalent chemistry are often host to economic concentrations of several elements whose enrichment can be explained by accumulation in residual melts during protracted magma fractionation (Christiansen *et al.*, 1983).

Several of these characteristics of fluorine-rich igneous rocks are readily explicable on the basis of the results of this and previous studies on the role of fluorine



in aluminosilicate melts.

Perhaps the most important consequence of fluorine concentration in late stage igneous melts is that fluorine can appreciably extend the magmatic "lifespan" of crystallizing granitic magmas by depressing the liquidus/solidus phase relationships several hundred degrees. This depression occurs in both dry (Koster van Groos and Wyllie, 1968) and wet (Manning, 1981) systems and one can reasonably infer, therefore, that the effect extends over the range of water-undersaturated conditions pertinent to the formation of many fluorine-rich silicic volcanics. Fluorine has a high melt/vapor partition coefficient (Hards, 1978) and appears to behave as an incompatible element in many silicic volcanic systems (Bailey, 1977). Progressive crystallization in such systems leads, therefore, to fluorine concentration in residual melts which in turn experience decreasing solidus temperatures. The fact that water-undersaturated, fluorine-rich rhyolites erupt at temperatures in the range 630 to 850°C (Bikun, 1980) is clear evidence of the influence of fluorine in such systems.

The influence of fluorine on melt diffusivities probably increases the nucleation and growth rates of observed phenocryst phases in fluorine-rich rhyolites. The effect is the "mineralizing action" that Buerger (1948) attributed to both  $F^-$  and  $OH^-$ . The concentration-independence of fluorine diffusion means that the effect of fluorine on melt diffusivities should be felt



at very low concentrations of dissolved fluorine, and that local enrichments of fluorine in the vicinity of growing crystals is unlikely. If protracted crystal fractionation is significant in the petrogenesis of fluorine-rich rhyolites, then crystal fractionation must operate as an efficient process in these melts. The viscosity-reducing effect of fluorine may be an important parameter that separates the crystal fractionation behavior of fluorine-rich rhyolites from that of fluorine-free rhyolites. Lower viscosities also result in the formation of large individual lava flows which travel considerable distances from their volcanic vents.

Finally, it is clear that some crystal-poor fluorine-rich magmas are sampled volcanically (Burt *et al.*, 1982). The result is rhyolites whose vesicles are lined with the quench products of an aqueous fluid phase which was released during eruption. Quench alkali fluorides in the lithophysae are rapidly leached by groundwaters, but the relatively insoluble fluor-topaz remains as evidence of the aluminum-carrying capacity of fluorine-bearing aqueous fluids.



## Bibliography

- Al-Dulaimy, J. A. M. (1978) A study of volatilisation from fluoride opal melts. unpub. M. Tech. Sci. thesis, Sheffield.
- Anderson, G. M. and Burnham, C. W. (1983) Feldspar solubility and the transport of aluminum under metamorphic conditions. American Journal of Science, 283-A, 283-297.
- Anfilogov, V. N., Glyuk, D. S. and Trufanova, L. G. (1973) Phase relations in interactions between granite and NaF at water vapor pressure of 1000 kg/cm<sup>2</sup>. Geochemistry International, 15, 30-32.
- Angell, C. A., Cheeseman, P. A. and Tamaddon, S. (1982) Pressure enhancement of ion mobilities in liquid silicates from computer simulation studies to 800 kilobars. Science, 218, 885-887.
- Arzi, A. A. (1978) Fusion kinetics, water pressure, water diffusion and electrical conductivity in melting rock, interrelated. Journal of Petrology, 19, 153-169.
- Bailey, D. K. and MacDonald, R. (1974) Fluorine and chlorine in peralkaline liquids and the need for magma generation





in an open system. Mineralogical Magazine, 40, 405-414.

Bailey, J.C. (1977) Fluorine in granitic rocks and melts : a review. Chemical Geology, 19, 1-42.

Barlow, D. F. (1965) Volatilisation of fluorides, borates and arsenic from glass. VII International Congress on Glass, Brussels, chapter 19, p.1-14.

Barton, M. D. (1982) Some aspects of the geology and mineralogy of the fluorine-rich skarn at McCullough Butte, Eureka County, Nevada. Carnegie Institute of Washington Yearbook 81, 324-328.

Barton, M. D. and Frantz, J. D. (1983) Exchange equilibria of alkali feldspars with fluorine-bearing fluids. Carnegie Institute of Washington Yearbook, 82, 377-381.

Bikun, J. V. (1980) Fluorine and lithophile element mineralization at Spor Mountain, Utah. U.S. Department of Energy Open File Report GJBX-225(80) , 167-377.

Bills, P. M. (1963) Viscosities in silicate slag systems. Journal of the Iron and Steel Institute, 201, 133-140.

Bockris, J. O'M. and Reddy, A. K. N. (1970) Modern Electrochemistry Vol. 1, Plenum Press, New York.



- Bond, W. L. (1951) Making small spheres. *Reviews of Scientific Instruments*, 22, 344-345.
- Bowen, N. L. (1928) *The evolution of the igneous rocks.* Princeton University Press, Princeton.
- Bowen, N. L. and Tuttle, O. F. (1950) The system  $\text{NaAlSi}_3\text{O}_8$ - $\text{KAlSi}_3\text{O}_8$ - $\text{H}_2\text{O}$ . *Journal of Geology*, 58, 489-511.
- Buerger, M. J. (1948) The structural nature of the mineralizer action of fluorine and hydroxyl. *American Mineralogist*, 33, 744-747.
- Burnham, C. W. (1964) Viscosity of a water-rich pegmatite. (abstr.) *Geological Society of America Special Paper*, 76, 26.
- Burnham, C. W. (1967) Hydrothermal fluids at the magmatic stage. In H. L. Barnes, ed. *Geochemistry of Hydrothermal Ore Deposits*, 34-76. Holt, Rinehart and Winston, New York.
- Burnham, C. W. (1975) Water and magmas: a mixing model: *Geochimica et Cosmochimica Acta*, 39, 1077-1084.
- Burnham, C. W. (1979) The importance of volatile constituents. In H. S. Yoder, ed. *The Evolution of the*



Igneous Rocks , . Princeton University Press.p. 439-482

Burnham, C. W. (1981) The nature of multicomponent aluminosilicate melts. Physics and Chemistry of the Earth, 13-14, 193-229.

Burnham, C. W. (1983) Deep submarine pyroclastic eruptions. In B. J. Skinner, ed. The Kuroko and related volcanogenic massive sulfide deposits. Economic Geology Monograph 5, p.142-148.

Burnham, C. W., Holloway, J. R. and Davis, N. F. (1969) Thermodynamic properties of water to 1000°C and 10,000 bars. Geological Society of America Special Paper 132.

Burnham, C. W. and Jahns, R. H. (1962) A method for determining the solubility of water in silicate melts. American Journal of Science, 260, 721-745.

Burnham, C. W. and Ohmoto, H. (1980) Late-stage processes of felsic magmatism. Mining Geology Special Issue, 8, 1-11.

Burt, D. M. (1981) Acidity-salinity diagrams - application to greisen and porphyry deposits. Economic Geology, 76, 832-843.

Burt, D. M., Sheridan, M. F., Bikun, J. V. and Christiansen,



E. H. (1982) Topaz rhyolites - Distribution, origin and significance for exploration. *Economic Geology*, 77, 1818-1836.

Carmichael, I. S. E., Turner, F. J. and Verhoogen, J. (1974) *Igneous Petrology*, McGraw Hill.

Carron, J-P. (1969) Vue ensemble sur la rheologie des magmas silicates naturels. *Bulletin de la Societe francaise de Mineralogie et de Cristallographie*, 92, 435-446.

Christiansen, E. H., Burt, D. M., Sheridan, M. F. and Wilson, R. T. (1983) The petrogenesis of topaz rhyolites from the western United States. *Contributions to Mineralogy and Petrology*, 83, 16-30.

Christiansen, E. H., Bikun, J. V., Sheridan, M. F. and Burt, D. M. (1984) Geochemical evolution of topaz rhyolites from the Thomas Range and Spor Mountain, Utah. *American Mineralogist*, 69, 223-236.

Clark, S. P. (1959) Effect of pressure on the melting points of eight alkali halides. *Journal of Physical Chemistry*, 31, 1526-1531.

Clark, S. P. (1966) *Handbook of physical constants*. Geological Society of America Memoir 97.





- Cooper, A. R. (1968) The use and limitation of the concept of an effective binary diffusion coefficient for multi-component diffusion. In J. B. Wachtman Jr. and A. D. Franklin, eds. Mass Transport in Oxides, National Bureau of Standards Special Publication, 296, p. 79-84.
- Cox, K. G., Bell, J. D. and Pankhurst, R. J. (1979) The Interpretation of Igneous Rocks. Allen and Unwin, London.
- Crank, J. (1975) The Mathematics of Diffusion. second edition, Oxford University Press.
- Czamanske, G. K., Ishihara, S. and Atkin, S. A. (1981) Chemistry of rock-forming minerals of the Cretaceous-Palaeocene batholith in Southwest Japan and implications for magma genesis. Journal of Geophysical Research, 86, 10431-10469.
- Danckwerth, P. A. (1980) Phase relations in the system  $\text{Na}_2\text{O}-\text{Al}_2\text{O}_3-\text{SiO}_2-\text{H}_2\text{O}-\text{HF}$ . Carnegie Institute of Washington Yearbook 80, 350-352.
- Day, H. W. and Fenn, P. M. (1982) Estimating the P-T-X( $\text{H}_2\text{O}$ ) conditions during crystallization of low calcium granites. Journal of Geology, 90, 485-507.



- Delaney, J. R. and Karsten, J. L. (1981) Ion microprobe studies of water in silicate melts: concentration-dependent diffusion in obsidian. *Earth and Planetary Science Letters* 52, 191-202.
- Druitt, T. H., Anderson, A. T., Jr. and Nagle, F. (1982) Water in rhyolitic magma, Bishop, California. (abstr.) *EOS Transactions of the American Geophysical Union*, 63, 451.
- Dumas, P., Corset, J., Carvalho, W., Levy, Y. and Neuman, Y. (1982) Fluorine-doped vitreous silica analysis of fiber optics preforms by vibrational spectroscopy. *Journal of Non-Crystalline Solids*, 47, 239-241.
- Dunn, T. (1982) Oxygen diffusion in three silicate melts along the join diopside-anorthite. *Geochimica et Cosmochimica Acta*, 46, 2293-2299.
- Dunn, T. (1983) Oxygen chemical diffusion in three basaltic liquids at elevated temperatures and pressures. *Geochimica et Cosmochimica Acta*, 47, 1923-1930.
- Eadington, P. J. and Nashar, B. (1978) Evidence for the magmatic origin of quartz topaz rocks from the New England batholith. *Contributions to Mineralogy and Petrology*, 67, 433-438.



- Eitel, W. (1965) Silicate Science II, Glasses, enamels and slags. Academic Press, New York.
- Fenn, P. M. (1973) Nucleation and growth of alkali feldspars from melts in the system  $\text{NaAlSi}_3\text{O}_8$ - $\text{KAlSi}_3\text{O}_8$ - $\text{H}_2\text{O}$ . unpub. Ph.D. dissertation, Stanford University, Stanford, CA.
- Frantz, J. D., Popp, R. K. and Boctor, N. Z. (1981) Mineral-solution equilibria - V. Solubilities of rock-forming minerals in supercritical fluids. *Geochimica et Cosmochimica Acta*, 45, 69-77.
- Friedman, I., Long, W. and Smith, R. L. (1963) Viscosity and water content of rhyolite glass. *Journal of Geophysical Research*, 68, 6523-6535.
- Friedman, I. and Long, W. (1976) Hydration rate of obsidian. *Science*, 191, 347-352.
- Glyuk, D. S. and Anfilogov, V. N. (1973a) Phase relations in the system Granite- $\text{H}_2\text{O}$ -HF at a pressure of 1000 kg/cm<sup>2</sup>. *Geochemistry International*, 9, 321-325.
- Glyuk, D. S. and Anfilogov, V. N. (1973b) Phase equilibria in the system granite-water-potassium fluoride at a water vapor pressure of 1000 kg/cm<sup>2</sup>. *Doklady Akademii Science USSR, Earth Science Section*, 210, 237-238.



- Goranson, R. W. (1931) The solubility of water in granitic magmas. *American Journal of Science*, 22, 481-502.
- Goranson, R. W. (1938) Silicate-water systems: phase equilibria in the  $\text{NaAlSi}_3\text{O}_8\text{-H}_2\text{O}$  and  $\text{KAlSi}_3\text{O}_8\text{-H}_2\text{O}$  systems at high temperatures and pressures. *American Journal of Science*, 35A, 71-91.
- Gotz, J., Hoebbel, D. and Wieker, W. (1976) Silicate groupings in glassy and crystalline  $2\text{PbO-SiO}_2$ . *Journal of Non-Crystalline Solids*, 20, 413-425.
- Gunow, A. J., Ludington, S. and Munoz, J. L. (1980) Fluorine in micas from the Henderson molybdenite deposit, Colorado. *Economic Geology*, 75, 1127-1137.
- Gustafson, L. B. (1978) Some major factors of porphyry copper development. *Economic Geology*, 70, 857-912.
- Hamilton, D. L. and MacKenzie, W. S. (1965) Phase equilibrium studies in the system  $\text{NaAlSiO}_4\text{-KAlSiO}_4\text{-SiO}_2\text{-H}_2\text{O}$ . *Mineralogical Magazine*, 34, 214-231.
- Hamilton, D. L., Burnham, C. W. and Osborn, E. F. (1964) The solubility of water and effects of oxygen fugacity and water content on crystallization in mafic magmas.





Journal of Petrology, 5, 21-39.

Hards, N. (1978) Distribution of elements between the fluid phase and silicate melt phase of granites and nepheline syenites. NERC Progress in Experimental Petrology IV, 88-90.

Harris, D. M. (1981a) The microdetermination of  $H_2O$ ,  $CO_2$  and  $SO_2$  in glass using a  $1280^\circ C$  microscope vacuum heating stage, cryopumping and vapor pressure measurements from 77 to 273 K. *Geochimica et Cosmochimica Acta*, 45, 2023-2036.

Harris, D. M. (1981b) Vesiculation and eruption of a subduction zone basalt. EOS Transactions of the American Geophysical Union, 62, 1084.

Harris, N. B. W. and Marriner, G. F. (1980) Geochemistry and petrogenesis of a peralkaline granite complex from the Midian Mountains, Saudi Arabia. *Lithos*, 13, 325-337.

Harris, P. G., Kennedy, W. Q. and Scarfe, C. M. (1970) Volcanism versus plutonism: the effect of chemical composition. in. G. Newall and N. Rast, eds. *Mechanisms of Igneous Intrusion*, Geological Journal Special Issue, 2, p.187-200.



- Hart, S. R. (1981) Diffusion compensation in natural silicates. *Geochimica et Cosmochimica Acta*, 45, 279-291.
- Henderson, J., Yang, L. and Derge, G. (1961) Self-diffusion of aluminum in  $\text{CaO-SiO}_2\text{-Al}_2\text{O}_3$  melts. *Transactions of AIME*, 221, 56-60.
- Hildreth, W. (1979) The Bishop Tuff: evidence for the origin of compositional zonation in silicic magma chambers. *Geological Society of America Special Paper* 180, 43-75.
- Hirayama, C. and Camp, F. E. (1969) The effect of fluorine and chlorine substitution on the viscosity and fining of soda-lime and potassium-barium silicate glass. *Glass Technology*, 10, 123-127.
- Hofmaier, G. and Urbain, G. (1968) The viscosity of pure silica. *Science of Ceramics*, 4, 25-32.
- Hofmann, A. W. (1980) Diffusion in natural silicate melts: a critical review. In R. B. Hargraves, ed. *Physics of Magmatic Processes* p. 385-415, Princeton University Press
- Holland, H. D. (1972) Granites, solutions and base metal deposits. *Economic Geology*, 67, 281-301.



- Hunnold, V. K. and Bruckner, R. (1979) Physikalische Eigenschaften und struktureller Feinbau von Natrium-Aluminosilicatglasern und -schmelzen. Glastechnische Berichte, 53, 149-161.
- Huspeni, J. R., Kesler, S. E., Ruiz, J., Tuta, Z., Sutter, J. F. and Jones, L. M. (1984) Petrology and geochemistry of rhyolites associated with tin mineralization in Northern Mexico. Economic Geology, 79, 87-105.
- Jahns, R. H. and Burnham, C. W. (1969) Experimental studies of pegmatite genesis I. A model for the derivation and crystallization of granitic pegmatites. Economic Geology, 64, 843-864.
- Jambon, A. (1982) Tracer diffusion in granitic melts: Experimental results for Na, K, Rb, Cs, Ca, Sr, Ba, Ce, Eu to 1300°C and a model of calculation. Journal of Geophysical Research, 87, 10797-10810.
- Jambon, A., Carron, J. P. and Delbove, F. (1978) Donneés preliminaires sur la diffusion dans les magmas hydrates: le cesium dans une liquide granitique a 3 kb. Comptes Rendus Academie Sciences, Serie D. 287, 403-406.
- Johannes, W. (1978) Melting of plagioclase in the system Ab-An-H<sub>2</sub>O and Qz-Ab-An-H<sub>2</sub>O and P(H<sub>2</sub>O)=5 kbars, an



equilibrium problem. Contributions to Mineralogy and Petrology, 66, 295-303.

Johannes, W, (1980) Metastable melting in the granite system Qz-Ab-An-H<sub>2</sub>O. Contributions to Mineralogy and Petrology, 72, 73-80.

Johnston, R. F., Stark, R. A. and Taylor, J. (1974) Diffusion in liquid slags. Ironmaking and Steelmaking 1, 220-227.

Karsten, J. L., Holloway, J. R. and Delaney, J. R. (1982) Ion microprobe studies of water in silicate melts: temperature-dependent water diffusion in obsidian. Earth and Planetary Science Letters, 59, 420-428.

Khitarov, N. I., Lebedev, E. B., Rengarten, E. V. and Arsen'eva, R. V. (1959) The solubility of water in basaltic and granitic melts. Geochemistry, 5, 479-492.

Khitarov, N. I., Kadik, A. A. and Lebedev, E. B. (1967) Separation of water from magmatic melts of granitic composition. Geochemistry International, 10, 41-49.

Kilinc, I. A. and Burnham, C. W. (1972) Partitioning of chloride between a silicate melt and coexisting aqueous phase from 2 to 8 kilobars. Economic Geology, 67,





231-235.

Kogarko, L. N. and Krigman, L. D. (1973) Structural position of fluorine in silicate melts (according to melting curves). *Geochemistry International*, 9, 34-40.

Kogarko, L. N., Krigman, L. D. and Shardilo, N. S. (1968) Experimental investigations of the effect of alkalinity on the separation of fluorine into the gas phase. *Geochemistry International*, 4, 782-790.

Koros, P. J. and King, T. B. (1962) The self-diffusion of oxygen in a lime-silica-alumina slag. *Transactions of AIME*, 224, 299-306.

Koster van Groos, A. F. and Wyllie, P. J. (1968) Melting relationships in the system  $\text{NaAlSi}_3\text{O}_8\text{-NaF-H}_2\text{O}$  to 4 kilobars pressure. *Journal of Geology*, 76, 50-70.

Kovalenko, V. I. (1973) Distribution of fluorine in a quartz keratophyre dyke (ongonite) and solubility of fluorine in granitic melts. *Geokhimiya*, 57-66 (transl. *Geochemistry International*, 10, 41-49, 1967).

Kovalenko, V. I. (1978) The reactions between granite and aqueous hydrofluoric acid in relation to the origin of fluorine-bearing granites. *Geochemistry International*,



14, 108-118.

Kozakevitch, P. (1954) Sur la viscosite des laitiers de hauts fourneaux. *Revue de Metallurgie*, 8, 569-584.

Kumar, D., Ward, R. G. and Williams, D. J. (1961) Effect of fluorides on silicates and phosphates. *Discussions of the Faraday Society*, 32, 147-154.

Kumar, D., Ward, R. G. and Williams, D. J. (1965) Infrared absorption of some solid silicates and phosphates with and without fluoride additions. *Discussions of the Faraday Society*, 61, 1850-1857.

Kushiro, I. (1976) Changes in viscosity and structure of melt of  $\text{NaAlSi}_2\text{O}_6$  composition at high pressures. *Journal of Geophysical Research*, 81, 6347-6350.

Kushiro, I. (1983) Effect of pressure on the diffusivity of network-forming cations in melts of jadeitic compositions. *Geochimica et Cosmochimica Acta*, 47, 1415-1422.

Magaritz, M. and Hofmann, A. W. (1978) Diffusion of Sr, Ba and Na in obsidian. *Geochimica et Cosmochimica Acta*, 42, 595-605.



- Manning, D. A. C. (1981) The effect of fluorine on liquidus phase relationships in the system Qz-Ab-Or with excess water. *Contributions to Mineralogy and Petrology*, 76, 206-215.
- Manning, D. A. C., Hamilton, D. L., Henderson, C. M. B. and Dempsey, M. J. (1980) The probable occurrence of interstitial Al in hydrous fluorine-bearing and fluorine free aluminosilicate melts. *Contributions to Mineralogy and Petrology*, 75, 257-262.
- Mysen, B. O. , Virgo, D. and Scarfe, C. M. (1980) Relations between the anionic structure and viscosity of silicate melts - a Raman spectroscopic study. *American Mineralogist*, 65, 690-710.
- Mysen, B. O. , Virgo, D. and Seifert, F. A. (1982) The structure of silicate melts: implications for chemical and physical properties of natural magma. *Reviews of Geophysics and Space Physics*, 20, 353-383.
- Naumov, V. B., Kovalenko, V. I., Ivanova, G. F. and Vladyskin, N. B. (1977) Genesis of topaz according to the data on microinclusions. *Geochemistry International*, 14, 1-8.
- Naumov, V. B., Kovalenko, V. I., Kuz'Min, M. I., Vladyskin,



- N. V. and Ivanova, G. F. (1971) Thermometric study of inclusions in topaz from topaz-bearing quartz keratophyres (ongonites). Doklady Academia Science, USSR, 199, 104-106.
- Navrotsky, A., Peraudeau, G., McMillan, P. and Coutures, J-P. (1982) A thermochemical study of glasses and crystals along the joins silica-calcium aluminate and silica-sodium aluminate. *Geochimica et Cosmochimica Acta*, 46, 2039-2047.
- Nedachi, M. (1980) Chlorine and fluorine contents of rock-forming minerals of the Neogene granitic rocks of Kyushu, Japan. *Mining Geology Special Issue*, 8, 39-48.
- Oishi, Y., Terai, R. and Ueda, H. (1975) Oxygen diffusion in liquid silicates and relation to their viscosity. In A. R. Cooper and A. R. Heuer, eds. *Mass Transport Phenomena in Ceramics*, p. 297-310, Plenum Press.
- Orlova, G. P. (1963) Solubility of water in albite melts - under pressure. *International Geology Reviews*, 6, 254-258.
- Orville, P. M. (1963) Alkali ion exchange between vapor and feldspar phases. *American Journal of Science*, 261, 201-237.





- Owens-Illinois Glass Company , General Research Laboratory  
(1944) Effect of fluorine and phosphorus pentoxide on properties of soda-dolomite lime-silica glass. *Journal of the American Ceramic Society*, 27, 369-372.
- Oxtoby, S. and Hamilton, D. L. (1978a) The discrete association of water with  $\text{Na}_2\text{O}$  and  $\text{SiO}_2$  in NaAl silicate melts. *Contributions to Mineralogy and Petrology*, 66, 185-188.
- Oxtoby, S. and Hamilton, D. L. (1978b) Calculation of the solubility of water in granitic melts, *NERC Progress in Experimental Petrology II*, 37-40.
- Pauly, H. (1960) Paragenetic relations in the main cryolite ore of Ivigtut, South Greenland. *Neues Jahrbuch fur Mineralogie Abhandlung*, 94, 121-139.
- Pichavant, M. (1981) An experimental study of the effect of boron on a water-saturated haplogranite at 1 kbar pressure. *Contributions to Mineralogy and Petrology*, 76, 430-439.
- Piwoinskii, A. J. (1967) The attainment of equilibrium in hydrothermal experiments with granitic rocks. *Earth and Planetary Science Letters*, 2, 161-162.



- Rabinovich, E. M. (1967) On the behavior of fluorine in silicate glasses. Inorganic Materials Consultants Bureau Translations 3, 762-766.
- Rabinovich, E. M. (1983) On the structural role of fluorine in glass. Physics and Chemistry of Glasses, 24, 54-56.
- Rau, K., Muhlich, A. and Treber, N. (1977) Progress in silica fibers with fluorine dopant. (abstr.) Topical Meeting on Optical Fiber Transmission II, Williamsburg - conference proceedings, TuC1-TuC4
- Riebling, E. F. (1966) Structure of sodium aluminosilicate melts containing at least 50 mole%  $\text{SiO}_2$  at  $1500^\circ\text{C}$ . Journal of Physical Chemistry, 44, 2857-2865.
- Roedder, E. and Coombs, D. S. (1967) Immiscibility in granitic melts, indicated by fluid inclusions in ejected granitic blocks from Ascension Island. Journal of Petrology, 83, 417-451.
- Rothwell, G. (1956) The crystalline phase in fluoride opal glasses. Journal of the American Ceramic Society 39, 407-414.
- Rubie, D. C. and Gunter, W. D. (1983) The role of speciation in alkaline igneous fluids during fenite metasomatism.



Contributions to Mineralogy and Petrology, 82, 165-175.

Scarfe, C. M. (1973) Viscosity of basic magmas at varying pressure. *Nature*, 241, 101-102.

Schairer, J. (1950) The alkali-feldspar join in the system  $\text{NaAlSiO}_4$ - $\text{KAlSiO}_4$ - $\text{SiO}_2$ . *Journal of Geology*, 58, 512-517.

Schairer, J. F. and Bowen, N. L. (1956) The system  $\text{Na}_2\text{O}$ - $\text{Al}_2\text{O}_3$ - $\text{SiO}_2$ . *American Journal of Science*, 254, 129-195.

Schwerin, L. (1934) The effect of fluorspar on the viscosity of basic slags. *Metals and Alloys*, 5, 117-123.

Seifert, F., Mysen, B. O. and Virgo, D. (1982) Three-dimensional network structure of quenched melts (glass) in the systems  $\text{SiO}_2$ - $\text{NaAlO}_2$ ,  $\text{SiO}_2$ - $\text{CaAl}_2\text{O}_4$  and  $\text{SiO}_2$ - $\text{MgAl}_2\text{O}_4$ . *American Mineralogist*, 67, 696-717.

Sharma, S. K., Virgo, D. and Mysen, B. O. (1979) Raman study of the coordination of aluminum in jadeite melts as a function of pressure. *American Mineralogist*, 64, 779-787.

Shaw, H. R. (1963) Obsidian- $\text{H}_2\text{O}$  viscosities at 1000 and 2000 bars in the temperature range 700°C to 900°C. *Journal of*



.Geophysical Research, 68, 6337-6343.

Shaw, H. R. (1972) Viscosities of magmatic silicate liquids : an empirical method of prediction. American Journal of Science, 272, 870-893.

Shaw, H. R. (1974) Diffusion of  $H_2O$  in granitic liquids. Part I. Experimental Data; Part II. Mass transfer in magma chambers. In A. W. Hofmann, B. J. Giletti, H. S. Yoder and R. A. Yund, eds. Carnegie Institute of Washington Publication 634, Geochemical Transport and Kinetics Conference, 1973, 139-170.

Shcherba, G. N. (1970) Greisens. International Geological Reviews, 12, 114-151 239-254.

Shimizu, N. and Kushiro, I. (1984) Diffusivity of oxygen in jadeite and diopside melts at high pressures. Geochimica et Cosmochimica Acta, 48, 1295-1304.

Shinozaki, N., Okusi, H., Mizoguchi, K. and Suginozaki, Y. (1977) Electrical conductivity and the infrared spectra of  $Na_2O-SiO_2-NaF$  melts. Japanese Institute of Metallurgy Journal, 41, 607-612.

Smart, R. M. and Glasser, F. P. (1978) Silicate anion constitution of lead silicate glasses and crystals.





Physics and Chemistry of Glasses, 19, 95-102.

Smith, D. G. W. and Gold, C. M. (1979) EDATA2: a FORTRAN IV computer program for processing wavelength and/or energy-dispersive electron microprobe analyses. In D. Newbury, ed., Microbeam Analysis Society Proceedings 14th Annual Conference, San Antonio., p.273-278.

Smith, J. V., Delaney, J. S., Hervig, R. L. and Dawson, J. B. (1981) Storage of F and Cl in the upper mantle : geochemical implications. *Lithos*, 14, 133-147.

Sparks, R. S. J. (1978) The dynamics of bubble formation and growth in magmas : A review and analysis. *Journal of Volcanological and Geothermal Research*, 3, 1-37.

Sparks, R. S. J., Sigurdsson, H. and Wilson, L. (1977) Magma mixing: a mechanism for triggering acid explosive eruptions. *Nature*, 267, 315-318.

Tagusagawa, N. (1980) Infrared absorption spectra and structure of fluorine-containing alkali silicate glasses. *Journal of Non-Crystalline Solids*, 42, 35-40.

Taylor, M. and Brown, G. E. (1979) Structure of mineral glasses. I. The feldspar glasses  $\text{NaAlSi}_3\text{O}_8$ ,  $\text{KAlSi}_3\text{O}_8$ ,  $\text{CaAl}_2\text{Si}_2\text{O}_8$ . *Geochimica et Cosmochimica Acta*, 43, 61-77.



- Titley, S. R. and Beane, R. E. (1980) Porphyry copper deposits I. Geologic settings, petrology and tectogenesis. In B. J. Skinner, ed. Economic Geology 75th Anniversary Volume, p. 214-235.
- Towers, H. and Chipman, J. (1957) Diffusion of calcium and silicon in a lime-alumina silica slag. Transactions of AIME, 209, 769-773.
- Tuttle, O. F. and Bowen, N. L. (1958) Origin of granite in the light of experimental studies in the system  $\text{NaAlSi}_3\text{O}_8$ - $\text{KAlSi}_3\text{O}_8$ - $\text{SiO}_2$ - $\text{H}_2\text{O}$ . Geological Society of America Memoir 74
- Valley, J. W., Petersen, E. U., Essene, E. J. and Bowman, J. R. (1982) Fluorophlogopite and fluortremolite in Adirondack marbles and calculated C-O-H-F fluid compositions. American Mineralogist, 67, 545-557.
- Voigt, D. E., Bodnar, R. J. and Blencoe, J. G. (1981) Water solubility in melts of alkali feldspar composition at 5 kbar, 950°C. (abstr.) EOS, Transactions of the American Geophysical Union, 62, 428.
- Watson, E. B. (1979) Calcium diffusion in a simple silicate melt to 30 kbar. Geochimica et Cosmochimica Acta, 43, 313-322.



- Watson, E. B. (1981) Diffusion in magmas at depth in the earth: the effects of pressure and dissolved water. *Earth and Planetary Science Letters*, 52, 291-301.
- Weisbrod, A. (1981) Fluid inclusions in shallow intrusives. In L. S. Hollister and M. L. Crawford, eds. *Mineralogical Society of Canada Short Course in Fluid Inclusions, Applications to Petrology*, p. 241-271.
- Westra, G. and Keith, S. B. (1981) Classification and genesis of stockwork molybdenum deposits. *Economic Geology*, 76, 844-873.
- Weyl, W. A. (1950) Fluorine compounds in glass technology and ceramics. In J.H. Simmons, ed., *Fluorine Chemistry*, Academic Press, New York
- White, W. H., Bookstrom, A. A., Kamilli, R. J., Ganster, M. W., Smith, R. P., Ranta, D. E. and Steininger, R. C. (1980) Character and origin of Climax-type molybdenum deposits. In B. J. Skinner, ed. *Economic Geology 75th Anniversary Volume*, p. 270-316.
- Whitney, J. A. (1975) The effects of pressure, temperature and  $X(\text{H}_2\text{O})$  on phase assemblage in four synthetic rock compositions. *Journal of Geology*, 83, 1-31.



- Whittaker, E. J. W. and Muntus, R. (1970) Ionic radii for use in geochemistry. *Geochimica et Cosmochimica Acta*, 34, 945-956.
- Wilson, L., Sparks, R. S. J. and Walker, G. P. L. (1980) Explosive volcanic eruptions - IV. The control of magma properties and conduit geometry on eruption column behavior. *Geophysical Journal of the Royal Astronomical Society*, 63, 117-148.
- Winchell, P. (1969) The compensation law for diffusion in silicates. *High Temperature Science*, 1, 200-215.
- Winchell, P. and Norman, J. H. (1969) A study of the diffusion of radioactive nuclides in molten silicates at high temperatures. In *High Temperature Technology Third international symposium, Asilomar, 1967*, p.479-492.
- Wyllie, P. J. (1979) Magmas and volatile components. *American Mineralogist*, 64, 469-500.
- Wyllie, P. J. and Tuttle, O. F. (1961) Experimental investigation of silicate systems containing two volatile components. Part II. The effects of  $\text{NH}_3$  and HF in addition to water on the melting temperatures of granite and albite. *American Journal of Science*, 259, 128-143.





Yoder, H. S., Stewart, D. B. and Smith, J. R. (1957) Ternary feldspars: Carnegie Institute of Washington Yearbook, 56, 206-217.











**B30423**